Light Chain Dimers Acquire Amyloidogenic Properties in the Absence of Selection

DISS. ETH NO. 25870

LIGHT CHAIN DIMERS ACQUIRE AMYLOIDOGENIC PROPERTIES IN THE ABSENCE OF SELECTION

A thesis submitted to attain the degree of
DOCTOR OF SCIENCE of ETH ZURICH
(Dr. sc. ETH Zurich)
Presented by

SARA RAVASIO

M.Sci. Medical Chemistry and Pharmaceutical Technology
University of Pavia, Italy

born on 23.04.1990
citizen of Italy

accepted on the recommendation of

Prof. Dr. Federica Sallusto, examiner
Prof. Dr. Antonio Lanzavecchia, co-examiner
Prof. Dr. Paola Picotti, co-examiner
Prof. Dr. Giampaolo Merlini, co-examiner

2019

Table of contents

1. Acknowledgements

The fulfillment of my doctoral studies would not have been possible without the support of many people, who deserve my deepest gratitude.

Firstly, I would like to thank my supervisors Professor **Federica Sallusto** and Professor **Antonio Lanzavecchia**, for granting me the possibility to work in their laboratory and for their ongoing support and mentoring throughout my doctoral studies.

I wish to thank also the members of my committee, Professor **Paola Picotti** and Professor **Giampaolo Merlini** for positively supporting my PhD.

Further, I would like to thank **Andrea Cavalli** for the proactive collaboration established during these years on the challenging Light chain project.

A special thanks goes to the whole **IRB community**; the support, advice and the teachings of many current and former members of the Institute have proven fundamental to guide me though the multiple phases of my PhD. I would like to thank **Sonia** for our endless scientific and philosophical discussion, **Chiara** and **Isabella** for their boundless support, **Philipp**, **Antonino**, **Corinne**, **Valentina**, **Marica**, **Yiwei**, **Alex**, **Egle** and many others for sharing many precious moments and raising my spirits during this rollercoaster called PhD.

Further, I am deeply grateful to my **parents** and my brother **Francesco** for their emotional support and for their trust, which I have felt every single day. **Gabriele** deserves the most sincere credit, for patiently standing by my side in any circumstance and for proactively encouraging me to live my Values more fully.

A special thanks goes to my wonderful house mates **Emiliano** and **Mariantonietta**, with whom I have not only shared a flat, but rather a piece of my soul, and to all my friends inside and outside Switzerland, who have affectionately accompanied all my endeavors during these years. I would like to thank **Silvia**, **Chiara**, **Luca** and all my old friends, who I have always felt close.

I wish to warmly thank some gorgeous people who made my stay in Bellinzona more joyful: **Maura**, who worked side by side me on the Light chain project, to which I owe having gained an invaluable colleague and a true friend in life; **Sarah**, for her exquisite creativity and restless determination, and **Anna** for her affection and for the mutual pieces of advices dispensed during our inspirational hikes up to the Castles of Bellinzona.

2. Abbreviations

ΔG	Difference of Gibbs free energy
AID	Activation-induced deaminase
AKT	Protein kinase B
AL	Amyloidogenic Light
AL	Immunoglobulin Light Chain amyloidosis
APC	Antigen presenting cell
Apo	Apolipoprotein
APRIL	A proliferation-inducing ligand
ASC	Antibody-secreting cell
ASCT	autologous stem cell transplantation
ATF6	activating transcription factor 6
Aβ	Amyloid beta
BAFF	B cell Activating Factor
BCAP	B cell adaptor for PI3K
BCL2	B cell lymphoma 2
BCL6	B cell lymphoma 6
BCR	B cell receptor
BER	base excision repair
BiP	Ig binding protein
BJ	Bence Jones
BLIMP1	B lymphocyte-induced maturation protein 1
BLNK	B cell linker protein
BM	Bone Marrow
BNP	B natriuretic peptide
bp	base pair
BTK	Bruton's tyrosine kinase
C	cytidine
C	constant
CCL	CC-chemokine ligand
CCND	cyclin D
CCR	CC-chemokine receptor
CD	Cluster of Differentiation

CD40L	CD40 ligand
CDR	Complementary Determining Region
CH1	Heavy chain Constant domain 1
CH2	Heavy chain Constant domain 2
CH3	Heavy chain Constant domain 3
CHOP	C/EBP homologous protein
CL	Light chain constant domain
CLP	common lymphoid progenitor
CMV	cytomegalovirus
CR	Congo Red
CSR	class-switch recombination
CXCL	CXC-chemokine ligand
CXCR	CXC-chemokine receptor
DAG	diacylglycerol
DC	Dendridic cell
DLBCL	diffuse large B cell lymphoma
DSB	double-strand breaks
E2A	E2A immunoglobulin enhancer-binding factors E12/E47
EBF	Early B-Cell Factor
EBV	Epstein-Barr virus
ECM	extracellular matrix
EGCG	epigallocatechin-3-gallate
ELISA	Enzyme-linked immunosorbent assay
ER	Endoplasmic Reticulum
ERAD	ER-associated degradation
Fab	fragment antigen binding
Fc	fragment crystallizable
FcR	Fc receptors
fDC	Follicular dendritic cell
FLC	serum free L chain
FOXO1	forkhead box protein O1
FR	Framework
FTIR	Fourier Transform Infrared Spectroscopy
GAG	glycosaminoglycan

GC	Germinal Center
GL	Germline
GRB2	growth factor receptor-bound protein 2
H	Heavy
ICOS	inducible T-cell costimulatory
Ig	Immunoglobulin
IL	Interleukin
InsP3	inositol-1,4,5-trisphosphate
InsP3R	inositol-1,4,5-trisphosphate (InsP3) receptor
IRE1α	inositol-requiring 1 α
IRF4	interferon regulatory factor 4
ITAM	immunoreceptor tyrosine-based activation motifs
ITIM	intracellular inhibitory motif
L	Light
LPL/WM	lymphoplasmacytic lymphoma/Waldenström macroglobulinemia
LPS	lipopolysaccharide
MAPK	mitogen-activated protein kinase
MEK	MAPK/ERK kinase
MGUS	monoclonal gammopathy of undetermined significance
MHC	major histocompatibility complex
miRNA	microRNA
moDCs	Monocyte-derived Dendritic cells
MM	Multiple Myeloma
MMP	matrix metalloproteinase
MW	Molecular Weight
MYD88	Myeloid differentiation primary response 88
NFAT	nuclear factor of activated T cells
NF−κB	nuclear factor−κB
NHEJ	non homologous end joining
NMR	nuclear magnetic resonance
OBF1	(OCT)-binding factor 1
PAX5	Paired box protein 5
PC	Plasma cell
PD-1	Programmed Cell Death Protein 1

PDK1	3-phosphoinositide-dependent protein kinase 1
pI	isoelectric points
PI3K	phosphoinositide 3-kinase
PKC	protein kinase C
PLCγ2	phospholipase Cγ2
POEMS	Polyneuropathy, Organomegaly, Endocrinopathy, Monoclonal protein and Skin
PtdInsP2	phosphatidylinositol-4,5-bisphosphate
PtdInsP3	phosphatidylinositol-3,4,5-trisphosphate
PTEN	phosphatase and tensin homologue
RAG	recombination-activating gene
RASGRP	RAS guanyl-releasing protein
RB1	retinoblastoma protein
ROS	reactive oxygen species
RSs	recombination signal sequences
S	switch
S1PR1	sphingosine-1-phosphate receptor 1
SAP	Serum amyloid P component
SAP	(SLAM)-associated protein
SAXS	Small-angle X-ray scattering
SFK	Src family kinases
SHIP	SH2-domain-containing inostil-5-phosphatase
SHM	somatic hypermutation
SHP1	SH2-domain- containing protein tyrosine phosphatase 1
SIAE	sialic acid acetyl esterase
Siglec	sialic acid-binding immunoglobulin-like lectin
siRNA	Short interfering RNA
SLC	surrogate light-chain
SLE	systemic lupus erythematosus
SOS1	son of sevenless 1
STC1	stanniocalcin-1
SYK	spleen tyrosine kinase
TAB1	TGF-β-activated protein kinase-1 binding protein-1
TCR	T cell receptor
TD	T cell-dependent

TEM	Transmission electron microscopy
Tfh	T follicular helper
TGF-β	transforming growth factor-β
THP	Tam Horsfall Protein
ThT	Thioflavin T
TI	T cell-independent
TLR	Toll-like receptor
TNF	tumor necrosis factor
TP53	tumor protein 53
U	uridine
UEX	urinary extracellular vesicles
UNG	uracil DNA N-glycosylase
UPR	unfolded-protein response
V	variable
VCAM1	Vascular Cell Adhesion Molecule 1
VH	Variable heavy chain domain
VL	Variable light chain domain
WT	Wild type
XBP1	X-box-binding protein 1

3. Abstract

3.1 Summary

It is well established that immunoglobulin Light (L) chains dimers, also known as Bence-Jones (BJ) proteins, are secreted by normal and malignant plasma cells (PCs) and, when produced in large amounts, can aggregate into amyloid fibrils in target tissues leading to organ failure and to the clinical manifestation of Immunoglobulin Light Chain amyloidosis (AL amyloidosis). The unique identity of the pathogenic L chain belonging to each AL amyloidosis patient, which originates from the mechanisms of generation of antibody diversity, has considerably hindered the identification of the structural determinants of L chains aggregation and consequent clinical manifestations.

The aim of my thesis is to examine AL amyloidosis from the B cell perspective, considering that in developing B cell clones, L chain variable (VL) domains undergo a process of somatic mutation and are selected for pairing with variable Heavy (H) chain (VH) domains to form a functional B cell receptor (BCR).

Therefore, by comparing the effect of L chains hetero-dimerization with H chains to L chains homo-dimerization, I could show that free L chains, which are not subject to antigen-driven selection, are intrinsically unstable and are characterized by the exposure of hydrophobic patches and free thiols; their instability is substantially increased by somatic mutations, leading to aggregation into Congo Red (CR)- and Thioflavin T (ThT)- positive amyloid fibers. I could also show that free L chains have unique specificities and can bind to cells and to the extracellular matrix, a property that may increase their local concentration and drive the nucleation phase of amyloid aggregation in the target tissues.

Taken together, these findings demonstrate that, in the absence of a negative selection mechanism, L chain dimers develop through somatic mutations into rogue proteins, leading to their concentration-dependent aggregation and organ accumulation. Consequently, these results suggest that a plausible explanation of AL amyloidosis pathogenesis could be represented by the deleterious combination of a break of tolerance with a break of protein homeostasis.

3.2 Riassunto

Le catene leggere immunoglobuliniche, note anche come proteine di Bence-Jones (BJ), sono secrete da plasmacellule normali e tumorali e, se prodotte in elevate quantità, possono aggregare formando fibrille amiloidi localizzate in specifici tessuti, causando insufficienza d'organo e la

manifestazione clinica dell'amiloidosi delle catene leggere (amiloidosi AL). L'identità della catena leggera patogenica appartenente a ciascun paziente affetto da amiloidosi delle catene leggere, che ha origine dai meccanismi di generazione della diversità anticorpale, ha considerevolmente ostacolato l'identificazione dei determinanti strutturali dell'aggregazione delle catene leggere e dei conseguenti meccanismi alla base delle manifestazioni cliniche della patologia.

Lo scopo della mia tesi è quello di esaminare l'amiloidosi delle catene leggere dal punto di vista della risposta immunitaria sostenuta dai linfociti B, considerando che durante il loro sviluppo e maturazione, i domini variabili delle catene leggere (VL) subiscono un processo di mutazione somatica e sono selezionati per l'appaiamento con i domini variabili delle catene pesati (VH) al fine di formare, sulla superficie dei linfociti B, un recettore funzionale (BCR).

Pertanto, confrontando l'effetto dell'etero-dimerizzazione delle catene leggere con le catene pesanti all'effetto dell'omo-dimerizzazione tra catene leggere, ho potuto dimostrare che le catene leggere, che, nella loro forma libera, non sono soggette alla selezione antigenica, sono intrinsecamente instabili e sono caratterizzate dall'esposizione di superfici idrofobiche e tioli liberi; la loro instabilità è notevolmente aumentata dalle mutazioni somatiche, che promuovono l'aggregazione in fibrille amiloidi positive al legame di Congo Rosso (CR) e Tioflavina T (ThT). I dati qui riportati dimostrano inoltre che le catene leggere hanno specificità uniche e possono legare antigeni cellulari e la matrice extracellulare, una proprietà che può contribuire ad aumentare la loro concentrazione locale e supportare la fase di nucleazione dell'aggregazione amiloide nei tessuti bersaglio.

Globalmente, questi risultati dimostrano che, in assenza di un meccanismo di selezione negativo, le catene leggere immunoglobuliniche, nella loro forma libera, divengono, mediante mutazioni somatiche, proteine atipiche, propense all'aggregazione dipendente dalla concentrazione e all'accumulo in organi bersaglio. Ne consegue che una plausibile spiegazione della patogenesi dell'amiloidosi delle catene leggere potrebbe essere rappresentata dalla deleteria combinazione di un fallimento dei meccanismi della tolleranza immunologica e di omeostasi proteica.

4. General introduction

Systemic immunoglobulin Light chain amyloidosis, referred to as AL amyloidosis, is a protein misfolding disease, whose distinctive feature is the conversion of immunoglobulin (Ig) light (L) chains from their native state into amyloid fibrillary aggregates in the extracellular space, leading to severe organ dysfunction.

In this section I will provide a summary of recently published and relevant literature, which will aid the understanding of the main results of this thesis. Firstly, I will discuss the events related to protein aggregation and amyloid formation. Subsequently, considering that the precursor protein involved in AL amyloidosis is produced by B lymphocytes and that Ig L chains are components of the antibody molecule, I will give a general introduction on the humoral immune response, focusing on the generation of antibody diversity and its inherent quality checkpoints. Finally, I will provide a comprehensive description of the current understanding of the determinants of AL amyloidosis.

4.1 The amyloid state and its association to protein conformational disorders

Following their synthesis by the ribosome, proteins can occupy highly diverse structural states. The conversion from one state to the other is governed by several factors, which include the rates of protein synthesis and degradation and the interaction with chaperones. An even more crucial element that can shift the equilibrium between the different protein states is represented by the thermodynamic stability and the free energy barrier that are associated to the each transition.

Most proteins, through their inherent folding pathway, tend to assume their functional state either as monomers or as components of precise multi-domain complexes, such as the proteasome or the ribosome. In parallel, all polypeptides have the generic tendency to generate aggregated forms, which can either consist of amorphous, disordered assemblies or display, on the ultrastructural level, a highly-ordered fibrillary structure rich in β-sheets, which represents a different type of protein aggregates, known as amyloid. Remarkably, the misfolding of soluble proteins, the resultant formation of amyloid fibrils and their deposition into specific target organs not only correlate with loss of function of the native protein, but also with the generation of toxic intermediates; these phenomena have been associated with a group of human diseases, known as protein conformational disorders or protein misfolding diseases (Knowles, Vendruscolo and Dobson, 2014). 36 human proteins (**Table 4.1**) have been described as able to form extracellular amyloid aggregates in several target tissues either in their wild-type (WT) form or due to

mutations, the former condition being known as acquired amyloidosis, the latter as hereditary amyloidosis. (Chiti and Dobson, 2009; Merlini *et al.*, 2018).

Table 4.1. Human proteins associated to amyloid formation and related disorders Adapted from (Merlini et al., 2018).

Acronym	Precursor Protein	Type	Syndrome or tissues involved
Aβ	Amyloid β precursor protein	Acquired	Sporadic Alzheimer's disease
		Hereditary	Hereditary cerebral amyloid prototypical angiopathy
APrP	Prion protein	Acquired	Sporadic Creutzfeldt-Jakob Disease
		Hereditary	Familial Creutzfeldt-Jakob Disease
ACys	Cystatin C	Hereditary	Cerebral amyloid angiopathy, Iceland-type
A β_2m	β_2-microglobulin	Acquired	Chronic Hemodialysis
AL	Immunoglobulin Light Chain	Acquired	Systemic Immunoglobulin Light chain amyloidosis
AH	Immunoglobulin Heavy Chain	Acquired	Primary amyloidosis myeloma-associated
AA	(apo)serum AA	Acquired	Secondary Amyloidosis, reaction to infection or chronic inflammation
ATTR	Transthyretin	Hereditary	Familial amyloid polyneuropathy
		Acquired	Senile heart, blood vessel
AApoAI	Apolipoprotein AI	Hereditary	Liver, kidney, heart
AApoAII	Apolipoprotein AII	Hereditary	Kidney, heart
AApoAIV	Apolipoprotein AIV	Acquired	Sporadic associated to ageing
AGel	Gelsolin	Hereditary	Hereditary Amyloid, Finland-Type
ALys	Lysozyme	Hereditary	Kidney, liver and spleen
AFib	Fibrinogen a chain	Hereditary	Kidney

The pathogenic mechanisms of amyloidosis are poorly characterized, but organ dysfunction seems to derive from a combination of the fibril-dependent distortion of tissue architecture and a direct effect of different molecular weight (MW) aggregates on cells, known as proteotoxicity (Merlini *et al.*, 2018). Once formed, amyloid deposits are stable, resistant to degradation and persistent, even if the endogenous immunological clearance mechanisms, usually involving tissue macrophages, can slowly reduce the amount of amyloid deposits (Nyström and Westermark, 2012). Such mechanisms are employed by current immunotherapies aimed at visceral amyloid clearance (Bodin *et al.*, 2010), which have recently shown preliminary clinical efficacy (Richards *et al.*, 2015).

Despite amyloid precursor proteins are characterized by diverse sequences, native structures and functions, the corresponding amyloid fibrils appear remarkably similar. As shown by pioneering

X-ray diffraction and electron microscopy studies (Shirahama and Cohen, 1967; Eanes and Glenner, 1968) and confirmed by cryo-electron microscopy, solid-state nuclear magnetic resonance (NMR) spectroscopy (Fitzpatrick *et al.*, 2013) and X-ray diffraction of peptide microcrystals (Sawaya *et al.*, 2007) amyloid fibrils are unbranched filaments with a diameter of 7.5–10.0 nm, characterized by a highly ordered cross-β structure with antiparallel β-strands arranged with a perpendicular orientation respect to the fiber length. Each mature fibril usually consists of multiple protofilaments coiled around each other.

The presence of amyloid was initially solely associated to human disorders, however during the last decades seminal research works have suggested that under appropriate experimental conditions almost any given protein could populate the amyloid state (Chiti *et al.*, 1999; Knowles, Vendruscolo and Dobson, 2014), due to the unique architecture of amyloid aggregates. Indeed, the common structural property of amyloid comprises extended intermolecular β-sheets, which are stabilized by hydrogen bonds between the backbones of each monomer; considering that the polypeptide backbone is by definition a common structural feature of all proteins and peptides, the ability to form amyloid aggregates can be considered a generic property of every polypeptide, which could in principle populate the amyloid state as an alternative to the native state. Nevertheless, the protein sequence and the resulting properties of the side-chains regulate whether the conversion of a given polypeptide to amyloid aggregates could be achievable, as the side-chains packing guides the interaction between different β-sheets, dictating whether β-sheets interactions could be structurally tolerated (Sawaya *et al.*, 2007) and accounting for variations of the fibrillary architecture (Fändrich and Dobson, 2002; Knowles, Vendruscolo and Dobson, 2014).

The conversion of polypeptides to amyloid aggregates is based on the formation of intermolecular interactions and is therefore favored at higher concentrations. In detail, above a specific concentration, known as critical concentration, owing to the extensive energy gain due to the a vast network of intermolecular hydrogen bonds, the free energy (G) level of the amyloid state could be lower than the one of the native state, implying that the thermodynamic stability of amyloid species might be higher than the one of their native precursor proteins. Despite the native state represents a metastable protein form, its conversion to the amyloid form is not usually spontaneous or is even inaccessible, due to the kinetic barriers that separate native and aggregated states (**Fig. 4.1**) (Baldwin *et al.*, 2011; Knowles, Vendruscolo and Dobson, 2014). Therefore, the description of the kinetics involved in amyloid formation is instrumental to study the conditions which favor amyloidogenesis in living organisms, despite it is necessary to consider that protein

misfolding diseases develop over several decades, whereas in vitro experiments need to employ suitable, sometimes even artificial, conditions to observe amyloid formation in a reasonable timescale (Knowles, Vendruscolo and Dobson, 2014).

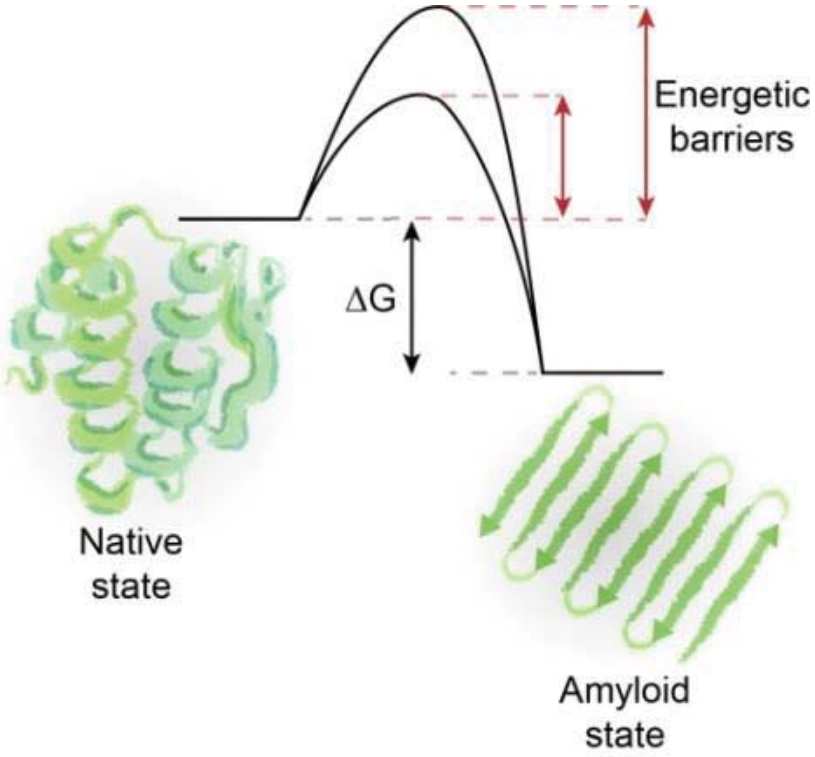

Figure 4.1. Thermodynamics and kinetics of the amyloid state. The free energy of the amyloid state can be lower than the one of the native state, as indicated by a the difference of Gibbs free energy (ΔG) associated to the transition. The propensity of such transition correlates with the energetic barrier separating the two states, which is subordinate to the critical concentration. Original artwork inspired by Knowles, Vendruscolo and Dobson, 2014.

Reaching the amyloid state can be related to nucleated polymerization reactions, which are described by a sigmoidal curves, where a lag phase precedes the onset of a growth phase, culminating in a plateau phase (**Fig. 4.2**) (Serio *et al.*, 2000); such phases correspond to a primary nucleation step, required for the initial formation of nuclei, an elongation step, where monomers are added to an already formed fibril, and to the depletion of soluble species. The conversion of a protein monomer to amyloid can be accelerated by the supplementation of pre-formed aggregates, known as seeds, which can reduce the extension of the lag phase (Jucker and Walker, 2011).

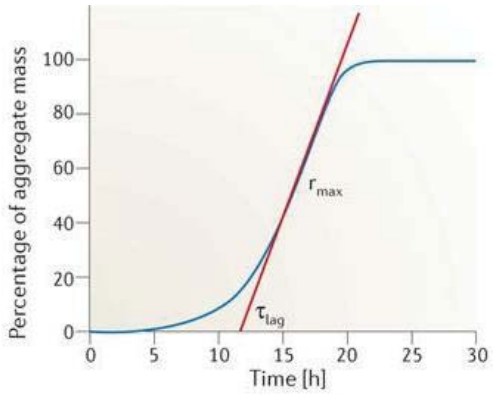

Figure 4.2. Sigmoidal curve typical of nucleated polymerization reactions, dysplaying a lag phase (τ_{lag}) and a maximal growth rate (r_{max}). Adapted with permission (Knowles, Vendruscolo and Dobson, 2014). Originally displayed in (Knowles *et al.*, 2009)

The process of amyloid aggregation has been widely studied for several amyloidogenic model precursors, such as Amyloid beta (Aβ), showing that new aggregates can be generated either by primary nucleation of monomers or by secondary events, namely secondary nucleation owing to the combination of monomers to pre-formed aggregates or by fragmentation of existing fibrillary species (**Fig. 4.3**); in the context of amyloid aggregation, secondary processes play a crucial role, as they contribute to the exponential growth of fibrillary species due to the catalytic role of fibrillary nuclei (Knowles, Vendruscolo and Dobson, 2014).

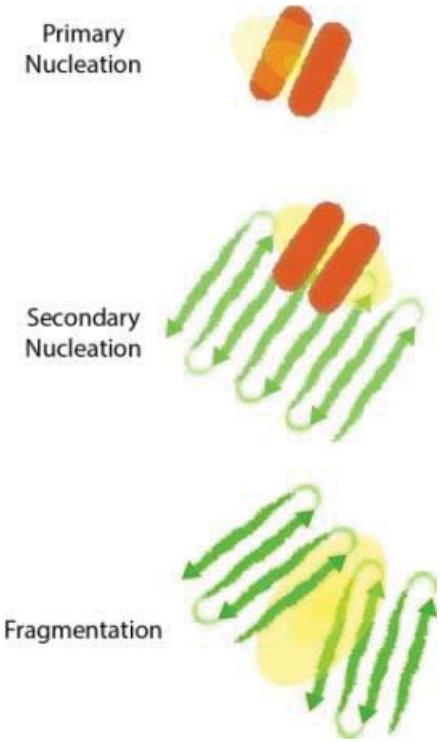

Figure 4.3. Mechanisms and microscopic steps involved in nucleated polymerization reactions. Amyloid aggregates can be formed from monomers via primary nucleation or from existing nuclei through secondary processes such as surface-catalyzed secondary nucleation or

fibrils fragmentation. Original artwork inspired by Knowles, Vendruscolo and Dobson, 2014. Originally displayed in (Lührs *et al.*, 2005).

Several factors have been demonstrated to favor amyloid formation, such as the intrinsic propensity of specific proteins to form amyloid material, mutations that destabilize the native structure of a protein and expose protease-sensitive or hydrophobic regions. Enhanced protein synthesis or reduced clearance can increase the precursor protein concentration until reaching the critical concentration, which is strictly dependent on the precursor protein stability and which is required for nucleation and aggregation initiation (Merlini and Bellotti, 2003; Knowles, Vendruscolo and Dobson, 2014). However, it is crucial to highlight that protein aggregation becomes apparent only after the failure of the mechanisms of protein homeostasis, known as proteostasis, which are designed to maintain the proteome in its native conformation, at the right concentration and in the correct location (Wyatt *et al.*, 2012; Labbadia and Morimoto, 2015).

4.2 Structural features of immunoglobulins

The precursor protein responsible for amyloid aggregation in AL amyloidosis is represented by Ig L chains. Ig L chains are structural components of antibodies, the distinctive effector molecules generated by B lymphocytes in the context of the adaptive immune response. Compared to the other types of protein misfolding diseases, where the amyloidogenic protein is a well characterized WT protein or a protein variant arising from genetic mutations inherited in an autosomal dominant manner, AL amyloidosis presents an apparent complexity deriving from the nature of its amyloid precursor protein. Ig L chains are characterized by high sequence variability, as the repertoire of Ig sequences can be considered almost unique for each individual. Thus, the identity of the amyloidogenic precursor protein is not shared by multiple individuals and is, by definition, patient-specific. Therefore, it is crucial to provide a detailed description of all the properties of B cell biology, which are involved in AL amyloidosis, starting from Ig structural features.

4.2.1. The antibody molecule

A central element of the adaptive immune system resides in the ability of lymphocytes to respond with high specificity to a potentially infinite diversity of antigenic structures within the constraints of a finite genome (Davis and Bjorkman, 1988; Jung *et al.*, 2006) thanks to the generation of an extraordinarily vast diversity of antigen receptors, namely the T cell receptor (TCR) and the B cell receptor (BCR). The broad diversity of unique receptor specificities is reached through a somatic recombination process, V(D)J recombination (Jung *et al.*, 2006), which takes place before

lymphocytes encounter their cognate antigen (Bernard, Hozumi and Tonegawa, 1978; Brack *et al.*, 1978). While the TCR exists only in a membrane-bound isoform, terminally differentiated B cells can also produce a soluble effector form of the BCR, called antibody. Secreted antibodies, which can bind pathogens and soluble products, are the main weapons through which B cells exert their effector function in the context of adaptive immunity.

Any antibody molecule, comprises two identical 50 kDa heavy (H) chains and two identical 25 kDa L chains, giving rise to a 150 kDa molecule. Disulphide bridges covalently connect the two H chains, and each H chain binds a L chains through a disulphide bond. Non-covalent interactions contribute to antibodies quaternary structure, stabilizing the pairing of the two H chains and of each H and L chain.

Both the H and the L chain comprise multiple Ig domains of approximatively 110 amino acids each. The C-terminal domain of both chains, named constant domain, is conserved within antibody classes and can be classified based on common determinants, termed isotypes. Higher vertebrates produce five H chain isotypes (IgD, IgM, IgG, IgA and IgE) and two L chain isotypes (κ and λ). Conversely, the N-terminal regions of H and L chains differ between antibodies and are therefore named variable domains (VH and VL). They comprise hypervariable regions composed of variable stretches of amino acids, which are responsible for the antibody unique specificity. Due to allelic exclusion, the greatest majority of B cells expresses only one H chain and L chain allele (Mostoslavsky, Alt and Rajewsky, 2004), therefore, as the unique combination of a given VH and VL pair creates the antigen binding site, each B cell produces antibodies with a unique specificity. As any antibody consists of two identical pairs of H and L chains, and therefore possesses two identical antigen-binding sites, each molecule can concurrently bind two identical antigens.

The term specificity reflects an antibody ability to discriminate between different antigenic structures, named epitopes. Hence, the interaction of antibodies and their cognate antigens can be described by two parameters: the strength of the non-covalent interaction between an antigen-binding site and a single epitope of its cognate antigen, called affinity, and the total strength of interaction due to the simultaneous interaction of the multivalent binding sites with antigens comprising multiple repeating epitopes, called avidity (Azimzadeh and Van Regenmortel, 1990).

4.2.2. From the Ig fold to antibody structure

H an L chains are multi-domains proteins, the former comprising four 12.5 kDa-domains, the latter comprising two 12.5 kDa-domains, all sharing a "β sandwich" structure, usually referred to

the “Ig fold”. The N-terminal Ig domains of the H and L chains correspond to their V domain (VH and VL), whereas their C-terminal domains are known as CH1-CH2-CH3 and CL, respectively.

The Ig fold is a crucial structural elementary unit of the extracellular recognition systems of vertebrates (Williams and Barclay, 1988; Barclay, 2003) and has also been described in viral and prokaryotic proteins, implying that it could have been acquired by horizontal gene transfer (Halaby and Mornon, 1998). The evolutionary selection of the Ig fold could have possibly originated from its unique combination of structural stability, granting resistance against proteases and extreme environmental conditions, and scaffolding ability for the presentation of binding loops to the surrounding environment (Feige, Hendershot and Buchner, 2010).

The Ig fold is distinguished by a greek-key β-barrel topology comprising two sheets, which create a sandwich-like structure. The V domain is composed of nine strands (abcc’c’’defg), whereas the C domain of seven strands (abcdefg) (Bork, Holm and Sander, 1994). The Ig fold of most antibody domains is stabilized by a buried disulfide bond connecting strands b and f, whose orientation is perpendicular to the two sheets (Huber *et al.*, 1976; Goto, Azuma and Hamaguchi, 1979; Bork, Holm and Sander, 1994), between two conserved cysteine residues. Other conserved features of the Ig fold of antibodies are a tryptophan residue in close proximity to the internal disulfide bond (Goto, Azuma and Hamaguchi, 1979) and a cis-proline residue located in the loop connecting b and c strands of C domains (Feige, Hendershot and Buchner, 2010).

Unlike other Ig domains, the V domain of H and L chains is characterized by a unique feature: its primary sequence can be functionally divided into three hypervariable amino acid strands known as complementary-determining regions (CDRs), which are located between four regions with seemingly constant sequence, named framework regions (FRs). The CDRs, especially CDR3, create solvent-exposed loops that are consistently interacting with the structure of the bound antigen (Schroeder *et al.*, 2010).

The multi-domain architecture of an antibody and the presence of an unstructured hinge region between the CH1 and the CH2 domains grant a substantial flexibility between its two arms (**Fig. 4.4**). The hinge region is also the site of proteolytic digestion by papain, which subdivides the antibody into three functional fragments (Kalmanson and Bronfenbrenner, 1942): two Fab (fragment antigen binding) segments, composed of a full L chain and the VH-CH1 domains of the H chain, endowed with antigen-binding ability, and one Fc (fragment crystallizable), comprising two identical two domain (CH2-CH3) segments, covalently linked by disulfide bridges in the hinge region. The Fc, despite devoid of antigen-binding properties, integrates antigen binding to

effector functions by mediating several downstream effects, namely the activation of the complement system, the binding to Fc receptors (FcR) (Ravetch and Kinet, 1991; Nimmerjahn and Ravetch, 2008) and recruitment of natural killer cells and macrophages (Lu *et al.*, 2018).

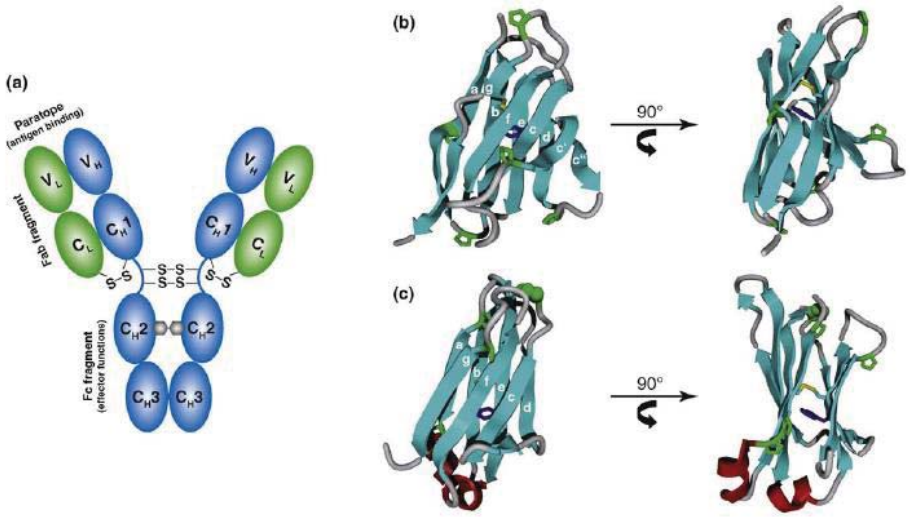

Figure 4.4. Structure and domain arrangement of antibodies. a, Structural description of an IgG antibody, where H chains are shown in blue, L chains in green and oligosaccharides between CH2 domains in gray; indications of the antigen-binding paratope, Fab fragment, Fc fragment and interchain disulfide bridges are shown. **b,c,** Domain architecture of VL (b) CL (c) with the indication of the intrachain disulfide bridge (yellow), the conserved tryptophan (blue) and proline residues (green). Short helical moieties (red) interconnect strands a and b and strands e and f only in the CL domain. Adapted with permission (Feige, Hendershot and Buchner, 2010).

In the BCR, the C-terminal region of the H chains contains an extra membrane-spanning domain, which is crucial for enabling BCR signaling (**Fig. 4.5**) thanks to its association with the transmembrane proteins Cluster of Differentiation 79A/79B (CD79A/CD79B) (formerly known as Igα/Igβ), which, due to the presence of tyrosine phosphorylation sites within immunoreceptor tyrosine-based activation motifs (ITAMs), are crucial docking sites for signal transduction (Reth, 1992).

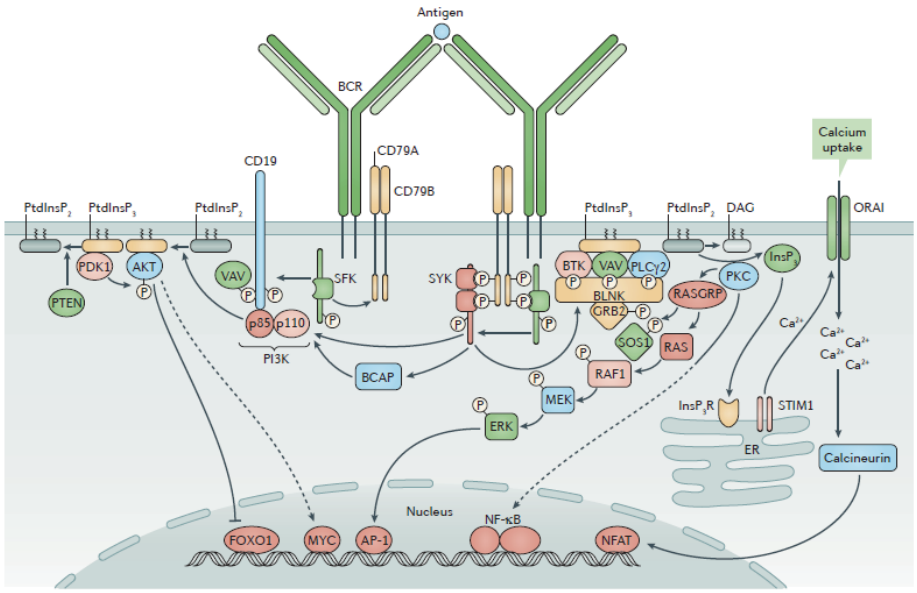

Figure 4.5. BCR signaling. BCR signaling and its regulation have been widely described (Packard and Cambier, 2013). Antigen binding promotes CD79A and CD79B phosphorylation by Src family kinases (SFKs) on ITAM, which are then able to recruit and upregulate the function of spleen tyrosine kinase (SYK). In this context, CD19 acts as BCR co-receptor, as phosphorylation of YXXM motifs within its cytoplasmic tail contributes to recruit phosphoinositide 3-kinase (PI3K) via interaction with its p85 regulatory subunit. Once activated through this pathway or via B cell adaptor for PI3K (BCAP), PI3K phosphorylates phosphatidylinositol-4,5-bisphosphate ($PtdInsP_2$), generating phosphatidylinositol-3,4,5-trisphosphate ($PtdInsP_3$), a crucial mediator that is able to recruit critical signal propagators, namely protein kinase B (AKT), 3-phosphoinositide-dependent protein kinase 1 (PDK1) and Bruton's tyrosine kinase (BTK). PI3K is counteracted by phosphatase and tensin homologue (PTEN), which catalyzes the reverse reaction. Alternatively, phosphorylation by SYK and SFK within B cell linker protein (BLNK) promotes the recruitment of a distinct array of signal propagators, like phospholipase Cγ2 (PLCγ2), BTK, VAV guanine nucleotide exchange factor proteins and growth factor receptor-bound protein 2 (GRB2). Specifically, PtdInsP2 hydrolysis by PLCγ2 generates two essential mediators, diacylglycerol (DAG) and inositol-1,4,5-trisphosphate ($InsP_3$). DAG can in turn recruit protein kinase C (PKC) isoforms, whose activation supports activation of nuclear factor−κB (NF−κB), and RAS guanyl-releasing proteins (RASGRPs), while $InsP_3$ sensing mediates Ca^{2+} mobilization by $InsP_3$ receptor ($InsP_3R$) and the plasma membrane Ca^{2+} channel ORAI, promoting calcineurin activation and the nuclear localization of the nuclear factor of activated T cells (NFAT). In parallel, BCR signaling can also proceed through a distinct pathway, which involves the guanine nucleotide exchange factor son of sevenless 1 (SOS1), the small GTPase RAS, serine kinase RAF1, MAPK/ERK kinase (MEK) and extracellular signal-regulated kinases (ERKs). Adapted with permission (Nemazee, 2017).

4.3 The B cell response

Considering that Ig L chains are building modules of antibodies and that their production is an outcome of humoral memory, Ig L chain biology is tightly associated to the events related to B cell development. In the following paragraphs I will provide an overview of the B cell response, focusing on B lymphocyte development.

In detail, B cell development and the combinatorial rearrangements at the Ig loci (Hozumi and Tonegawa, 1976) originate a repertoire of naïve B lymphocytes, which, after a first interaction with specific antigens (known as primary response), can generate memory responses (known as secondary responses) through the expansion and differentiation of B cell clones recognizing antigens, a phenomenon known as clonal selection (Burnet, 1976). Memory responses provide two lines of defense against invading pathogens: the first one is represented by pre-existing neutralizing antibodies secreted by long-lived plasma cells (PCs), the second one by the rapid reactivation of memory B cells and subsequent secretion of antibodies. Differentiation memory B cells and PCs from this continuously evolving population is responsible for an increase in the affinity of antibodies during a primary response and following secondary immunization or infections (Eisen and Siskind, 1964; Berek and Milstein, 1987; Mesin, Ersching and Victora, 2016). Thus, compared to primary responses, secondary responses are usually faster, of greater magnitude, and characterized by antibody with increased affinity (Kurosaki, Kometani and Ise, 2015).

In the following paragraph I will delineate an overview of the molecular and cellular mechanisms of B cell development. I will start from the generation of diversity in naïve B lymphocytes and move to the following stages of B cell differentiation, focusing on the impact of affinity maturation on the antibody repertoire.

4.3.1 B cell development

B lymphocytes development is a multifaceted process that involves several differentiation steps (**Fig. 4.6**) orchestrated by a network of transcription factors and environmental cues (Lin *et al.*, 2010); at least ten distinct transcription factors have been confirmed to act in the early stages of B-cell development, with E2A immunoglobulin enhancer-binding factors E12/E47 (E2A), Early B-Cell Factor (EBF), and Paired box protein 5 (PAX5) being predominantly involved in promoting B-lineage commitment and differentiation (Nutt and Kee, 2007). B lymphocytes are generated in the bone marrow (BM) from progenitor cells, known as pro-B cells, arising from common lymphoid progenitor (CLP) cells and committed to the B cell lineage (Nemazee, 2017).

At the pro-B cell developmental stage combinatorial rearrangements at the H chain locus take place until a productive H chain gene assembly occurs. IgM H-chain (μ chain) can therefore associate with surrogate light-chain (SLC) λ5 and Vpre-B, allowing surface expression of the pre-B cell receptor (pre-BCR) in the so called large pre-B cells (Melchers, 2005). Antigen-independent triggering of the pre-B cell receptor promotes transient proliferation and the end of recombination events at the H chain locus. Subsequently, B cells enter the small pre-B cell state, which involves the exit from the cell cycle, SLCs downregulation and recombination events at the L chain locus until a productive L chain protein is expressed. Expression and pairing of correctly rearranged H and L chains as membrane Ig on the B cell surface as IgM BCR is a crucial step and requires association to CD79A/CD79B in order to fulfill correct trafficking to the plasma membrane and consequent antigen recognition (Hombach *et al.*, 1990).

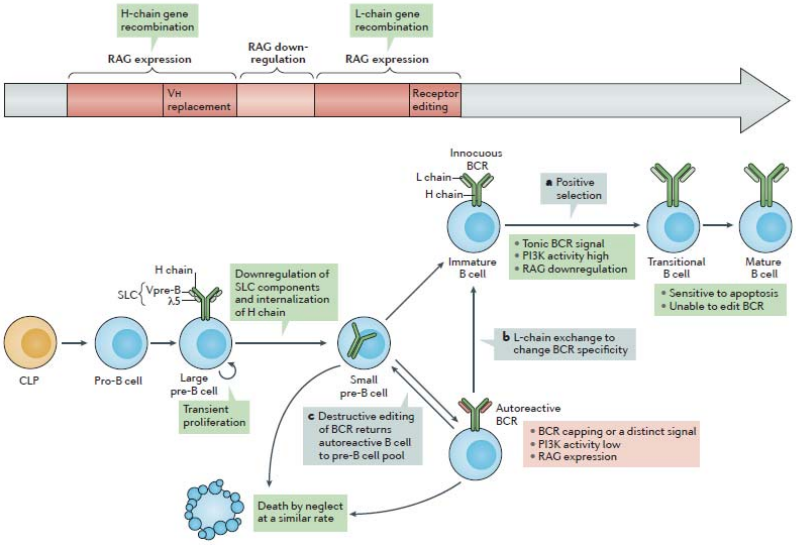

Figure 4.6. Cellular and molecular mechanisms involved in B cell development. Adapted with permission (Nemazee, 2017).

At this immature B cell developmental stage, BCRs, present in equilibrium as dimer or higher order complexes (Yang and Reth, 2010), can start interacting with antigens; concurrently, B cells undergo a selection process, involving receptor editing and clonal deletion, to preclude the expansion of self-reactive clones (Cambier *et al.*, 2007). After this stage, B cells can leave the BM as transitional B cells and acquire surface expression of IgD, together with substantial changes in the expression of other receptors (Chung, Silverman and Monroe, 2003).

4.3.2 Mature B cell development

Before encountering their cognate antigens, thus undergoing clonal proliferation and terminal differentiation into memory B cells and PCs, B lymphocytes can be referred to as naïve B cells. Transitional B cells (T1 and T2) undergo an additional round of negative selection in the spleen before becoming fully mature. A fraction of transitional B lymphocytes migrates to the splenic marginal zone and resides at the margin of the red and white pulp as non-circulating marginal zone B cells; conversely, the majority of B cells mature into follicular B cells, which continue circulating into the follicles within secondary lymphoid organs until they interact with their cognate antigen, thus undergoing further maturation steps (Shapiro-Shelef and Calame, 2005).

Mature B cells express the transcription factors PAX5, PU.1, interferon-regulatory factor 8 (IRF8), and BTB and CNC homologue 2 (BACH2) (Nutt *et al.*, 2015). Subsequent differentiation steps are not solely mediated by antigen-dependent BCR engagement, but, according to the "two-signal model", also require costimulatory signals. Therefore, based on antigen properties and on the nature of costimulatory signals, B cell activation can be defined either as T cell-independent (TI) or as T cell-dependent (TD).

BCR ligation by TI antigens, like lipopolysaccharide (LPS) – a type 1 TI antigen – or large molecular weight (MW) molecules with repetitive epitopes like phospholipids and polysaccharides – typical type 2 TI antigens (Mond *et al.*, 1995) –, together with costimulation by Toll-like receptors (TLRs) elicit rapid antibody responses without major histocompatibility complex (MHC) class II-restricted T cell help (Lebien and Tedder, 2008). Nevertheless, the breath and extent of a TI response, in terms of memory B cell restimulation capacity, lifespan and PC secretion ability, are considered to be modest (Defrance, Taillardet and Genestier, 2011).

Most B lymphocytes respond to TD antigens, consisting of polypeptides that can be processed and presented by antigen presenting cells (APCs) to T cells bound to MHC class II molecules; TCR ligation and binding of co-receptors and co-stimulatory molecules trigger activation and proliferation of T cells, which can activate their cognate B cells, allowing them to directly differentiate into PCs or enter germinal center (GC) reaction. In the GC phase, cycles of BCR diversification and antigen-driven selection support high-affinity memory B cells and PCs development and export (McHeyzer-Williams *et al.*, 2012).

TD responses are associated to secondary lymphoid organs, namely the spleen and lymph nodes, which, under pathogen-free conditions, contain follicles mainly composed of naïve B cells, known as primary follicles. Around 6 days after exposure to antigen, GCs develop within these B cell areas, creating secondary follicles. Multiphoton laser-scanning microscopy unveiled the dynamic nature of GCs, where B cells move constantly throughout the entire GCs and are continuously involved in short, dynamic contacts with T cells and antigen (Allen *et al.*, 2007).

GCs are the main site for affinity maturation through somatic hypermutation (SHM) – a stochastic process that introduces point mutations in the V region of H and L chains – and class-switch recombination (CSR) – a recombination event that changes the expression of the H chain C region–, ultimately generating the humoral memory compartment, consisting of long-lived memory B cells and high-affinity antibody-secreting PCs (Jacob *et al.*, 1991). As mentioned earlier, B cells can also attain an extrafollicular pathway, forming extrafollicular foci where they differentiate into short-lived PCs secreting low-affinity antibodies.GCs can be divided in a dark zone (DZ) and a light zone (LZ) (**Fig. 4.7**).

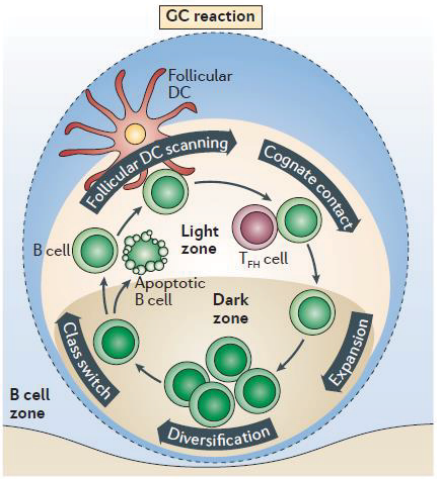

Figure 4.7. The iterative cycle of the GC reaction. The micro-anatomical architecture of GCs highlights the distinct molecular events occurring in the T cell zone-proximal DZ and in the T cell zone-distal LZ. Adapted with permission (McHeyzer-Williams *et al.*, 2012).

B lymphocytes in the context of the DZ, named centroblast, undergo extensive proliferation, SHM and CSR. After exiting the cell cycle, centroblasts become centrocytes and move to the LZ where they compete for antigen binding. Iterative cycles of DZ-LZ trafficking allow the generation and selection of high-affinity antibodies and ultimately regulate the clonal composition and the long-term immune function of humoral memory (McHeyzer-Williams *et al.*, 2012).

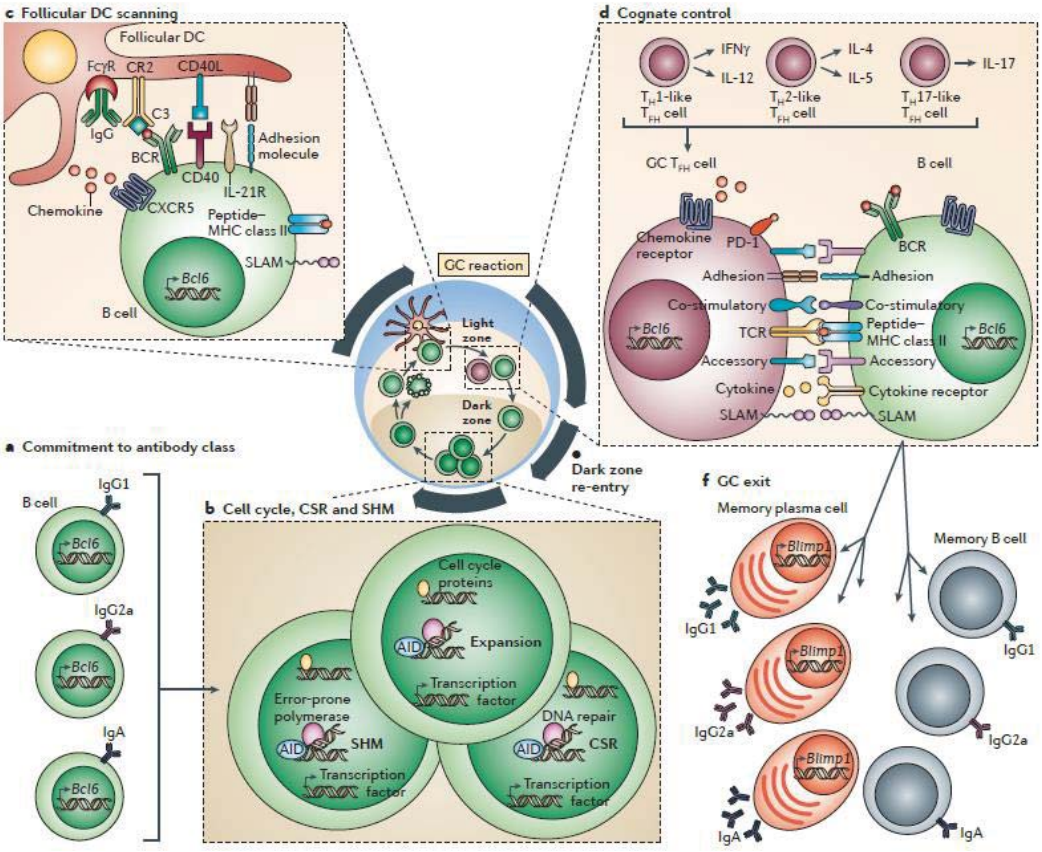

Figure 4.8. The evolution of B cell memory. Several distinct pathways, including FDCs scanning, cognate control by Tfh cells, the molecular control of cell cycle, BCR diversification via AID-mediated SHM and CSR, the commitment to antibody class and commitment to memory B cell or PC fate are involved in the evolution of B cell memory. Adapted with permission (McHeyzer-Williams *et al.*, 2012).

B cells are not the only components of GCs. Indeed, highly specialized subsets of T cells and stromal cells are crucial for efficient TD responses and the evolution of B cell memory (**Fig. 4.8**). The GCs architecture itself is closely linked to the molecular processes orchestrating affinity maturation.

Follicular dendritic cells (FDCs) are stromal cells forming a reticular network in primary follicles and especially in the LZ of GCs. FDCs play a dual role: on one hand they serve as antigen depot as they trap antigens on their surface in the form of immune complexes bound to complement receptors CD35 and CD21, previously known as complement receptor 1 and complement receptor 2. On the other hand FDCs secrete chemokines and cytokines that either guide homing to the GCs – like CXC-chemokine ligand 13 (CXCL13), the ligand for CXC-chemokine receptor 5 (CXCR5) – or sustain B cells survival within GCs – like Interleukin 6 (IL-6) and B cell Activating Factor (BAFF) (Aguzzi, Kranich and Krautler, 2014).

T cells represent a small fraction of the cells in GCs, but they are fundamental for GCs maintenance and for affinity maturation. Follicular helper cells (Tfh) are CD4+ T lymphocytes that, thanks to the expression of CXCR5, are able to home to B cell follicles, where they support B cell growth and differentiation through a combination of different stimuli. Not only they express Programmed Cell Death Protein 1 (PD-1) and the activation markers CD69 and inducible T-cell costimulatory (ICOS), but they also upregulate the expression of IL-21, B cell lymphoma 6 (BCL-6), a transcription factor instrumental for acquiring Tfh phenotype, CD40 ligand (CD40L), which by binding CD40 on B cell allows GC B cell proliferation, class-switch recombination and differentiation into memory B cells, and signaling lymphocytic activation molecule (SLAM)-associated protein (*SAP*) – an adaptor protein capable of modulating Tfh signaling. Recent data have suggested that Tfh are a highly heterogeneous T cell subset, comprising helper and regulatory cells, postulating a possible division of labor in GC B cell selection and elimination (Vinuesa *et al.*, 2016).

As for Tfh, also follicular B cells, through expression of CXCR5, can home to follicles within secondary lymphoid organs where they upregulate CC-chemokine receptor 7 (CCR7) expression, thus redirecting themselves to the margins of the outer T cell zone, sensing the gradient of CC-chemokine ligand 21 (CCL21). In the context of this location, follicular B cells upregulate BCL-6 and repress interferon regulatory factor 4 (IRF4) expression, and, through binding, internalization and processing of their cognate antigen, they can present a series of deriving peptides to Tfh cells, which can detect the same peptide as presented by a matching MHC class II molecule they had previously recognized on a dendritic cell (DC) or macrophage (Lanzavecchia, 1985).

Affinity maturation in GC reflects a series of local iterative rounds of Darwinian-like selection of high-affinity mutants produced by SHM (Lebien and Tedder, 2008). Indeed, B cells expressing a BCR with higher affinity will be able to outcompete those cells whose BCRs have lower affinity for antigen binding, leading to a feed-forward loop of efficient antigen presentation to Tfh, resulting in substantial T cell help to sustain B cell survival and differentiation; conversely, centrocytes characterized by self-reactive or low-affinity BCRs will be abrogated due to lack of T cell help resulting in the apoptosis of approximatively 50% of GC B lymphocytes every 6 hours, a mechanism that maintains GC homeostasis (Mayer *et al.*, 2017). However, recent studies unveiled how GC responses could be permissive to retain B cells harboring low affinity receptors (Kuraoka *et al.*, 2016; Tas *et al.*, 2016), showing that GCs can accommodate multiple B cells clones for extensive periods of time, instead of being rapidly conquered by a single dominant clone (Bannard and Cyster, 2017).

Exit from the GC entails either the acquisition of a memory phenotype, maintaining the B cell program gene regulators (including PAX5), or an additional differentiation step toward antibody-secreting cells (ASC), which is orchestrated by mechanisms not fully resolved yet but putatively dependent on antigen affinity (Smith *et al.*, 1997; Nutt *et al.*, 2015).

Memory B cells

Crucial functional features of memory B cells are their longevity and their fast and robust responsiveness to antigen re-exposure, which are the basis of the so-called "reactive humoral memory" (Kurosaki, Kometani and Ise, 2015): they can respond more rapidly than naïve B cells, and upon secondary encounter with antigen they show an extensive clonal expansion (Tangye *et al.*, 2003). However, despite post-GC memory B cells retain the expression of the BCR on their surface, memory B cells are not endowed with antibody secretion ability. Yet, it is acknowledged that memory B cells can directly contribute to short- and long-term humoral immune protection, by virtue of their proliferative capacity. On one other hand, memory B cell proliferative burst is required to expand the pool of antigen-specific cells and provides the tools needed to generate effector cells (Nutt *et al.*, 2015); on the other, all memory B cells, regardless of antigen presence, are able to proliferate at low rate generating PCs of all memory specificities (Traggiai, Puzone and Lanzavecchia, 2003).

Plasma cells

Several developmental pathways can lead to ASCs formation (**Fig 4.9**). B1 cells, a specialized subset mainly located in the peritoneal and pleural cavities and the gut lamina propria, is able to differentiate into ASCs either secreting natural antibodies in the absence of external antigen or secreting IgA in the gut. Additionally marginal zone B cells and follicular B cells, after interaction with antigens, can directly differentiate into ASCs, despite the lifespan of such PCs is generally short. Conversely, post-GC PCs can become long-lived if they reach suitable survival niches. In this scenario, it is still debated whether memory B cells and PCs fates derive from a single differentiation pathway or represent alternative fates of post-GC B cells (Shapiro-Shelef and Calame, 2005).

Despite the observation that continuous differentiation of memory B cells through bystander T cell signals and TLR9 stimulation by CpG-containing oligodeoxynucleotides could represent a mechanism to replenish and/or maintain memory and PCs in the absence of antigen exposure (Bernasconi, Traggiai and Lanzavecchia, 2002), at least some persistent antibodies are derived from long-lived PCs, independent of memory B cells and antigen (Manz *et al.*, 1998) and the BM

is generally the primary site for long-lived PCs survival (Slifka, Matloubian and Ahmed, 1995; Shapiro-Shelef and Calame, 2005).

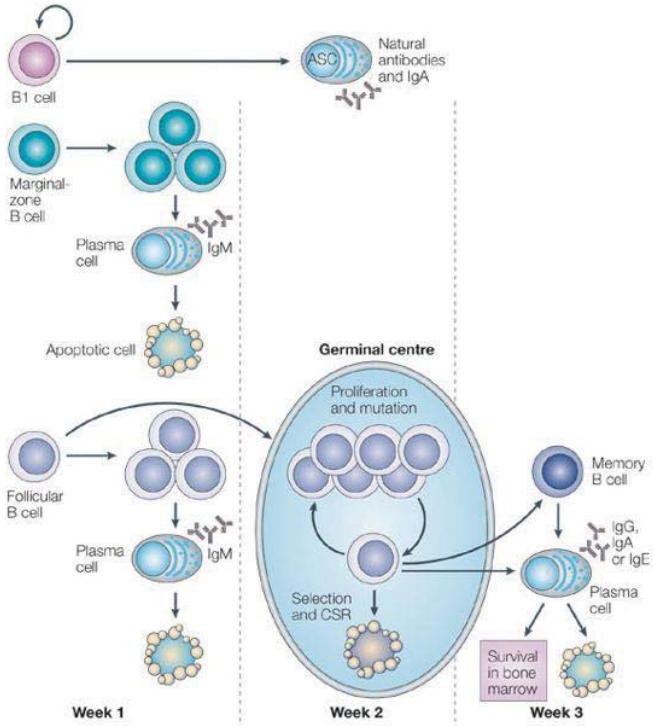

Figure 4.9. The formation of PCs. Adapted with permission (Shapiro-Shelef and Calame, 2005)

Despite the observation that continuous differentiation of memory B cells through bystander T cell signals and TLR9 stimulation by CpG-containing oligodeoxynucleotides could represent a mechanism to replenish and/or maintain memory and PCs in the absence of antigen exposure (Bernasconi, Traggiai and Lanzavecchia, 2002), at least some persistent antibodies are derived from long-lived PCs, independent of memory B cells and antigen (Manz *et al.*, 1998) and the BM is generally the primary site for long-lived PCs survival (Slifka, Matloubian and Ahmed, 1995; Shapiro-Shelef and Calame, 2005).

Short-lived plasmablasts express high levels of IRF4 and X-box-binding protein 1 (XBP1) and intermediate levels of B lymphocyte-induced maturation protein 1 (BLIMP1), while long-lived plasma cells express high levels of BLIMP1, IRF4 and XBP1 (Nutt and Kee, 2007). The expression of BLIMP1 by all PCs highlights their general pro-apoptotic tendency and involves the repressions of anti-apoptotic proteins, like BCL-2 family protein A1, and the expression of pro-apoptotic proteins, like C/EBP homologous protein (CHOP) (Shapiro-Shelef and Calame, 2005). Despite it is established that PCs also silence the cell cycle program, through BLIMP1-mediated repression of MYC, how short-lived cycling plasmablast differentiate to long-lived, post-mitotic

PCs is not fully understood (Nutt and Kee, 2007). In this regard, PCs longevity seems to be non-intrinsic and is thought to be dependent on several environmental factors that are able to mediate PC long-term survival.

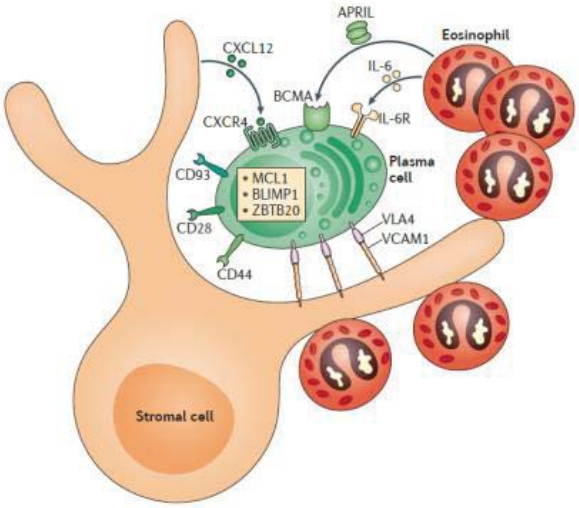

Figure 4.10. Model for the survival niche of BM PCs. Putative secondary components of the plasma cell niche, secreting PC survival factors are shown. Adapted with permission (Nutt and Kee, 2007).

ASCs enter the bloodstream after egressing secondary lymphoid organ thanks to the expression of sphingosine-1-phosphate receptor 1 (S1PR1). Signaling through different chemokine receptors guides ASCs homing to specific sites: activation of CXCR3 by inflammatory chemokines, such as CXCL9, CXCL10 and CXCL11 supports the homing to sites of inflammation, including non-lymphoid organs; conversely signaling through CXCR4 by CXCL12 ligation promotes recruitment and retention in the BM (Nutt *et al.*, 2015). Therefore, PCs survival niches can be located both in lymphoid organs, in non-lymphoid organs in disease conditions and in the BM (Slifka, Matloubian and Ahmed, 1995). PCs survival in the BM is tightly associated to microenvironmental structures known as "niches" that provide crucial trophic factors, namely IL-6, tumor necrosis factor (TNF) and a proliferation-inducing ligand (APRIL) (**Fig 4.10**). Several cellular lineages have been proposed as niche components, but there is a general agreement that CXCL12+ Vascular Cell Adhesion Molecule 1 (VCAM1) + stromal cells and eosinophils could be the most important components. Considering both that the number of BM niches is finite (Radbruch *et al.*, 2006) and the intrinsic pro-apoptotic tendency of PCs, the PCs repertoire in the BM is tightly regulated by complex competing circuits (Nutt *et al.*, 2015).

4.4 Generation of diversity in B lymphocytes

The unique identity and the distinctive properties of each amyloidogenic L chain derive from the huge diversity of possible Ig sequences that can arise from the recombination events occurring at the Ig loci during B cell development. In order to understand the origin of L chain diversity it is necessary to dig into the principles of the generation of diversity of the antibody repertoire.

4.4.1 V(D)J recombination

The remarkable diversity of the antibody repertoire and the resulting ability of antibodies to bind highly structurally-heterogeneous antigens derives from the site-specific recombination events occurring in developing B lymphocytes, named V(D)J recombination. Unlike C domains, V regions of antigen receptors, including BCR and TCR chains, are assembled from three different gene segments, namely the variable (V), the diversity (D) and the joining (J) segments (Bassing, Swat and Alt, 2002; Jung and Alt, 2004). V genes encode FR1, FR2, and FR3 together with CDR1, CDR2 and the N-terminal portion of CDR3, whose C-terminal portion is encoded by J genes, together with FR4. D segments are present only in the IgH locus and encode the central portion of the H chain CDR3.

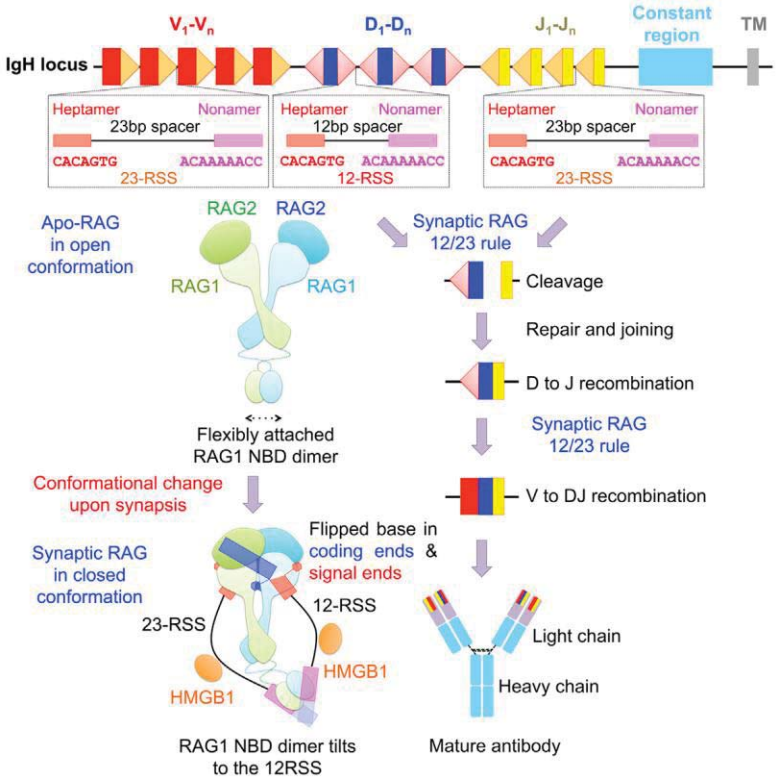

Figure 4.11 Schematic representation of V(D)J recombination mechanism. Shown are the 12-RSS and 23-RSS flanking V, D, and J segments. RAG conformational changes allow RSS-mediated synapses formation and cleavage, which are followed by repair and joining phases. Adapted with permission (Ru *et al.*, 2015).

The V(D)J recombination is tightly regulated in a lineage-, stage-, and allele-specific manner and requires a complex orchestration of several factors, including chromatin structure, transcriptional activation, DNA breakage and repair mechanisms (**Fig 4.11**) (Jung *et al.*, 2006).
V(D)J recombination is initiated by the action of an endonuclease complex, named RAG, composed of two subunits, the recombination-activating genes 1 and 2 (RAG1 and RAG2). RAG complex introduces DNA double-strand breaks (DSBs) at specific positions located between two coding segments and their flanking recombination signal sequences (RSs), which consist of a conserved heptamer and nonamer, separated by a spacer of either 12 or 23 base pairs (bp) (Fugmann *et al.*, 2000; Jung *et al.*, 2006). DSBs are repaired by ubiquitously expressed non homologous end joining (NHEJ) machinery (Rooney, Chaudhuri and Alt, 2004), which creates imprecise joints at the coding ends, where non-germline-encoded nucleotides (N nucleotides) are randomly added by the enzyme terminal deoxynucleotidyl transferase (TdT) (Schroeder *et al.*, 2010).

4.4.2 The pre- and post-immune antibody repertoire

V(D)J recombination is estimated to lead to the generation of 10^{16} Igs in naïve B lymphocytes, due not only to the potential rearrangements of all the functional Vκ genes to Jκ genes, Vλ to Jλ genes and VH to DH to JH genes, but also to the pairing of any produced H chain with any L chain. Additionally, several mechanisms can contribute to further diversify Ig repertoire, such as the insertion of N-nucleotides by TdT, the rearrangement of D genes by inversion or deletion and their possible translation in three different reading frames, the formation of palindromic sequences to solve hairpin structures deriving from gene rearrangement and the loss of terminal nucleotides at the site of rearrangement (Schroeder *et al.*, 2010).

In mature B cells the Ig repertoire breath can also be substantially broadened by SHM, which introduces point mutations at an extremely high rate in mutational hotspots of the V domain, especially in the CDRs. SHM, combined to GC affinity-based selection, increases the range of affinity through which low-affinity germline rearrangements can bind antigenic determinants, thus contributing to affinity maturation. SHM relies on two phases: the introduction of mismatches by the enzyme activation-induced deaminase (AID) their subsequent error-prone repair.

During transcription, stalled RNA Polymerase II and associated factors recruit AID to target sites, where it can deaminate cytidines (C) into uridines (U) in single-strand DNA-bubbles, generating G:U mismatches that can be processed by alternative mechanisms. In “phase 1” mutations U can either be interpreted as T leading to a C-to-T transition in one of the daughter cells, or it can be excised by a uracil DNA N-glycosylase (UNG), creating an abasic site, then repaired through

short-patch base excision repair (BER), where error-prone polymerases lead to transitions and transversions to any of the four bases at the abasic, nicked site. Conversely, in "phase 2" mutations the mismatch-repair (MMR) machinery recognizes the U:G mismatch and the U-containing strand is excised and repaired by error-prone polymerases, like DNA polymerase η, creating transitions and transvertions also in neighboring G:C and (preferentially) A:T base pairs. In order to avoid aberrant and untargeted mutations, AID activity is strictly regulated by both transcription factors (like PAX5) and microRNA (miRNA) (like miR155 and miR181b), ensuring that AID is highly expressed only in GC-B cells properly activated by Tfh and FDCs. In addition, it has been demonstrated that AID tends to act on specific target regions, preferentially deaminating C within WRC motifs (W = A/T, R = A/G) (Laffleur *et al.*, 2013).

AID also plays a foremost role in another Ig diversification mechanism, CSR, which is made possible by the organization of the IgH locus, where a switch (S) region is located upstream each CH gene (each encoding for a different IgH class, therefore named Cμ, Cγ, Cα and Cε. AID activity on transcriptionally active S regions and subsequent processing of U bases generates DNA DSBs in the upstream (donor) and downstream (acceptor) S region, which are resolved by NHEJ culminating in the deletion of the intervening DNA as an extrachromosomal switch circle and the formation of a S-S junction, connecting the downstream CH region with the V-D-J rearranged gene. AID-mediated CSR is dependent on the combination of primary and secondary stimuli: primary stimuli (CD40-CD40L interaction) induce AID expression, whereas secondary stimuli (specific cytokines) guide CSR to specific isotypes by inducing the transcription through the acceptor S region of sterile RNAs (germline transcripts) (Xu *et al.*, 2012).

4.5 Quality checkpoints of humoral immunity

The above mentioned diversification mechanisms are essential to generate a broad germline (GL) repertoire of rearrangements, which can undergo additional fine-tuning through affinity maturation; nevertheless, they can also increase the probability of generating proteins that can aberrantly interact with self molecules or that cannot even fold correctly. For these reasons, sustained expression of a repertoire of protective, correctly assembled and non-self-reactive antibodies relies on tightly regulated mechanisms (Nemazee, 2017), among which the quality-control system of the ER and the unresponsiveness to self antigens, known as tolerance, play a crucial role (Feige, Hendershot and Buchner, 2010). In the next paragraphs I will firstly delineate the process and the regulation of antibody folding and subsequently I will describe the mechanisms underlying immunological tolerance.

4.5.1 Antibody folding

Expression of properly folded, secretory Igs is regulated at several levels. At the transcriptional level, BLIMP1 and XBP1 are required for Ig secretion. BLIMP1 represses PAX5 expression, thus de-repressing H and L chain transcription, and induces expression of IRF4, which activates L chain loci enhancers, and of octamer-binding transcription factor (OCT)-binding factor 1 (OBF1), which can activate a 3' enhancer of the H chain locus and some κ-locus promoters. Additionally, BLIMP1, regulating a differential polyadenylation, splicing and polymerase pausing, is able to dictate the switch from the expression of the membrane isoforms of IgM to the expression of its secreted isoform. Also XBP1 is fundamental for PCs secretory programme and is induced by BLIMP1-dependent PAX5 repression, IL-4 and activating transcription factor 6 (ATF6) (Shapiro-Shelef and Calame, 2005).

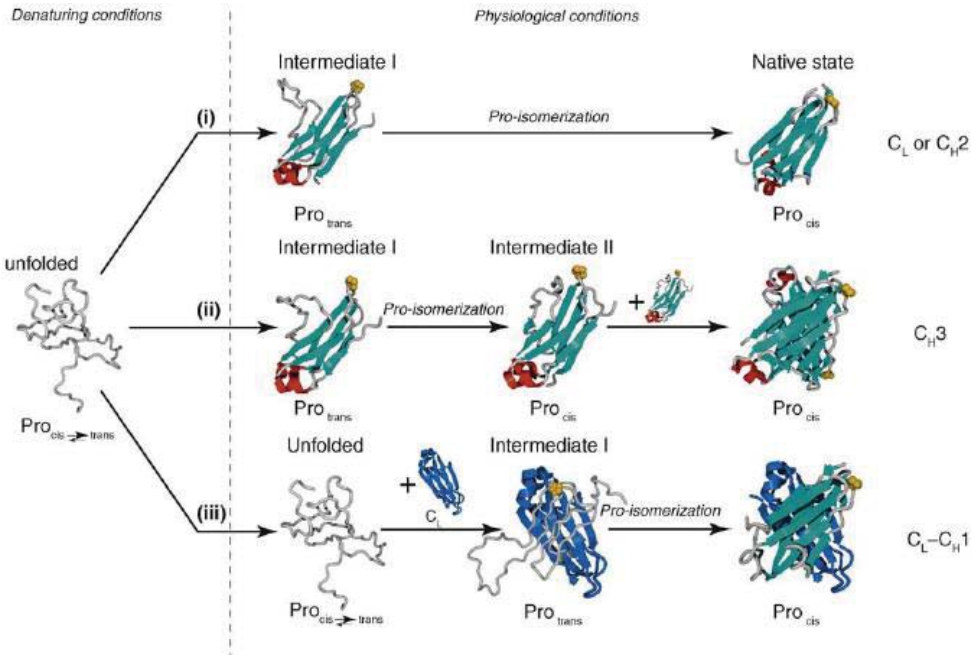

Figure 4.12 Distinct folding pathways of antibody domains. **i,** CL and CH2 fold via a highly structured intermediate, whose limiting folding step is represented the isomerization state of the proline residue (yellow) in the b-c loop, whereas the helical moieties and the core β structure are already formed. **ii,** CH3 is an obligate dimer, which folds through two intermediates; the critical isomerization of b-c loop proline residue (yellow) allows the formation of the CH3 dimer, which can then complete its folding. **iii,** The CH1 domain forms a loosely folded intermediate even in association with CL. The critical isomerization of the b-c proline residue (yellow) can take place at this stage, leading to the native state and to the formation of the interchain disulfide bridge between the two domains. Adapted with permission (Feige, Hendershot and Buchner, 2010).

It is acknowledged that H and L polypeptides chains are co-translationally translocated to the ER, where the folding of Igs occurs. Despite the Ig domains of H and L chains present highly similar structures and the slow proline isomerization reactions represent a rate-limiting step for the

folding of both chains, they fold following different pathways (**Fig. 4.12**). CL and CH2 domains are able to reach autonomously a monomeric state and a crucial folding step is represented by the formation of the internal disulphide bond between strand b and f, which favors the clustering of the hydrophobic core of the protein, thus facilitating the formation of a folding nucleus and preventing unproductive conformations. In this regard, the short CL α-helical moiety and the CH2 N-linked glycans have been suggested to promote, at least to some extent, the domains folding and are absent in Ig domains, like the VL domain, which are less foldable and more prone to aggregation (Qin *et al.*, 2007; Feige, Hendershot and Buchner, 2010). The CH3 domain folds following a distinct pathway, where a critical proline isomerization generates a folding intermediate, which can homo-dimerize to fulfill its folding. Conversely, the CH1 domain relies on a template-assisted mechanism to overcome a folding barrier, dictated by its intrinsically disordered nature (Feige *et al.*, 2009). Indeed, CH1 domains can initiate the rate-limiting proline isomerization only after association with CL domains.

The three distinct folding pathways characteristic of each antibody Ig domain emphasize that, despite a very similar domain topology, each Ig domain is intended for a different purpose: CH3 domains guide via non-covalent interactions Fc fragment dimerization, which is then stabilized by disulphide bridges within the hinge region, while CH1 domains represent quality-control sensors for the quaternary structure assembly (**Fig. 4.13**) (Feige, Hendershot and Buchner, 2010).

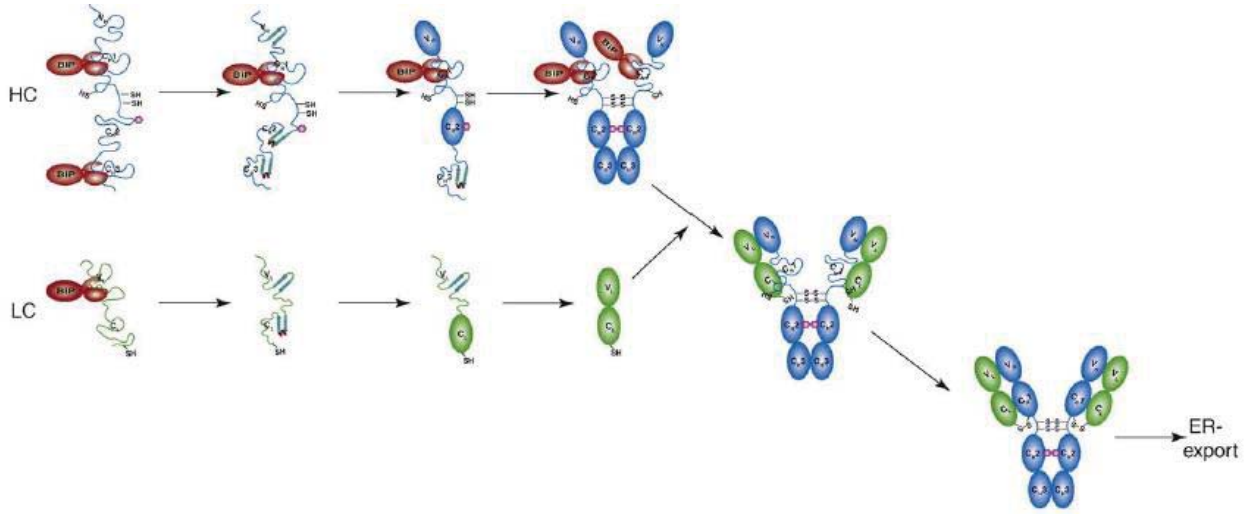

Figure 4.13 The folding of the distinct Ig domains guides antibody assembly. Folding and assembly of antibodies occurs in the ER, where all Ig domains interact transiently with the chaperone BiP (red). CH3 folding induced antibody dimerization, which is strengthened by intermolecular disulphide bridges formation at the hinge region. However, CH1 remains unfolded, unoxidized and tightly bound to BiP until an already folded L chain (green) displaces BiP, thus inducing the correct folding of CH1 domain. Only at this stage, the critical b-c proline

isomerization can occur, followed by the formation of an intermolecular disulphide bridge between CH1 and CL. Adapted with permission (Feige, Hendershot and Buchner, 2010).

In this regard, two layers of stringent quality checkpoints, consisting of the ER quality machinery control and of a signaling feedback provided only by folded, secreted protein monitor antibody integrity by sensing CH1 folding during B cells development and differentiation to PCs. The ability of CH1 domains to fold properly is firstly assessed by assembling with their L chain counterpart in pre-B cells where the rearranged H chain assembles with SLCs and subsequently by assembly with rearranged L chains in mature B cells; in both cases only a proper pairing will allow folding and transport to the cell surface of a pre- BCR or a BCR able to convey proper signals. Conventional H chains unable to associate with L chains are retained and degraded in the ER, whereas truncated H chains, lacking the CH1 domain, can dispense with L chain association and can be secreted as camel-like antibodies typical of a rare B cell lymphoproliferative disorder known as heavy chain disease (Seligmann *et al.*, 1979).

Not only the ER provides crucial assistance for folding, but it also monitors the maturation of nascent secretory proteins, assessing whether a protein is able to reach its native state and can proceed along the secretory pathway or cannot fold properly, thus needing to be retained and eventually retro-translocated to the cytoplasm where it will be degraded through ER-associated degradation (ERAD) by the 26S proteasome. Due to the burden of intensive antibody production, all B cells, and PCs in particular, experience continuous ER-stress and therefore rely stringently on the unfolded-protein response (UPR) to overcome it. A “physiologic” UPR is activated in PCs by an increased expression of H chains, which leads to processing of XBP1 mRNA by a protein kinase with endoribonuclease activity, inositol-requiring 1 α (IRE1α), thus creating an active isoform of XBP1. XBP1 induces the expression of UPR-associated genes that are involved in an array of functions, namely decreasing protein synthesis, enlarging the ER and increasing the ER ability to fold and translocate proteins (Shapiro-Shelef and Calame, 2005).

A crucial chaperone required for Ig folding is the Ig binding protein (BiP), the ER ortholog of Hsp70 family chaperones, which does not interact with fully assembled antibodies (H-L heterotetramers) but is able to interact transiently with Ig domain assembly intermediates (Haas and Wabl, 1983), retaining them until properly folded by virtue of its C-terminal ER-retention signal sequence KDEL (**Fig. 4.13**). As mentioned, Ig domains can attain different folding schemes and, despite all possessing BiP binding sites (Knarr *et al.*, 1995), they rely on BiP association accordingly: the CL domain are able to fold rapidly without requiring BiP association, while VL, VH, CH2 and CH3 domains are transiently bound by BiP, which, conversely, tightly binds CH1

domains until fully folded LCs (both in their VL and CL domains) assemble with the CH1 domain, displacing BiP (Feige, Hendershot and Buchner, 2010).

4.5.2 Immunologic tolerance and fate of autoreactive B cells

The antibody repertoire of each individual is generated by antigen-driven selection and subsequent fine-tuning of available antibody rearrangements. On one hand the diversification mechanisms occurring at the Ig loci, spanning from V(D)J recombination to SHM, are instrumental for the generation of a vast pool of Igs, on the other only BCRs that encountered and interacted with sufficient strength with their cognate antigens can lead to BCR signaling, clonal expansion and commitment to the memory or PC fate. It is straightforward that, in the absence of suitable control mechanisms, B cells binding to self-antigens could be constantly selected, leading to deleterious effects, emphasizing the fundamental role of antigen-driven selection and of the tolerance mechanisms aimed at hindering harmful responses to host tissues.

Given that antibody gene recombination events proceed randomly, it was demonstrated that more than 50% of BCRs assembled during B cell development are self-reactive (Wardemann *et al.*, 2003); therefore, specific tolerance mechanisms ensure that self-reactive clones are either abrogated, rescued by editing or made unresponsive and grant that the secondary repertoire generated through SHM is devoid of auto-reactivity (Brink, 2014; Nemazee, 2017). By virtue of the combination of these mechanisms most mature B cells – approximatively the 95% of them – lack self- or poly-reactivity (Wardemann *et al.*, 2003; Kara and Nussenzweig, 2018).

Immune tolerance mechanisms work at various B cell developmental stages and can be roughly divided in central and peripheral tolerance. The term central tolerance refers to the regulatory mechanisms occurring in mature IgM+ B cells in the BM, while peripheral tolerance involves regulatory checkpoints in the spleen, lymph nodes and other tissues. BCR signaling plays a foremost role in both immune tolerance mechanisms.

Central tolerance

Central tolerance checkpoints take place in the BM and stringently rely on BCR ability to signal in different ways (Monroe, 2006).

In pre-B cell development several feedback mechanisms select for cells expressing exactly one functional H chain and prevent the survival of cells lacking any H chain thanks to the association to SLCs creating a pre-BCR; subsequently, a correct L chain rearrangement allows the formation of a functional IgM BCR. In their unligated forms both the pre-BCR and the BCR convey a tonic signal that is crucial for B cell survival. Specifically, it has been shown that the pre-BCR is able to

convey spontaneous signals due to self-aggregation or interaction with invariant host antigens, thus resembling self-reactive BCRs. Additionally, it has been suggested that only intermediate strength of unligated-BCR signaling could allow positive selection and promote developmental progression, guiding B cell maturation and migration to peripheral lymphoid organs. At the molecular level, in immature B cells unligated BCR promotes PI3K signaling via SYK- and SFK-mediated tonic phosphorylation of CD19 cytoplasmic tail and BCAP adaptor protein, leading to $PtdInsP_3$ formation, which is able to activate AKT. AKT in turn phosphorylates the transcription factor forkhead box protein O1 (FOXO1), thus sequestering it from the nucleus and leading to RAG genes downregulation and B cell survival via the transcription factor MYC. Alternatively, positive selection can be guided by low levels of RAS activation, which, together with activation of the ERK pathway, can restore impaired tonic BCR signaling and rescue immature B cell differentiation (Nemazee, 2017).

Conversely, if H-L chain pairing is inefficient or BCR expression is too low, lack of BCR signaling implies B cell failure to mature and induces apoptosis; insufficient positive selection signal retains B cells in a developmental arrest state with a limited lifespan of approximatively 3 days, during which additional rearrangements at the L chain locus could occur. In the same line, BCR ligation by BM-resident antigens could lead to receptor editing or apoptosis. In detail, BCR ligation, via transient activation of the BLNK pathway, leads to downregulation of surface IgM, a condition which resembles the low surface BCR expression of pre-B cells and, reducing PI3K signaling, supports nuclear localization of FOXO1, RAG-dependent L chain recombination and consequently receptor editing; unsuccessful BCR editing will result in cell starvation, developmental arrest, inability to home to secondary lymphoid tissues due to lack of CD62 ligand (or L-selectin) expression (Hartley *et al.*, 1993) and eventually cell death after approximatively 3 days, driven by the pro-apoptotic protein BIM.

Receptor editing is a directional phenomenon, progressing from upstream to downstream Jκ elements on the κ locus, before continuing on λ L chain locus. Receptor editing efficiency is remarkable (Halverson, Torres and Pelanda, 2004) and allows several editing attempts in a limited time, substantially contributing to the usage of less efficiently rearranged genes and of λ L chain genes, hence supporting antibody repertoire diversity. Occasionally, B cells can express more than one L and H chain leading to the so called allelic inclusion, a crucial mechanism that, by diluting an aberrant BCR on the B cell surface, allows the generation of polyreactive cells able to escape clonal selection (Wardemann and Nussenzweig, 2007; Basten and Silveira, 2010).

Globally, central tolerance mechanisms prevent the development of B cells lacking a functional BCR and limit the frequency of B cells harboring self-reactive rearrangements (Nemazee, 2017). However, central tolerance checkpoints are partial, especially because not all self-antigens are accessible in the BM; therefore additional tolerance mechanisms are required to ensure the abrogation of autoreactive B lymphocytes in peripheral tissues.

Peripheral tolerance

Peripheral tolerance regulates activation and survival of B lymphocytes, after their egress from the BM via distinct reversible mechanisms, such as anergy (Goodnow *et al.*, 1988), BCR desensitization, tolerance to antigens via sialic acid-binding immunoglobulin-like lectin (Siglec) inhibitory receptors (Duong *et al.*, 2010). Also in the context of peripheral tolerance the strength of BCR signaling plays a foremost role. In the absence of T cell help or TLR costimulation, BCR engagement with moderate to high affinity by antigens, like membrane molecules or soluble, highly repetitive antigens, favors clonal deletion through a BIM-dependent pathway (Basten and Silveira, 2010). Conversely, low avidity BCR ligation triggers anergy or ignorance. Anergic B lymphocytes are characterized by dramatically reduced BCR surface expression, desensitization of BCR signaling leading to low responsiveness, failure to efficiently present antigen and produce antibody. At the molecular level, anergy results from reduced activation of the kinases downstream of BCR, leading to poor activation of NF−κB, culminating in downregulation of pro-survival factors like BCL-2 and upregulation of pro-apoptotic factors like BIM; additionally, inhibitory receptors such as CD5 can further dampen BCR signaling via their intracellular inhibitory motif (ITIM), which can recruit tyrosine and lipid phosphatases like SH2-domain-containing protein tyrosine phosphatase 1 (SHP1) and SH2-domain-containing inostil-5-phosphatase (SHIP), thus increasing the threshold required for B cell activation (Hippen, Tze and Behrens, 2000; Ravetch and Lanier, 2000; Goodnow *et al.*, 2005). Anergic IgM-IgDhi B cells subsets, which have been identified also in humans (Duty *et al.*, 2009), are usually short-lived, more difficult to activate than non-autoreactive B cells (Goodnow *et al.*, 1988), and are usually excluded from B cell follicles. Hence, anergic B cells are at disadvantage for GC entry, but, upon strong receptor cross-linking by high affinity, multivalent antigens and suitable co-stimulation, can undergo positive selection, enter GCs and experience affinity maturation (Cambier *et al.*, 2007; Basten and Silveira, 2010). In this context, SHM can also edit self-reactive BCRs in a process named “receptor revision” (Burnett *et al.*, 2018), consisting of the expansion of clones capable of acquiring mutations that were simultaneously able to reduce affinity to self and increase affinity to foreign antigens (Kara and Nussenzweig, 2018), further highlighting that the reversibility of peripheral tolerance mechanisms allows the maintenance of autoreactive B cells

that could respond to invading pathogens carrying epitopes that are similar to the self-antigens ones (Klinman, 1996; Nemazee, 2017).

Autoreactive cells recognizing tissue-specific or intracellular antigens, such as nucleic acids released in the GC after apoptosis of negatively selected centrocytes, can survive as normal follicular B cells in a state known as clonal ignorance. To prevent the development of autoimmunity, such cells receive inhibitory signals through Siglec-2 (CD22) and sialic acid acetyl esterase (SIAE) (Duong *et al.*, 2010) to counteract TLR stimulation by the nucleic acid itself (TLR9 sensing CpG-containing DNA and DNA-associated autoantigens and TLR7 interacting with single-stranded RNA and RNA-associated autoantigens) (Leadbetter *et al.*, 2002; Lau *et al.*, 2005), which could favour autoreactive B cell activation and production of anti-nuclear antibodies as observed in patients affected by systemic lupus erythematosus (SLE) (Detanico *et al.*, 2013).

In addition to pre-immune autoreactive rearrangements, SHM can also be responsible of the generation of self-reactive B cells (Shlomchik *et al.*, 1987), which have been identified at high frequencies in the serum of healthy individuals (Tiller *et al.*, 2007) and kept in check by regulatory mechanisms, suggesting that GC self-tolerance is not an absolute concept.

4.6 Systemic immunoglobulin Light Chain Amyloidosis (AL amyloidosis)

AL amyloidosis can be defined as a protein misoflding disease arising from an underlying PC malignancy. In order to give a comprehensive introduction on AL amyloidosis, I will firstly provide an overview of the B cell malignancies usually related to AL amyloidosis and subsequently I will describe in detail the biology and the structural features of free L chains. I will conclude with a synopsis of the current understanding of AL amyloidosis pathophysiology, focusing on the areas of current research.

4.6.1 B cell malignancies

Late B cell differentiation represents a prominent source of lymphoproliferative disorders and, unsurprisingly, many of the chief transcriptional regulators of B cell terminal differentiation are also involved in several lymphomas and in PCs disorders, like BCL-6 and PAX5, which are often dysfunctional or translocated to the Ig H chain locus. Production of abnormal amounts of Igs by an expanded B cell o PC clone results in a series of conditions globally known as monoclonal gammopathies. The overproduced monoclonal Ig (M-component), which is not associated to a response to an offending immunogen, can be recognized as a band of restricted migration via serum or urine electrophoresis and can be attributed to full length Igs of different isotypes or to monoclonal free L chains, named Bence Jones proteins (BJ).

Monoclonal gammopathies result from dysregulated proliferation of B cells, often deriving from abnormal GC reactions, as seen in leukemias and lymphomas; contrariwise, if the disease originates from a PC line, the condition is known as PC dyscrasia (Attaelmannan and Levinson, 2000; Nutt *et al.*, 2015).

Due to the high proliferation of GC B lymphocytes and the expression of AID, both of which are DNA-altering processes, different types of lymphomas resemble unique stages of B cell maturation, in which multiple pathways are hijacked leading to malignant transformation (Basso and Dalla-Favera, 2015; Nutt *et al.*, 2015). Burkitt lymphomas present molecular characteristics analogous to DZ B cells, where MYC is ectopically expressed and PI3K signaling is altered; conversely, GC B cell-like diffuse large B cell lymphoma (DLBCL) and follicular lymphoma resemble LZ B cells, which are characterized by ectopic expression of BCL-2 and/or MYC; activated B cell-like DLBCL bears molecular characteristics of plasmablasts committed to PCs differentiation and is characterized by inactivation of the gene encoding BLIMP1 (Basso and Dalla-Favera, 2015).

Conversely, PC dyscrasias are an heterogeneous group of disorders characterized by the presence of an M-component, also known as monoclonal paraprotein, and a monoclonal PC population in the BM or, rarely, in other districts. PC dyscrasias include monoclonal gammopathy of undetermined significance (MGUS), multiple myeloma (MM), lymphoplasmacytic lymphoma/Waldenström macroglobulinemia (LPL/WM), POEMS syndrome (Polyneuropathy, Organomegaly, Endocrinopathy, Monoclonal protein, and Skin changes) and AL amyloidosis (Castillo, 2016). AL amyloidosis can occur in combination with any of the above mentioned PC disorders.

MGUS is a clinically asymptomatic pre-malignant PC or lymphoplasmacytic disorder, characterized by a prevalence of 4% in Caucasians over the age of 50. Non-IgM MGUS patients usually progress at average rates of 1% to MM and, in smaller proportions, to other disorders like AL amyloidosis, while IgM MGUS patients usually progress to chronic lymphocytic leukemia, lymphoma, lymphoplasmacytoma and WM (Kuehl and Bergsagel, 2012; Castillo, 2016).

MM is a PC disorder characterized by an increased number of monoclonal PCs, referred to as plasmacytoma, in multiple sites of the BM. PCs usually represent less than 4% of total BM cells, whereas MM patients present more than 30% PCs infiltrate in the BM. Compared to normal BM PCs, MM PCs retain a low rate of proliferation of approximatively 1-3% cycling cells and are phenotypically described as CD38+ CD138+, usually CD19– and CD45–, and and mostly

CD56+ (Pérez-Persona *et al.*, 2007). Excluding approximatively 5% of cases, in which the abnormal clone does not secrete Igs, the malignant clone secretes high amounts of M-protein, which is represented by somatically hypermutated, isotype switched IgG or IgA antibodies, while IgM is expressed by only approximatively 1% of tumors (Attaelmannan and Levinson, 2000). MM is considered a mostly incurable disease, due to the extensive organ damage, which includes anemia, lytic bone lesions, immunodeficiency and reduced renal function (Kuehl and Bergsagel, 2012).

MM is preceded by a pre-malignant precursor tumor and is characterized by the presence of defined disease stages. Indeed, symptomatic MM is preceded by MGUS (Landgren *et al.*, 2009), a condition which is clinically different from MM due to the absence of end-organ damage, the reduced levels of M-component and the presence of less than 10% BM mononuclear cells. An intermediate, still asymptomatic, condition is represented by smoldering myeloma, which can progress to symptomatic MM with a frequency of 10% per year. The genetic events leading to MM have been classified in three phases: a first set of genetic events including IgH translocations, hyperdiploidy and chromosome 13 deletions (del13), leading to cyclin D (CCND) dysregulation are typical of MGUS; phenomena like increased MYC expression and KRAS mutations are usually associated to the transition from MGUS to MM, while MM progression is generally linked to late MYC rearrangements involving an Ig locus, deletions of tumor protein 53 (TP53), inactivation of retinoblastoma protein (RB1) and activation of the NF-κB pathway (Kuehl and Bergsagel, 2012). Moreover, BLIMP1 is frequently mutated in MM, together with XBP1 and IFR4 (Leung-Hagesteijn *et al.*, 2013; Lohr *et al.*, 2014), the latter being suggested to be fundamental for MM cells survival through "non-oncogene addiction" (Shaffer *et al.*, 2008; Nutt *et al.*, 2015). In MM patients, as observed in healthy individuals, κ L chains are usually more represented, with a λ/κ ratio of approximatively 1:2 (Kyle and Gertz, 1995).

LPL/WM is a rare B-cell disorder characterized by the malignant expansion of clonally related B cells, lymphoplasmacytic cells, and PCs in the BM or in other body districts. The production of monoclonal IgM by WM clones can be associated to hyperviscosity syndrome, type I or II cryoglobulinemia, which are causative agents of vasculitis, Raynaud syndrome and peripheral neuropathy (Attaelmannan and Levinson, 2000; Castillo, 2016). More than 90% of LPL/WM patients are characterized by Myeloid differentiation primary response 88 (MYD88) L265P mutation, which is also present in IgM MGUS patients.

POEMS syndrome is a rare B cell dyscrasia characterized by highly variable clinical manifestations and a more indolent clinical course compared to MM, usually involving peripheral

neuropathy, organomegaly, endocrine deficiency, monoclonal gammopathy, and skin pigmentation (Miralles, O'Fallon and Talley, 1992).

4.6.2 Free L chains: synthesis, folding and metabolisms

Increased levels of free L chains, the causative agent of AL amyloidosis, are frequently observed in PC disorders (Perfetti *et al.*, 2012). The secretion of free L chains by normal and malignant B cells revolves around the mechanisms underlying antibody production. As anticipated in the previous sections of this thesis, the folding of the intrinsically-disordered CH1 domain (Feige *et al.*, 2009) in association with the L chain CL domain is seen a critical focus of quality-control mechanisms during the B cell development, culminating in H chains retention in the ER and consequent degradation unless properly assembled with L chains (Feige, Hendershot and Buchner, 2010). To ensure that PCs, which have been predicted to synthesize more than 100 antibody molecules per second (Hendershot and Sitia, 2003; Feige, Hendershot and Buchner, 2010), do not secrete misassembled domains unable to interact properly with their specific antigen or perform effector functions, there is a 40% overproduction of L chains compared to H chains (Mian, Bradwell and Olson, 1991). Considering that most L chains fold freely and can be secreted as such (Dul *et al.*, 1996; Leitzgen, Knittler and Haas, 1997), around 500 mg/day of polyclonal free LCs are released into the circulation (Waldmann, Strober and Mogielnicki, 1972; Solomon, 1985; Basnayake *et al.*, 2011). Free L chains are kept at levels as low as 3.3 to 19.4 mg/L and 5.71 to 26.3 mg/L for κ and λ L chains respectively (Lavatelli *et al.*, 2011), as they are primarily removed by catabolism in proximal tubular epithelial cells and, under physiological conditions, their serum half-lives are 2–4 h and 3–6 h, for κ and λ L chains respectively (SOLOMON *et al.*, 1964; Miettinen and Kekki, 1967; Wochner, 1967; Basnayake *et al.*, 2011). Uptake occurs at the brush border (Nielsen and Christensen, 2010; De Matteis *et al.*, 2017) through rapid and saturable megalin–cubilin receptor-mediated endocytosis in clathrin-coated pits, which provides a highly efficient physiological mechanism for conserving amino acids and essential protein-bound molecules (Batuman, Dreisbach and Cyran, 1990; Batuman and Guan, 1997; Batuman *et al.*, 1998; Klassen *et al.*, 2005; Basnayake *et al.*, 2011).

4.6.3 Introduction on AL amyloidosis

Only in some circumstances free L chains have been described to be able to lose their native conformation and aggregate over several years into amyloid fibrils (Merlini and Stone, 2006), giving rise to AL amyloidosis, an hematologic protein conformational disorder whose distinctive feature is the systemic stromal deposition of BM-derived monoclonal L chains in form of amyloid fibers, which tend to display a predominant organ tropism, including kidney, heart, liver,

gastrointestinal tract, soft tissue and peripheral nervous system (Perfetti *et al.*, 2012). The incidence of AL amyloidosis is still difficult to estimate due to the lack of extensive population studies, but studies performed in Europe and in the United States have estimated AL amyloidosis incidence to be between 10-12.5 individuals per million persons per year (Kyle *et al.*, 1992; Duhamel *et al.*, 2017). The main risk factor for developing AL amyloidosis is a pre-existing monoclonal gammopathy; indeed, the risk of developing AL amyloidosis in patients affected by MGUS is much higher compared to individuals without MGUS and approximatively 1% of MM patients are estimated to develop AL amyloidosis (Madan *et al.*, 2010). Based on the cohorts assessed, AL amyloidosis has been reported in 10-15% or 38% of patients with MM (Merlini *et al.*, 2018)

The amyloidogenic clone, producing λ L chains in 75-80% of the cases (Merlini *et al.*, 2018), is usually indolent (Merlini and Stone, 2006) and of small size, with a median PC infiltration of 7% (Obici *et al.*, 2005), even if, not uncommonly, PCs infiltration can be greater, even up to 30% of the total BM cellularity, but usually no signs of MM (anemia, hypercalcemia, bone lesions, progressive increase in PC number) are described (Perfetti *et al.*, 2012). In parallel to the increased production of free L chains by the progressively-expanding malignant PC clone, also the reduction of L chains renal catabolism occurring in the context of severe kidney disease can increase serum free L chains levels, which can in turn be responsible for enhanced renal failure through binding and subsequent co-aggregation with Tam Horsfall Protein (THP), obstructing flow through the renal tubule (Sanders and Booker, 1992; Huang *et al.*, 1993; Huang and Sanders, 1997). In severe renal failure, the reticuloendothelial system becomes the main route of removal of free L chains and their serum half-life increases to 32 hours or more (Miettinen and Kekki, 1967; Basnayake *et al.*, 2011), further sustaining free L chains serum levels. Recently, it was shown that patients with AL amyloidosis have a monoclonal L chains component up to 10 years before clinical presentation, supporting the notion that prolonged and sustained production of amyloidogenic L chains results in the development of AL amyloidosis (Weiss *et al.*, 2014).

4.6.4 L chains structural features

From the structural perspective, in line with pioneering high resolution X-ray structures (Schiffer *et al.*, 1970), free L chains are characterized by the Greek key barrel fold typical of all Igs, which is composed of nine and seven β-strands for the VL and CL domains respectively. Four and five (three for the CL domain) β-strands combine to form two β-sheets that pack together, thanks to a conserved disulphide bridge and hydrophobic moieties located at the interface between the two β-sheets, like a Tryptophan in position 35. The β-strand G, the last strand of the VL domain, is

encoded by the J gene, which therefore contributes greatly not only to the correct folding of the domain, but also to the overall structural variability of the protein (Ramirez-Alvarado, 2013).

L chains monomers can dimerize in a way that resembles the association to an H chain; indeed, the dimerization interface used for homo-dimerization and hetero-dimerization is mostly the same, despite the orientation of the two L chain monomers can vary, in terms of a different angle between the VL and CL domains of the two monomers (Oberti *et al.*, 2017). κ and λ L chains present highly similar structural features, however λ L chains were reported not only to have lower isoelectric points (pI) compared to κ L chains, but also to have longer and more hydrophobic CDR3 loops, features that arise from germline-encoded differences and are independent from SHM (Townsend *et al.*, 2016). Moreover, κ and λ L chains differ regarding to the β-strand A, a structural moiety which adopts a conformation known as β-sheet switch that has been described to prevent non-native intermolecular interactions; specifically, the size of such design was reported to be bigger in κ L chains (Richardson and Richardson, 2002; Blancas-Mejia *et al.*, 2018). As V-J recombination at the λ L chain locus occur after rearrangements at the κ locus, λ L chain usage is promoted by receptor editing and it has been suggested that, due to their distinct biophysical properties, including the characteristics of their CDR3 loop, λ L chains may have a specialized role in editing (Wardemann, Hammersen and Nussenzweig, 2004; Townsend *et al.*, 2016; Nemazee, 2017). In healthy individuals or MM patients κ L chains are usually more represented, with a λ/κ ratio of approximatively 1:2; conversely it is described that in AL amyloidosis λ L chains are overrepresented, with a λ/κ ratio of 3:1 (Kyle and Gertz, 1995), but the reasons accounting for λ L chains enrichment in the pool of amyloidogenic sequences are still unknown.

4.6.5 The amyloidogenic clone

Despite the immunophenotypic profile of AL amyloidosis PCs tends to overlap to the one of MM PCs, genome-wide associations studies provide evidence for a genetic susceptibility signature for AL amyloidosis (Da Silva Filho *et al.*, 2017). The ten loci showing evidence of association are related to translocations between chromosomes 11 and 14 (t(11;14)) within the oncogene CCND1 or are related to proteins, like SWI/SNF-related matrix-associated actin-dependent regulator of chromatin subfamily D member 3 (SMARCD3), involved in chromatin remodeling. Indeed, common cytogenetic abnormalities include chromosomal t(11;14), juxtaposing the H chain locus to CCND1, which is observed in approximatively 40-60% of AL amyloidosis clones (Bochtler *et al.*, 2011; Merlini *et al.*, 2018). However, considering that the causative agent of AL amyloidosis

is the secreted L chain, it is enigmatic to envision how cytogenetic abnormalities of the malignant PCs could dictate a pathogenic phenotype at distal organs.

Interestingly, the distinctive perinuclear distribution of mitochondria and the upregulation of cellular redox sensors in AL amyloidosis PCs compared to PCs from MGUS and MM suggests that amyloidogenic L chain expression is a stressor, resulting in enhanced oxidative stress and sensitization to proteasome inhibitor therapy (Oliva *et al.*, 2017). In the same line, AL amyloidosis PCs are considered to be less proliferative than PCs from MM patients, a reason that could account for the lack of cellular models for AL amyloidosis PCs, which rely solely on two sister cell lines, ALMC-1 and ALMC-2 (Arendt *et al.*, 2008).

4.6.6 Composition of amyloid deposits and tissue tropism

Resembling all the 36 human amyloid diseases, amyloid deposits of patients affected by AL amyloidosis contain, together with the amyloid precursor protein, a number of co-factors (Vrana *et al.*, 2009). Such ubiquitous components include apolipoprotein E (ApoE), A-I and A-IV, serum amyloid P (SAP), and proteoglycans – glycoproteins comprising core proteins connected to glycosaminoglycans (GAGs) including hyaluronic acid, heparan sulfate, dermatan sulfate, chondroitin sulfate A and keratan sulfate (Zhang, Huang and Li, 2017; Blancas-Mejia *et al.*, 2018). The pro-amyloidogenic role of ApoE is widely recognized and has been extensively studied in Alzheimer's disease, indicating the association of the genetic variant ApoE4 to the development and to the severity of the disease (Schmechel *et al.*, 1993). The presence of extracellular matrix (ECM) components, namely GAGs, collagen and lipids, in amyloid deposits as assessed by in situ Fourier Transform Infrared Spectroscopy (FTIR) (Ami *et al.*, 2016) suggests that the tissue microenvironment could play a crucial role in the process of amyloid fibrils formation, by further destabilizing the precursor protein or due to shear forces, interaction with metals and proteases. Oligomers and amyloid fibrils can also be protected from degradation by the calcium-dependent binding of SAP, a circulating plasma pentraxin (Pepys *et al.*, 1994; Tennent, Lovat and Pepys, 1995), further promoting amyloid formation through seeding effects.

Accumulation of amyloid fibrils in the parenchyma of affected organs alters the tissue morphology, with organ-specific histologic features. In detail, cardiac AL amyloidosis deposits are characterized by specific patterns of distribution (perifiber and mixed) and by a frequent vascular involvement, while renal AL amyloidosis usually involves amyloid deposition in the glomeruli and, to a lower extent, in the blood vessels, tubular-basement membranes and interstitium (Zhang, Huang and Li, 2017). In this context, the ECM is progressively replaced by amyloid fibrils, thus causing organs dysfunction by impairing the exchange of nutrients, building

a mechanical barrier around the cells, causing microvascular dysfunction and by recruiting immune cells, like macrophages, that eventually cause tissue damage. Additionally, it has been suggested that amyloid fibrils could contribute to ECM remodeling via inhibition of transforming growth factor-β (TGF-β), the cytokine responsible for ECM renewal (Zhu *et al.*, 1995) and via the activation of matrix metalloproteinases (MMPs), a family of zinc-dependent proteases involved in tissue remodeling (Zhang, Huang and Li, 2017). Additional mechanisms of amyloid-driven organ toxicity have been widely studied focusing on models of cardiac damage, given that cardiac involvement is a crucial factor for prognosis and survival. The observation that organ damage decreased in parallel to reduction of free L chain levels after chemotherapy (Palladini *et al.*, 2006) supports the concept that circulating L chains might directly contribute to organ toxicity.

4.6.7 L chain proteotoxicity: in vitro studies

Several studies explored L chains putative proteotoxity. In vitro studies employing rat and mouse cardiac fibroblasts and cardiomyocytes (Brenner et al., 2004; Trinkaus-Randall et al., 2005; Shi et al., 2010; Levinson et al., 2013) or human-derived cardiomyocytes and cardiac fibroblasts (Lavatelli *et al.*, 2015; McWilliams-Koeppen *et al.*, 2015; Marin-Argany *et al.*, 2016) investigated L chains internalization and their impact on cellular homeostasis, showing increased oxidative stress, reduced contractility and ultimately increased apoptosis after exposure to amyloidogenic L chains. These studies suggest that organ dysfunction may derive from the proteotoxicity of prefibrillar species – especially oligomers – which were proposed to contribute to reactive oxygen species (ROS) production, perturbation of cellular membranes, mitochondrial damage due to non-physiological L chains-mitochondrial proteins contacts and were shown to globally lead to reduced cell viability (Brenner *et al.*, 2004; Shi *et al.*, 2010; Lavatelli *et al.*, 2015; Imperlini *et al.*, 2017). Different cell types, such as rat cardiomyocytes and mesangial cells, can internalize L chains through diverse routes, either via receptor-mediated endocytosis, through a still unknown receptor, or via pinocytosis into the endosomal-lysosomal pathway (Monis *et al.*, 2006; Ramirez-Alvarado, 2013). L chains internalization into cardiomyocytes was shown to mediate lysosomal dysfunction, consisting of loss of acidity and downregulation of lysosomal proteins (Guan *et al.*, 2014) and was suggested to promote amyloidogenesis, putatively through the acidic lysosomal environment; lysosomal dysfunction was also associated to a defective autophagic flux, an observation that could represent a functional link to the previously reported mitochondrial dysfuntion, which could derive from impaired autophagic clearance of damaged mitochondria (Zhang, Huang and Li, 2017).

From the mechanistic point of view, pioneering studies indicated that isolated adult cardiomyocytes, once exposed to L chains from patients affected by AL amyloidosis cardiomyopathy, displayed higher activation of p38 mitogen-activated protein kinase (MAPK) signaling. This process relies on p38 autophosphorylation mediated by TGF-β-activated protein kinase-1 binding protein-1 (TAB1) and subsequent activation of stanniocalcin-1 (STC1) that is responsible for ROS production and impaired calcium homeostasis, which are mechanisms associated to cell dysfunction (Shi *et al.*, 2010; Guan *et al.*, 2013). Interestingly, the fact that p38 MAPK pathway is also a selective regulator of type B natriuretic peptide (BNP) transcription, a serum biomarker of heart damage (Ma, Ogawa and De Bold, 2004), supports the use of the serum biomarker NT-proBNP (the amino-terminal fragment of BNP) for the clinical management of AL amyloidosis patients. As mentioned previously, internalization of L chains by mesangial cells via clathrin-mediated endocytosis to the lysosomal pathway was shown on one hand to support amyloid material formation (Comenzo *et al.*, 2001), on the other to promote a phenotypic transformation from smooth muscle-type cells to macrophage-like cells, characterized by accumulation of lysosomes, increased expression of CD68 and activation of NF-κB (Keeling, Teng and Herrera, 2004; Zhang, Huang and Li, 2017).

In vitro studies proved fundamental to elucidate some mechanisms underlying AL amyloidosis, however it is necessary to emphasize that such experimental approaches are far from the real organ systems, in which amyloid deposition and toxicity occur and do not fully reflect the pathophysiology of the disease, urging the establishment of suitable, more sophisticated in vitro and in vivo models. In this regard, recent data analyzing urinary extracellular vesicles (UEX), vesicles containing cytosolic proteins engulfed in kidney-derived membranes, from AL amyloidosis patients revealed the presence of oligomeric L chains, suggesting that UEX might be exploited as diagnostic tools and as an experimental platform to understand AL amyloidosis pathophysiology (Ramirez-Alvarado *et al.*, 2012). Moreover, also endothelial cells should represent a valuable experimental system to study the role of microvasculature dysfunction and injury in AL amyloidosis, as suggested by some preliminary studies (Migrino *et al.*, 2011).

4.6.8 In vivo models of AL amyloidosis

Due to the heterogeneous and elusive pathophysiology of the disease, it has been so challenging to generate suitable animal models of AL amyloidosis that there is no reported in vivo model displaying the full spectrum of features of this disorder (Buxbaum, 2009) and the current – still incomplete – understanding of the molecular mechanisms underlying the disease relies on reductionist cellular studies. Non-mammalian model organisms, namely Danio rerio and

Caenorhabditis elegans, have been widely used in recent years to study amyloidogenic L chains cardiotoxicity (Mishra et al., 2013; Diomede et al., 2014; Guan et al., 2014). Despite non-mammalian model organisms display significant advantages, such as the ease of handling and the reduced amount of L chains that need to be used to reach critical pathological concentrations, the equivalence between such animal models and the human disease phenotype may be ambiguous (Zhang, Huang and Li, 2017). Several mouse models of AL amyloidosis have been generated and rely on diverse strategies to trigger the disease. One approach is based on repeated injection of patient-derived BJ proteins in dehydrated mice in order to produce histopathologic lesions typical of AL amyloidosis especially in renal blood vessel walls and parenchyma (Solomon, Weiss and Pepys, 1992) or on injection of solubilized human amyloid deposits into the animal, giving rise to a mass consisting of aggregated material surrounded by neutrophils and macrophages (Hrncic *et al.*, 2000). More sophisticated models are represented by transgenic mouse strains, which express monoclonal L chains using the cytomegalovirus (CMV) promoter, resulting in gastric amyloid deposit formation after 24-30 months (Ward *et al.*, 2011), or by a conditional transgenic mouse generated via Cre/loxP system to allow regulated expression of L chains (Nuvolone *et al.*, 2017).

4.6.9 Clinical presentation and diagnosis

The clinical presentation of AL amyloidosis depends on the organs affected. All organs, apart from the central nervous system, can be affected by Ig L chains amyloid deposits. The symptoms range from asymptomatic proteinuria or nephrotic syndrome related to kidney involvement (observed in 70% of patients), restrictive cardiomyopathy or arrhythmias related to heart involvement (observed in 60% of patients), numbness, paresthesia, carpal tunnel syndrome, orthostatic hypotension related to peripheral (observed in 20% of patients) or autonomic (observed in 15% of patients) nervous system involvement, bleeding, gastroparesis, malabsorption, liver enzyme elevation related to gastrointestinal tract and liver involvement, macroglossia, purpura, easy bruisability, subcutaneous nodules related to soft tissue and skin involvement (Castillo, 2016).

A diagnosis of AL amyloidosis should be considered in any patient with a monoclonal gammopathy or atypical MM (Merlini *et al.*, 2018). AL amyloidosis diagnosis requires histopathological analysis on tissue biopsies in the affected organ or in less invasive sites such as rectal and abdominal subcutaneous fat pad and relies on the observation of Congo Red (CR) apple-green birefringence (Linke, 2012) demonstrating the presence of amyloid fibrils due to its regular intercalation between the ordered ultrastructure of amyloid fibrils. Accurate identification of the causative precursor protein is performed by immunohistochemistry, electron microscopy, or

mass spectrometry, the latter technique displaying a 88% higher sensitivity and a 96% higher specificity than immunochemical techniques (Merlini *et al.*, 2018); the evaluation of serum free L chains (FLC) concentration and ratio, 24-hour urine protein, immunofixation electrophoresis of the serum and urine, imaging with radio-iodinated SAP and NT-proBNP are fundamental for evaluation of patients where AL amyloidosis is suspected (Castillo, 2016; Merlini *et al.*, 2018).

4.6.10 L chain aggregation

A general paradigm for the initiation of amyloidogenesis contemplates that reduced protein stability allows a native protein to populate partially-folded states, which are the initiators triggering the aggregation reaction (Chiti and Dobson, 2009); hence, destabilized proteins, which require less energy to unfold, are considered to be more prone to amyloidogenesis. In the same line, decreased VL domains thermodynamic stability has been associated with enhanced propensity to form amyloid material (Hurle *et al.*, 1994; Blancas-Mejia *et al.*, 2018) and some reports suggest that, at least in some cases, AL amyloidosis L chains are less stable than non amyloidogenic L chains, such as MM L chains (Kim *et al.*, 2000; Oberti *et al.*, 2017). Several factors could impact on a L chain thermodynamic stability, ranging from destabilizing mutations, which allow the protein to sample partially unfolded states, mutations that impair the interaction with the H chain counterpart, and environmental factors. It is acknowledged that AL amyloidosis PCs underwent antigen-driven selection and somatic hypermutation (Perfetti *et al.*, 1998), implying the presence of mutations in amyloidogenic L chains; preliminary reports suggest that, at least for the amyloidogenic L chain AL-09, the germline protein could be more stable than its amyloidogenic counterpart, leading to slower kinetics of aggregation (Baden *et al.*, 2008). As for the environmental factors, interestingly, solutes and especially sulphated GAGs, which are ubiquitous components of amyloid deposits, have been described to affect the thermodynamic stability of AL amyloidosis VL domains (Mclaughlin *et al.*, 2006). In detail, GAGs like heparan-sulphate moieties are known to be able to interact with several ligands, namely cytokines, growth factors and enzymes; it was suggested that GAGs could form transient, electrostatic interactions also with amyloidogenic L chains (Martin and Ramirez-Alvarado, 2011), thus inducing or stabilizing their amyloidogenic conformations and subsequently acting as a scaffold responsible for the stabilization of inter-protofilament interactions, leading to mature fibrils formation (Zhang, Huang and Li, 2017). In the same line, several in vitro factors were described to influence L chain aggregation, either by promoting the sampling of misfolded states, such as low pH, ionic strength, protein concentration, chaotropic agents like urea and guanidine hydrochloride, reducing agents, agitation and pressure (Chiti *et al.*, 1999; Ramirez-Alvarado, 2013; Andrich *et al.*, 2017), or by stabilizing and enhancing fibril growth rates, such as the presence of surfaces and the addition of

preformed seeds. Additionally, structural studies also indicate that some L chains could dimerize in different conformations, as observed for the recombinant bacterially produced VL domain AL-09. Specifically, alterations of the dimeric interface, putatively due to somatic mutations, suggest that some L chains could populate, in a dynamic equilibrium, different dimeric interfaces (Baden *et al.*, 2008). Globally, current studies highlight that lack of stability does not trigger amyloid fibrils formation per se, rather, in order to sustain amyloid fibrils formation, it is necessary that the precursor protein, also in combination with external factors, populates a critical concentration of partially folded states (Ramirez-Alvarado, 2013).

In parallel to L chains thermodynamic stability, also their kinetic stability and their dynamics could play a crucial role. Amyloidogenic L chains were shown to be characterized by increased protein dynamics, as assessed by limited proteolysis (Oberti *et al.*, 2017). In this regard, proteolysis can be considered one of the post-translational modifications implicated in fibrillogenesis (Zhang, Huang and Li, 2017). In contrast to other types of amyloidosis, where the role of proteases is well established, the pathogenic role of proteolytic fragments is still controversial, despite the identical fragmentation pattern observed in different organs of the same patient implies a universal, rather than organ specific, process (Enqvist, Sletten and Westermark, 2009). Recent studies suggested that somatic mutations in the L chain variable region could reduce the fold stability of the native protein, thus increasing protein dynamics and favoring endoproteolysis and subsequent aggregation of V domains (Morgan and Kelly, 2016). In this context, it is crucial to highlight that the misconception that amyloid fibrils from AL amyloidosis patients contained only the entire VL domain and a portion of the CL domain (Glenner *et al.*, 1969) may be ascribed to technical limitations, which have been recently overcome thanks to the use of mass spectrometry on subcutaneous fat aspirates and biopsy tissues, allowing to reveal the presence of the CL domain in patient-derived amyloid material (Lavatelli *et al.*, 2008; Vrana *et al.*, 2009). Prior to such reports biochemical and biophysical studies on amyloidogenic L chains had been performed focusing only on VL domains and it is not surprising that, despite decades of active research, no conclusive results have been obtained. The pioneering finding of Lavatelli *et al.* cast new light on the potential role of the CL domain, suggesting that the interaction between VL and CL domain could be involved in the process of amyloidogenesis. Indeed, the linker between VL and CL domains was shown to contribute to L chain stability and amyloid formation propensity (Nokwe *et al.*, 2015); however, due to the challenges related to the study of full-length L chains, a conclusive interpretation of the role of the CL domain still needs to be achieved (Oberti *et al.*, 2017; Blancas-Mejia *et al.*, 2018).

A typical property of all amyloid fibrils is their ability to self-propagate, known as seeding, implying a continuous recruitment of additional molecules to the fibrils, resembling an autocatalytic reaction. Amyloidogenic L chains have been reported to be recruited by homologous and heterologous seeding (Blancas-Mejía and Ramirez-Alvarado, 2016); however, the results obtained from seeding experiments are quite controversial as it was shown either that preformed seeds cannot affect the kinetic of amyloid formation, implying that the provided seeds were not able to act as a catalyst, or that seeds could act as excellent nucleators and elongators for aggregation reactions (Blancas-Mejia *et al.*, 2018). Seeding was proposed to occur also via fibrils attachment to cell membranes in cell-mediated seeding mechanism (Marin-Argany *et al.*, 2016).

4.6.11 L chains diversity and Amyloidosis

Compared to the other types of amyloidosis, AL amyloidosis, due to the nature of its amyloid precursor protein, presents an additional complexity. Amyloidogenic L chains, as any Ig L chain, can originate from the unique rearrangements of 40 κ and 33 λ germline V genes with 5 κ and 4 λ J genes, on top of which an additional level of complexity is added by SHM. Therefore, each AL amyloidosis patient is characterized by a unique amyloidogenic precursor protein sequence and this level of diversity results in a varying degree of propensity to form amyloid fibrils and toxic species and might be implicated in the severity of the disease or in the organ involvement (Ramirez-Alvarado, 2013). It should be emphasized that L chains sequence diversity does not represent the only source of diversity in AL amyloidosis, as L chains serum concentration, tissue tropism and a virtually infinite array of still underappreciated factors occurring at the site of amyloid formation may be responsible for the unique features of each amyloidogenic L chain aggregation. Amyloidogenic L chains diversity has been widely documented and several groups attempted to discover structural features that could account for L chains enhanced propensity to form amyloid fibrils and become pathogenic (Stevens, 2000; Poshusta *et al.*, 2009). These studies, which focused on κ L chains, evidenced that the introduction of glycosylation sites and mutations of proline residues in β-turns were associated to amyloidogenesis and suggested that L chains with amyloidogenic-promoting mutations were present at lower levels in the sera of AL amyloidosis patients, an observation that could be ascribed to the intracellular quality-control checkpoints retaining destabilized proteins (Ramirez-Alvarado, 2013).

It has been suggested that structural features encoded by certain L chain variable genes could correlate with higher risk of specific organs involvement, as indicated by the over-representation of specific V genes in AL amyloidosis. A representative example is the germline gene IGLV6-57, which is poorly represented in the normal repertoire of healthy individuals B cells, but is

extremely common in AL amyloidosis patients who present kidney involvement (Comenzo *et al.*, 2001; Kourelis *et al.*, 2017). In the same line, IGLV3-1 and IGLV1-44 have been associated to predominant deposition of amyloid in cardiac tissue (Perfetti, 2002; Perfetti *et al.*, 2012). However, it is still enigmatic whether such V genes encode for inherently aggregation-prone proteins, or somatic mutations and other still elusive factors drive amyloidogenic properties (Blancas-Mejia *et al.*, 2018). Nevertheless, recent reports have at least partially excluded an inherent amyloidogenic potential of germline-encoded L chains (Garay Sánchez *et al.*, 2017), emphasizing that, despite tentative correlations between germline usage and AL amyloidosis, the factors accounting for specific germline gene products over-representation in AL amyloidosis still need to be fully addressed and the determinants of the disease are undoubtedly multifactorial (Ramirez-Alvarado, 2013).

4.6.12 Therapeutic approach against AL amyloidosis

Early diagnosis and prompt treatment are essential to improve survival in AL amyloidosis. Unfortunately for most patients, the disease goes unrecognized until severe organ dysfunction develops and nearly half of the patients die soon after diagnosis, generally as a result of cardiac involvement, which limits their options for chemotherapy (Kumar *et al.*, 2011). Ideal treatments for AL amyloidosis should eradicate the malignant PC clone, deplete the circulating amyloidogenic L chains and promote amyloid deposits clearance, putatively reversing organ dysfunction. Despite AL amyloidosis PCs are characterized by distinct cytogenetic abnormalities as compared to MM, current treatments targeting the amyloidogenic clone mirror MM therapeutic schemes; the amyloidogenic clone is usually targeted by chemotherapy, also including proteasome inhibitors, and autologous stem cell transplantation (ASCT). The outcome of current therapies and the frequent therapeutic failures, due to poor response of several patients, who display severe and irreversible organ dysfunction, are far from satisfactory and urge the application of new therapeutic schemes. An additional source of complexity is represented by the presence of two reservoirs of L chains, namely the amyloidogenic clone and the amyloid deposit itself. It is established that reduction of circulating L chains results in improved organ function (Palladini *et al.*, 2006), however an hematologic response does not necessarily imply an organ response, as long as amyloid fibrils are still present in affected tissues; amyloid deposits could continue to cause structural damage to the tissue and, if partially degraded, could provide a source of oligomers leaching from the fibrils (Zhang, Huang and Li, 2017). For these reasons anti-amyloid therapies targeting amyloid deposits and the precursor protein itself are urgently needed.

In this context, it was recently reported that NEOD001, an anti-free L chains monoclonal antibody, led to organ response in most of the patients treated in a Phase I/II study (Gertz *et al.*, 2016), while the use of a monoclonal antibody (mAb 11-1F4) targeting amyloid fibrils but not soluble L chains was tested for amyloid clearance (Solomon, Weiss and Wall, 2003). The last approach resamples the therapeutic strategy exploiting SAP targeting for immune-mediated amyloid fibrils degradation thanks to a combination of a small molecule to deplete circulating SAP and a monoclonal antibody to target amyloid-bound SAP (Bodin *et al.*, 2010; Richards *et al.*, 2015). In parallel, the ability of several small molecules, including doxycycline and epigallocatechin-3-gallate (EGCG), to remodel L chains aggregation has been tested in in vitro and in vivo experimental systems (Ward *et al.*, 2011; Andrich *et al.*, 2017). A novel strategy to reduce circulating L chains levels could rely on the use of small interference RNA (Phipps *et al.*, 2010) that presents encouraging results but apparent challenges for in vivo targeting, delivery and specificity.

5. Research plan

5.1 Study aims

As seen in the introduction, the origin of immunoglobulin L chains is intimately connected to the generation of antibody diversity, substantially contributing to the complexity of AL amyloidosis. Indeed, each patient suffering from AL amyloidosis carries a unique malignant B cell clone secreting a different L chain generated by a V-J rearrangement followed by the addition of somatic mutations. Several studies have shown that AL amyloidosis displays a bias for certain VL sequences (Kourelis *et al.*, 2017), but these sequences are rearranged to different J segments and carry different somatic mutations. Therefore, an unambiguous connection between specific structural determinants and L chains aggregation and consequent clinical manifestations still needs to be uncovered.

In this process, whether somatic mutations are the main drivers of L chains amyloidogenesis is still is subject to considerable debate. Thus, **the main goal of my thesis was to assess how and to what extent somatic mutations influence amyloidogenic L chains biophysical properties and their propensity to aggregate into amyloid fibrils**.

Considering that somatic mutations on the VL domain are a consequence of antigen-driven selection at the level of BCR, **a second goal of my thesis was to compare the effect of L chains hetero-dimerization with H chains and L chains homo-dimerization.** We aimed to address not only if L chains homo-dimerization could influence the biophysical properties of the complex, fostering a pro-amyloidogenic phenotype, but also if free L chains could be involved in interactions with antigens, which would be inherently able to escape immunological tolerance mechanisms.

5.2 Experimental approach

In order to provide enough flexibility to address the fundamental aspects of L chains biology, we selected amyloidogenic L chain sequences (AL) from the Amyloid Light Chain Database (ALBase) (Bodi *et al.*, 2009) or from a dataset provided by the group of our collaborator Prof. Merlini, together with suitable L chains and antibody controls in the Fab format. The role of somatic mutations was established by analyzing "germline sequences" (GL), as determined by the international ImMunoGeneTics information system database (IMGT) (Lefranc *et al.*, 2009).

To achieve a protein folding state resembling the one of immunoglobulins secreted by B cells, all proteins were produced by transfection of mammalian cells. The biophysical properties of recombinant proteins were assessed by several in vitro assays including size exclusion chromatography, thermal denaturation (Sypro Orange thermal shift assay) and free thiols quantification. In parallel, fibrillogenesis experiments were performed to assess the propensity of AL and GL L chains to form oligomers or fibrillary species, which were assessed by turbidity measurements, binding of amyloid specific dyes and TEM. Our in vitro data were compared to in silico analysis performed by our collaborators Maura Garofalo and Dr. Andrea Cavalli, namely the analysis of in silico thermal stability and the computed binding affinity of L chains homodimers and heterodimers.

In order to investigate the ability of L chains to interact with antigens, I followed two strategies: an unbiased, target-agnostic screening of a peptide library using the phage display technology, aimed at providing a proof of principle of our hypothesis, and a targeted analysis by flow cytometry, immunofluorescence and enzyme-linked immunosorbent assay (ELISA) of L chains and Fab binding to cells and the ECM. To further assess L chains ability to be retained in the ECM, I developed an ECM binding assay, which allowed to monitor the kinetic of protein interaction with three-dimensional ECM structures.

6. Results

In the following section I will present the results obtained in my thesis using the experimental approaches mentioned in the previous chapters. We reasoned that L chains are selected, as part of the BCR, for pairing with H chains, but not with themselves. Therefore, we considered the possibility that, in the absence of selection for the formation of functional homodimers, L chains may be intrinsically unstable and develop, through somatic mutations, amyloidogenic properties.

Production of recombinant L chains. To investigate the possibility that L chains could be intrinsically unstable and that amyloidogenic properties could derive from somatic mutations, we selected a panel of amyloidogenic L chains from AL amyloidosis patients (**Table 6.1**) from a dataset provided by our collaborator Prof. Merlini. In view of the issue of L chains sequence variability and to avoid analyzing germline-specific properties, we focused on L chains belonging to different V genes, which displayed a considerable homology to their corresponding GL. We selected λ rather than κ L chains, due to λ over-representation in AL amyloidosis. Considering that cardiac involvement, as assessed by the levels of the serum biomarker NT-proBNP, is regarded as a crucial factor for prognosis and survival and that a plausible mechanism of L chain cardiac toxicity has been recently described, all the selected L chains, besides two controls, were associated to cardiac dominant syndrome. We aimed to reproduce the conformation of the L chains circulating in the sera of AL amyloidosis patients, which represent the pool of aggregation prone material; therefore, full-length L chains, comprising VL and CL domains, were produced by transfection of HEK 293 cells in the mutated (AL) and unmutated, germinalized (GL) form. The recombinant L chains were purified by affinity chromatography; to verify that the purification strategy employed allowed the isolation of correctly folded species, purified samples were analyzed by Far-UV Circular Dicroism spectroscopy (**Figure 6.1a,b**). The analyzed proteins were characterized by a predominant β-sheet and irregular secondary structure, which was comparable to the predicted secondary structure of an IgG antibody.

Characterization of L chains heterogeneity. Subsequently, in order to characterize the MW distribution of the samples, L chains were examined by size exclusion chromatography (**Fig. 6.2a**). Compared to a Fab, which eluted as a single peak, corresponding to the 50 kDa H-L chains dimer, all the L chains tested showed heterogeneous profiles with major peaks corresponding to the 50 kDa dimeric form, as well as multimers and monomers. Likewise, non-reducing SDS-PAGE characterization of the samples confirmed the L chains heterogeneity and the co-existence of disulphide-linked dimers and monomers; interestingly, both AL and GL L chains presented a significantly different MW distribution as compared to Fabs, where no monomers or non-

covalently linked dimers could be detected (**Fig. 6.2b,c**). We further examined the peaks separated by size exclusion chromatography by incubating the different fractions at 37 °C for increasing time intervals; non-reducing SDS-PAGE analysis of the fractions showed an overall stability of the different MW isoforms as well as further heterogeneity of the major peak, with stable disulphide-linked and non-covalently linked dimers (**Fig. 6.2f**). Importantly, not only we could observe the presence of L chains dimers and monomers in free L chains secreted by EBV-immortalized memory B cells (**Fig. 6.2d**), but we were also able to isolate and immortalize memory B cells from healthy donors that did not secrete any IgG, IgM or IgA antibody, but could produce large amounts of free L chains (**Fig. 6.2e**). These findings support the use of eukaryotic cells, namely HEK 293 cells, to produce recombinant L chains, which are characterized by the same level of heterogeneity observed in free L chains expressed by B lymphocytes.

L chains intrinsic instability is aggravated by somatic mutations. To assess the L chains thermodynamic stability we employed two parallel approaches. Via Sypro orange thermal shift assay, which takes advantage of the significant increase in quantum yield of the Sypro orange dye upon binding hydrophobic moieties, we were able to evaluate the proteins unfolding curves and the exposure of hydrophobic residues to the solvent. Concurrently, our collaborators Maura Garofalo and Dr. Andrea Cavalli estimated by FoldX energy function calculation, both for L chains monomers and dimers, the free-energy change upon mutation ($\Delta\Delta G$), a thermodynamic parameter correlated to the gain or loss of free Gibbs energy due to the introduction of somatic mutations on a GL sequence, leading to the corresponding AL L chain sequence.

While four different Fabs showed an overall high thermal stability, with exposure of hydrophobic patches only after their melting temperatures, all L chains exposed hydrophobic patches already at 37 ^{o}C and showed a poor thermal stability with strong aggregation following the melting phase (**Fig. 6.3a,b**). Most L chains showed a defined unfolding curve, which could be mainly descriptive of a two-step process; however, it was not possible to extrapolate the melting temperature of some L chains, which displayed a high exposure of hydrophobic residues already at low temperatures, as observed also for proteins with solvent-exposed hydrophobic surfaces like Bovine Serum Albumin, which is characterized by a similar Sypro orange thermal shift assay profile.

Interestingly, the melting temperatures of all the AL L chains were lower as compared to their GL forms (**Fig. 6.3c**). Accordingly, the positive value of the computed free-energy change upon mutation for all the sample tested, both in the monomeric and in the dimeric form, suggested that the introduction of the somatic mutations observed in AL L chains could destabilize GL

sequences (**Fig. 6.3d**); indeed, positive ΔΔG values are associated to thermodynamic destabilization, while negative ΔΔG values are associated to thermodynamic stabilization. Collectively, these findings indicate that free L chains are intrinsically unstable and present varying degrees of solvent-exposed hydrophobic residues. In the context of AL amyloidosis, these properties are aggravated by somatic mutations.

VL/VL homo-dimerization mediates destabilization of stable VL/VH heterodimers. Following on these results, we compared the thermal shift assay profiles of two recombinant Fabs previously isolated against viruses and self-antigens and their BJ protein counterparts; interestingly, we observed that in both cases the BJ proteins were markedly less stable as compared to their precursor Fabs (**Fig. 6.4a,b**). Prompted by these observations, we assessed whether the pairing with an H chain could also stabilize AL L chains. We could firstly show a partial rescue of the L chain destabilization by testing AL17 BJ protein and a Fab comprising AL17 L chain and the H chain of an unrelated antibody (**Fig. 6.4c**). In one case we were able to obtain paired VH and VL sequences from the amyloidogenic clone AL153 and the comparison of the corresponding BJ protein and Fab showed a striking difference in thermal stability and hydrophobicity (**Fig. 6.4c**). We hypothesized that the dramatically different biophysical properties of AL153 Fab and its BJ counterpart might be due to a destabilization of the dimeric interface of the VL/VL homodimer. Indeed, despite a remarkable similarity in their three-dimensional structures (**Fig. 6.4d,e**), our collaborators Maura Garofalo and Dr. Andrea Cavalli investigated the binding affinity of the VL/VL homodimer and the VH/VL heterodimer. This analysis showed a markedly higher binding affinity, corresponding to a lower predicted free energy of binding (ΔG_{GB}), for the Fab VH/VL complex as compared to the binding affinity for the BJ protein VL/VL complex, indicating that Fabs stability is higher than the one of BJ proteins (**Fig. 6.4f**). Collectively, these results indicate that in contrast to Fabs, free L chains are inhomogeneous, have low melting temperatures and expose hydrophobic patches. Remarkably, our data suggest that the homo-dimerization of VL domains generates BJ proteins that are intrinsically unstable compared to their Fab counterparts.

L chains expose free thiols. The presence of non-disulphide-linked L chain dimers prompted us to investigate the redox status of L chains cysteines. Using the thiol-reactive probe 7-Diethylamino-3-(4'-Maleimidylphenyl)-4-Methylcoumarin (CPM) we determined that, in contrast to Fabs, both GL and AL free L chains have variable levels of exposed free cysteines, with a mean value of approximately 2 free thiols/L chain dimer (**Fig. 6.5a**). As mentioned in the introduction, each L chain monomer presents 5 cysteine residues, four of which are involved in

the formation of two intra-molecular disulphide bonds in the VL and CL domains respectively, while one of them, located in the terminal position of the CL domain (C105), is responsible for the formation of an inter-molecular disulphide bridge with the CH1 domain of H chains or the CL domain of a L chain. To measure the contribution of the terminal cysteine to the global level of free thiols, we compared two wild type L chains with the corresponding C105S mutants and found that the mutation reduced, but did not abrogate the number of free thiols (**Fig. 6.5b**). Interestingly, when two AL L chains, which as BJ proteins displayed high levels of exposed free thiols, were expressed as Fabs, free thiols were not detected (**Fig. 6.5c,d**). Taken together, these findings indicate that inter-chain and even intra-domain disulphide bonds are not fully oxidized in free L chains and are therefore accessible to the thiol-reactive probe; our observations suggest that the exposure of free thiols should not be regarded as a L chain-intrinsic property, as it can be reduced to baseline through the pairing with an H chain.

L chains aggregation into amyloid-like material is promoted by reducing conditions and is aggravated by somatic mutations. The formation of amyloid fibers in vivo is a very slow process since elevations of free L chains in the serum have been observed years before clinical symptoms. To evaluate the aggregation potential of free L chains in vitro we subjected the samples to shaking at 37 ^{o}C; since in native conditions L chains aggregation cannot be observed in the time frame of an in vitro experiment (**Fig. 6.6a**), we tested whether reducing conditions could affect the formation of aggregates. While aggregation was not observed in the absence of reducing agents, at least over a period of 10 hours, the addition of 10 mM DTT resulted in rapid aggregation as measured by turbidity and Thioflavin T (ThT) (**Fig. 6.6a,b**). Strikingly, when compared to their germline versions, mutated amyloidogenic L chains showed a much higher rate and extent of aggregation into Congo Red (CR) positive material (**Fig. 6.6c-f**). We further characterized the aggregates by negative staining and transmission electron microscopy (TEM) and found aggregates of different morphologies ranging from large oligomers to amyloid fibers (**Fig. 6.6g**). Interestingly, the lag time before the onset of aggregation differs among the L chains analyzed, consistent with the requirement for a specific nucleation event. To address this possibility, we added preformed aggregates to a fresh sample and observed a faster aggregation kinetics (**Fig. 6.6h,i**). Collectively these data indicate that, under reducing conditions, mutated free L chains, and to a much lower extent their unmutated counterparts, rapidly aggregate into amyloid material in a process that is accelerated by addition of preformed seeds.

DCs provide a reducing extracellular microenvironment. Based on these results, we aimed to assess if the presence of free thiols, which is required to trigger L chains aggregation into

amyloid-like material in vitro, could be compatible with the extracellular microenvironment. Considering that a reducing environment accompanies immune responses, we quantified the levels of free thiols that are produced by monocyte-derived dendritic cells (moDCs) upon maturation. moDCs maturation was induced and the secretion of thiols in fresh serum-free medium was analyzed. Interestingly, already 6 hours after stimulation, moDCs were able to secrete discrete amounts of thiols; remarkably, in our experimental setting also unstimulated moDCs, when cultured at high density, could secrete low levels of free thiols, which were dramatically increasing upon maturation (**Fig. 6.7a,b**). Hence, our results suggest that the presence of free thiols is compatible with the extracellular microenvironment, the location of L chain aggregation in vivo, at concentrations as high as 80 μM, corresponding to the production of 80 fmol of free thiols by a single moDC.

Light chain dimers have unique specificities and bind to cells and to the extracellular matrix. Clinical amyloidosis is associated with the deposition of amyloid fibers in target organs such as the kidney, the liver and the heart. To address the basis of the tissue tropism, we investigated the possibility that L chain dimers may have a distinct specificity encoded by the paired VL/VL domains. We therefore produced IgG-like molecules displaying two identical VL domains on the L and H chains. Two such constructs and a control antibody reactive against multiple peptides of *Plasmodium falciparum* circumsporozoite protein (CSP) were tested for their capacity to select peptides from a phage display library (**Fig. 6.8a**). Peptides selected by one of the VL/VL constructs and by the CSP-specific antibody showed high affinity and specific binding to the selecting antibodies, demonstrating that VL/VL dimers, as conventional antibodies, have a distinct specificity. We therefore tested whether L chain dimers could bind to cells, tissues or to the extracellular matrix. Strikingly, all the L chains tested bound to Hep2 cells and mouse myeloma Ag8.653 cells as assessed by flow cytometry and confocal microscopy using the same experimental approach employed for auto-antibody detection, while control Fabs failed to do so, indicating that L chain dimers have a broad reactivity to cellular antigens (**Fig 6.8b,d)**. Interestingly, the binding of the patient-derived Fab counterpart of an AL L chain was negligible (**Fig 6.8c)**. In addition, two AL L chains tested, but neither their GL versions, nor Fabs and antibodies bound to mouse heart tissue sections (**Fig 6.8e)**. To investigate the binding to the extracellular matrix, we measured the interaction of free L chain dimers with ECM proteins and glycosaminoglycans contained in commercially available Matrigel arranged in 2 or 3 dimensions. With a single exception, all free L chains bound to Matrigel-coated ELISA plates while some of them also bound, to a lower extent, to uncoated plates, a property characteristic of hydrophobic antibodies (**Fig. 6.8f**). Furthermore, free L chains were also retained in 3-dimensional Matrigel

droplets, while control antibodies and Fabs were rapidly washed out (**Fig 6.8g,h**). Collectively, these data suggest that free L chains have a unique specificity and can bind in a promiscuous fashion to cell surfaces and to the extracellular matrix.

6.1 Tables and figures

Table 6.1. V gene usage and homology (%) to GL of the L chains selected from AL amyloidosis patients with indication of the dominant syndrome and the levels of the serum biomarker of cardiac damage NT-proBNP (pg/ml)

L chain	V gene	Homology	Syndrome	NT-proBNP
AL17	IGLV3-19*01	97.85%	skin	139.6
AL57	IGLV2-14*01	94.79%	heart	12027
AL93	IGLV1-44*01	95.44%	heart	13513
AL95	IGLV3-1*01	91.76%	heart	22102
AL97	IGLV2-23*01 or IGLV2-23*03	95.83%	kidney	2019
AL105	IGLV3-21*02	92.83%	heart	12877
AL109	IGLV3-21*02	96.42%	heart	5244
AL153	IGLV3-19*01	96.06%	heart	5289

Figure 6.1. Secondary structure of recombinant L chains. a, Representative Far-UV spectra of purified L chains. **b,** Secondary structure prediction via spectra analysis of the L chains tested and an IgG antibody as control.

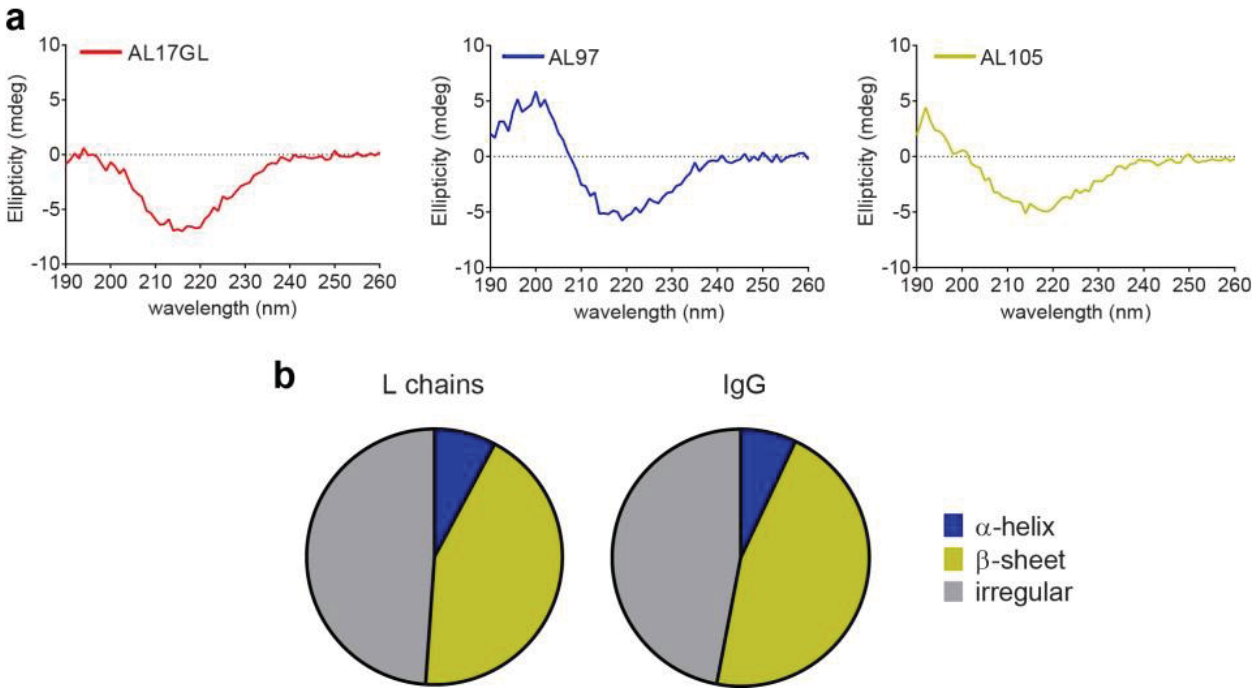

Figure 6.2. Heterogeneity of free L chains. L chains were produced in transiently transfected HEK 293 cells and characterized for their biophysical properties. **a,** Size exclusion chromatography profiles of amyloidogenic L chains (AL, blue) and their germline-reverted counterparts (GL, red) and a representative recombinant Fab (green). **b,** Non-reducing SDS-PAGE of AL, GL L chains and 4 Fabs. **c,** MW distribution of AL, GL L chains and Fabs analyzed via non-reducing SDS-PAGE expressed as Monomer/Dimer ratio (%).*** $P \leq 0.001$, as determined by unpaired t-test. **d,** WB of 3 EBV-immortalized B cell lines supernatants after non-reducing SDS-PAGE. **e,** Detection by ELISA of IgA (purple), IgG (black), IgM (green), κ L chains (blue), λ L chains (red) in EBV-immortalized B cell clones supernatants. Controls expressing full antibodies (first and second row) and clones secreting L chains-only (third and second rows) are shown. **f,** Stability of monomeric and dimeric fractions of AL93 assessed by non-reducing SDS-PAGE after 0-30 h incubation at 37 °C.

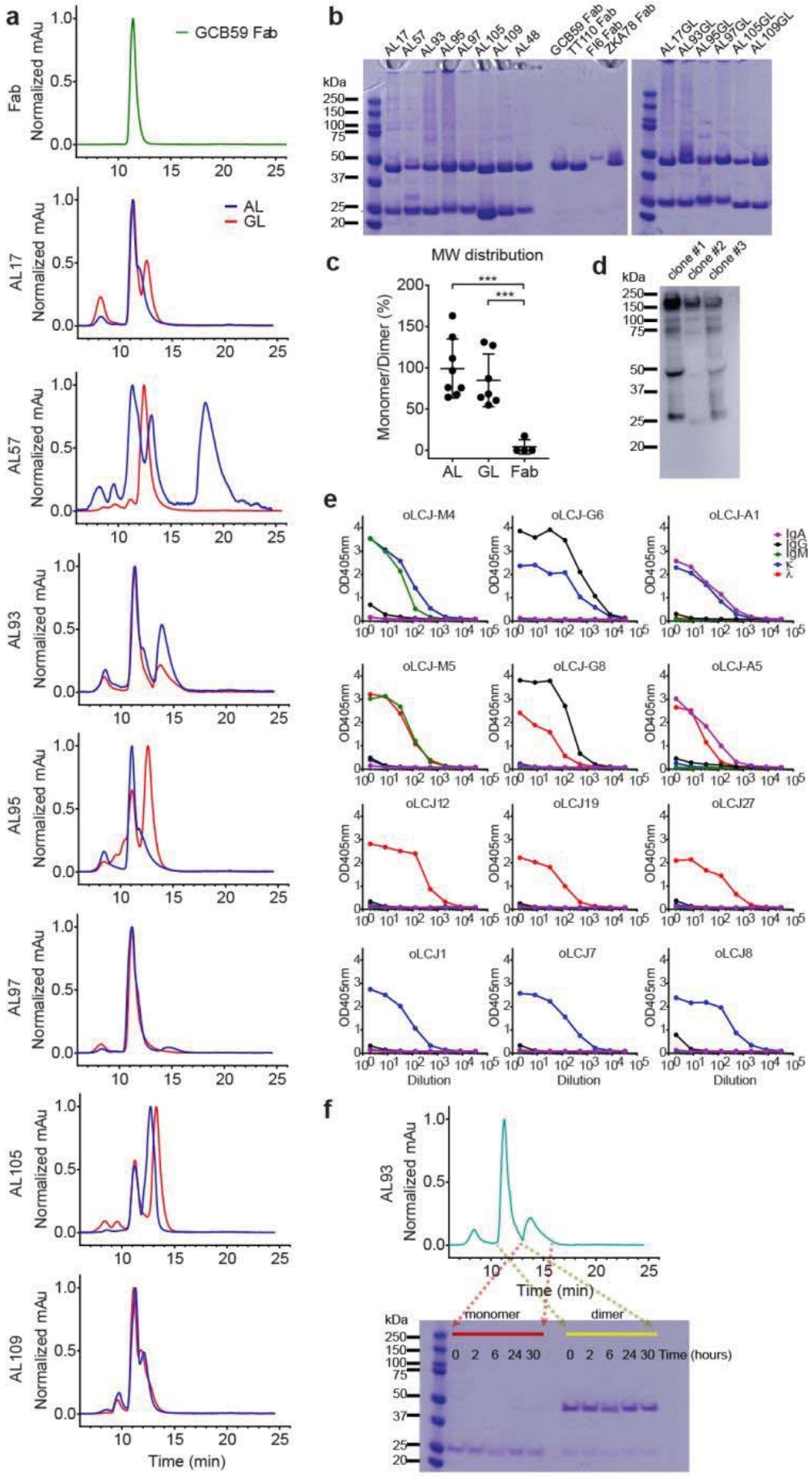
a
Fab
Normalized mAu
GCB59 Fab
AL17
AL
GL
AL57
AL93
AL95
AL97
AL105
AL109
Time (min)
b
AL17
AL57
AL93
AL95
AL97
AL105
AL109
AL48
GCB59 Fab
TT110 Fab
F16_Fab
ZKA78 Fab
AL17GL
AL93GL
AL95GL
AL97GL
AL105GL
AL109GL
kDa
250
150
100
75
50
37
25
20
c
MW distribution
Monomer/Dimer (%)
***
***
AL
GL
Fab
d
kDa
clone #1
clone #2
clone #3
e
oLCJ-M4
oLCJ-G6
oLCJ-A1
oLCJ-M5
oLCJ-G8
oLCJ-A5
oLCJ12
oLCJ19
oLCJ27
oLCJ1
oLCJ7
oLCJ8
OD405nm
IgA
IgG
IgM
κ
λ
Dilution
f
AL93
Normalized mAu
Time (min)
kDa
monomer
dimer
0 2 6 24 30
0 2 6 24 30 Time (hours)

Figure 6.3. Thermodynamic stability of recombinant L chains. a, Sypro orange thermal shift assay performed of AL and GL L chains and on 4 recombinant Fabs with κ or λ L chains. **b,** Hydrophobicity index of AL, GL and Fab measured by the emitted Sypro orange fluorescence at 37 ^{o}C. * P ≤ 0.05, as determined by unpaired t-test. **c,** Apparent thermal melting temperatures (first and second transitions) for AL and GL L chains extrapolated from the inflection points of the derivative curves of the Sypro orange thermal shift assay. * P ≤ 0.05,** P ≤ 0.01, as determined by paired t-test. **d,** Free-energy change upon mutation (ΔΔG) (kcal/mol) from GL to AL L chains estimated by FoldX energy function calculation. Dimer ΔΔG (red) and monomer ΔΔG (orange) are shown.

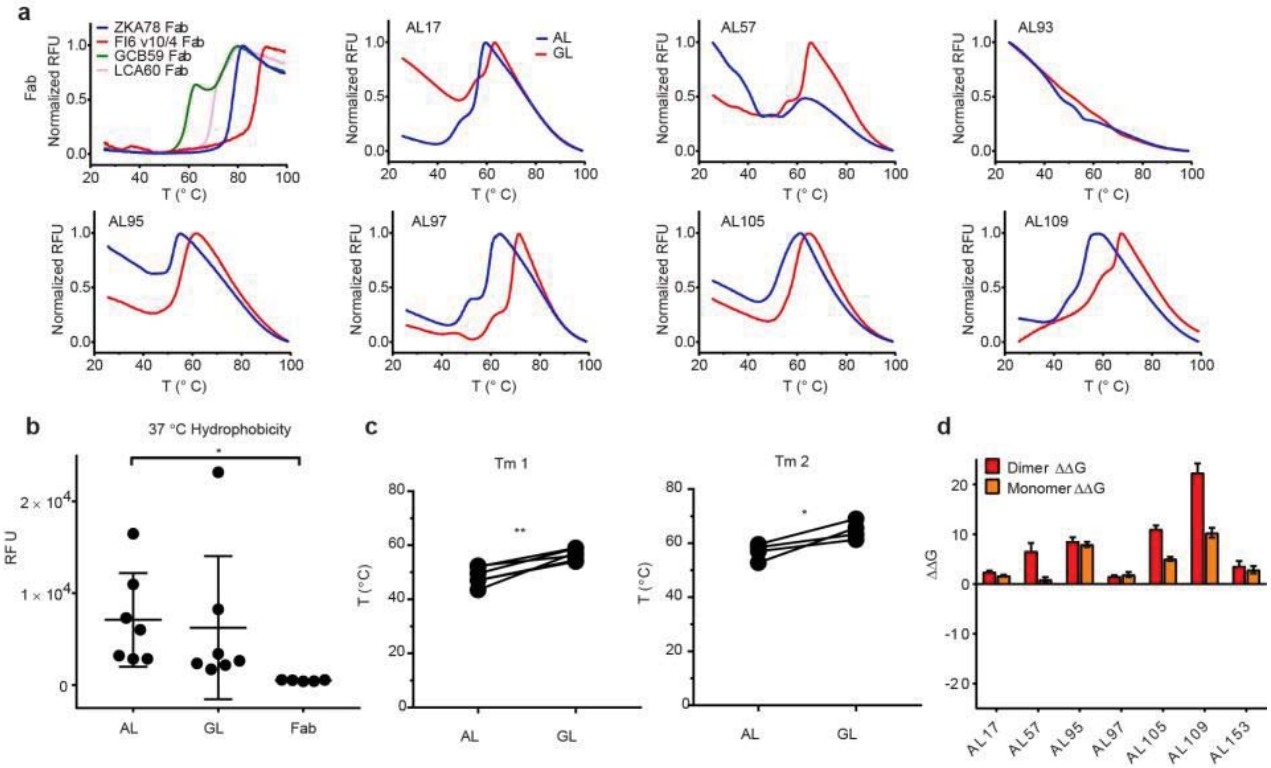

Figure 6.4. Divergent stability of L chains homo- and hetero-dimers. a, Sypro orange thermal shift assay of GCB59 BJ (orange) and its corresponding Fab (red, dotted). **b,** Sypro orange thermal shift assay of LCA60 BJ (dark green) and its corresponding Fab (light green, dotted). **c,** Sypro orange thermal shift assay of AL17 BJ (light blue) and a Fab comprising AL17 L chain and GCB59 H chain (blue, dotted). **d,** Sypro orange thermal shift assay of AL153 BJ (black) and its corresponding Fab (gray, dotted). **e,** 3D models obtained with Rosetta Antibody of AL153 BJ and AL153 Fab. L chains are shown in green and H chain in cyan. **f,** Predicted free energy of binding (ΔG_{GB}) according to the MM-GBSA calculations estimating the binding affinity of BJ and Fab complexes. **** $P \leq 0.0001$, as determined by unpaired t-test.

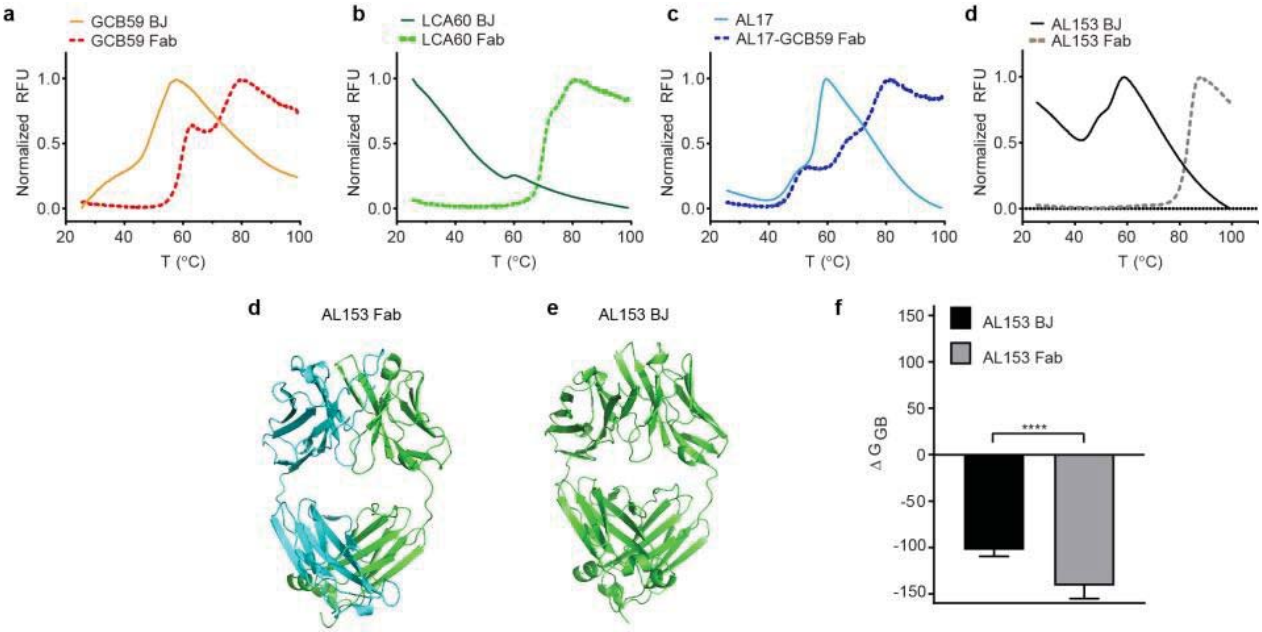

Figure 6.5. L chain dimers expose free thiols. Free thiols were quantified using the thiol-reactive probe CPM. **a,** Free thiol quantification of AL, GL and two λ-containing Fabs. **b,** Free thiol quantification of wild type (WT) and mutant L chains with a serine substitution of the terminal cysteine (CL_C105S) for two free L chains. **c,** Free thiol quantification of AL153 BJ protein and AL153 Fab. Paired VH VL sequences were obtained from an AL amyloidosis patient. **d,** Free thiol quantification of AL17 BJ protein and AL17-GBB59 Fab counterpart. The Fab was obtained by pairing with an unrelated H chain.

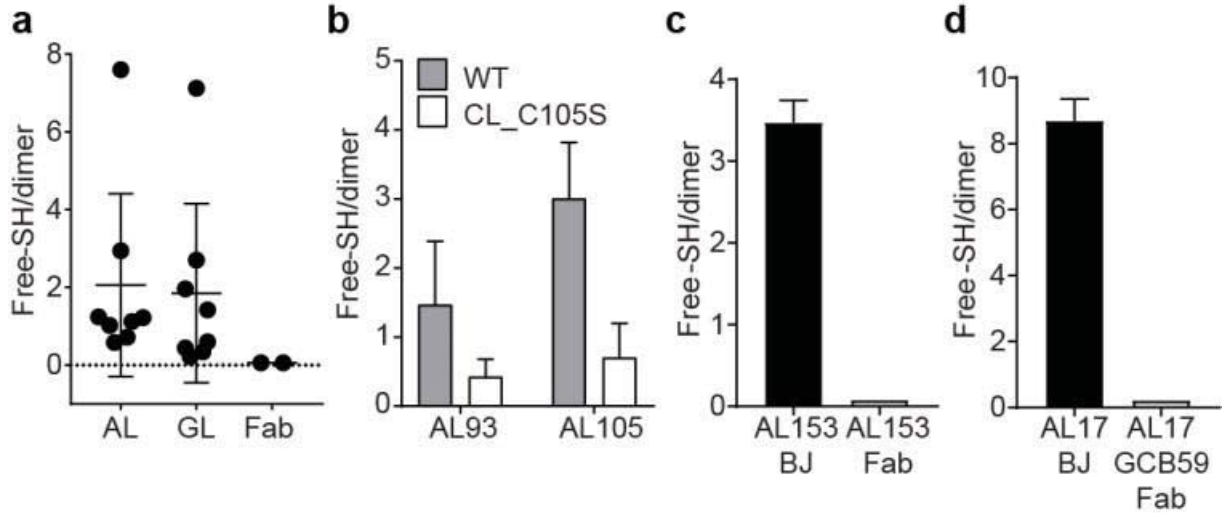

Figure 6.6. L chains aggregation into amyloid-like material is promoted by reducing conditions and is aggravated by somatic mutations. L chains were incubated with shaking at 37 °C in the presence or absence of DTT and the formation of aggregates was monitored by turbidity measurement (OD560nm), ThT fluorescence (RFU) and Congo Red binding (a.u.). **a,** Reducing agent dependency of AL93 aggregation (0.5mg/mL). **b,** Kinetics of aggregation measured by ThT and turbidity of AL93 (0.5mg/mL) in the presence of 50 mM DTT. **c,** Aggregation kinetics of 1mg/mL AL (left) and the corresponding GL (right) in the presence of DTT. **d,** End-point Congo Red binding (a.u.) of AL and GL in the presence or absence of DTT. **e,f,** Kinetics parameters of AL and GL aggregation assessed by end-point turbidity and $t_{1/2}$ (h). **g,** TEM imaging of prefibrillar aggregates. Scale bar 200 nm **h, i,** Enhanced kinetics of aggregation via addition of homologous seeds.

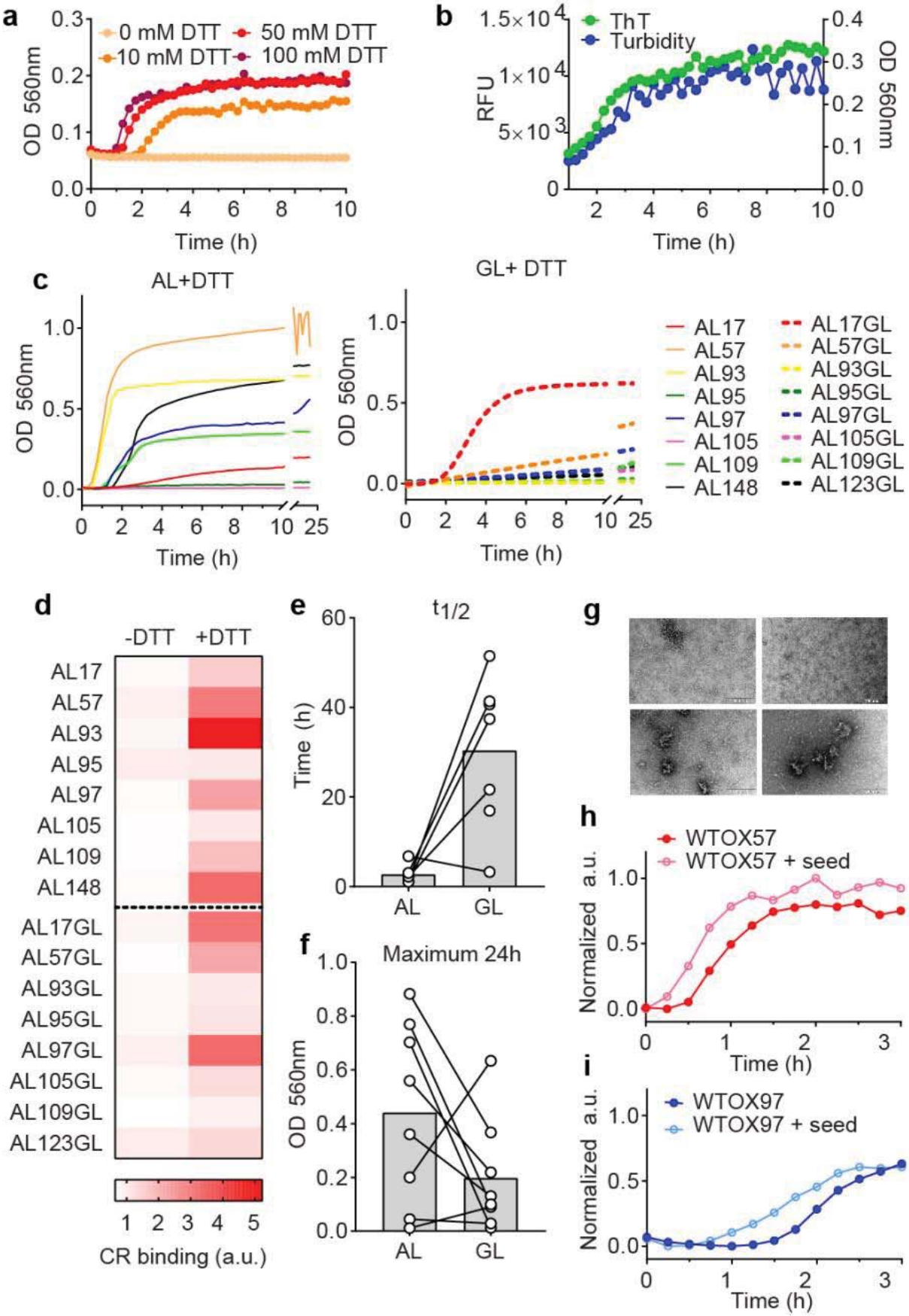
a
0 mM DTT
10 mM DTT
50 mM DTT
100 mM DTT
OD 560nm
Time (h)
b
ThT
Turbidity
RFU
OD 560nm
Time (h)
c
AL+DTT
GL+ DTT
OD 560nm
Time (h)
AL17
AL57
AL93
AL95
AL97
AL105
AL109
AL148
AL17GL
AL57GL
AL93GL
AL95GL
AL97GL
AL105GL
AL109GL
AL123GL
d
-DTT
+DTT
CR binding (a.u.)
e
t1/2
Time (h)
AL
GL
f
Maximum 24h
OD 560nm
g
h
WTOX57
WTOX57 + seed
Normalized a.u.
Time (h)
i
WTOX97
WTOX97 + seed
Normalized a.u.
Time (h)

Figure 6.7. DCs provide a reducing extracellular microenvironment. Monocytes-derived Dendritic cells (moDCs) maturation was induced with LPS or R848 and free thiols content of the supernatant was quantified using the thiol-reactive probe CPM. **a,** Free thiol content after 6 hours of stimulation. **b,** Free thiol content after 18 hours of stimulation.

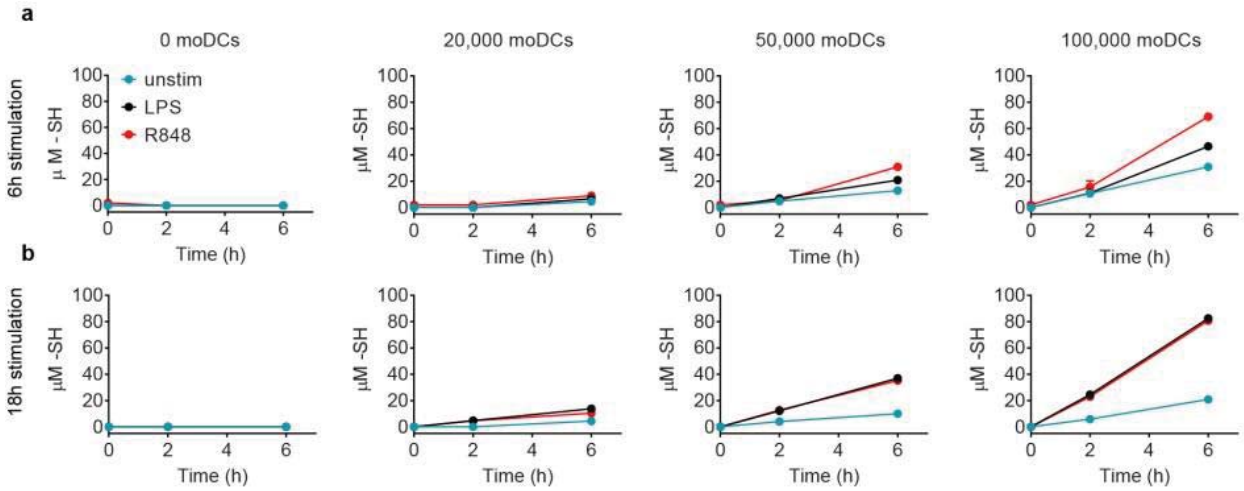

Figure 6.8. Free L chains have unique specificities and bind to cells and to the extracellular matrix. **a,** IgG1 molecules displaying identical N-terminal VL domains (LCA and LCB) and a control IgG_1 antibody (MGU10, NANP18-specific) were used to select peptides from a peptide display library. Shown is the binding of the three antibodies to the peptides selected by LCA (peptide 1 and peptide 2) and by MGU10 (peptide 5). **b,** Binding of 1 μM AL, GL L chains and 2 λ-containing Fabs to fixed and permeabilized Ag8.653 cells Hep2 cells assessed by flow cytometry. Shown is the mean fluorescence intensity (MFI) of the peaks. ns non significant, * $P \leq 0.0332$, ** $P \leq 0.0021$, as determined by unpaired t test with Welch's correction. **c,** Binding of 1 μM AL153 BJ, AL153 Fab and controls to fixed and permeabilized Ag8.653 cells Hep2 cells assessed by flow cytometry. **d,** Immunofluorescence staining of fixed and permeabilized Hep2 cells by AL93 and secondary control (mock). DAPI (blue) and anti- λ L chain (gray) staining are shown. Scale bar 50 μm. **e,** Quantification of immunofluorescence staining on mouse heart section of AL, GL, Fabs (λ, control) and antibodies (Ab, λ, control) probed with anti-λ L chain-AF647 secondary antibody (normalized to DAPI staining). **f,** Binding ELISA of AL, GL, BJ L chains and Fabs (λ, control) to Matrigel or PBS. Shown is the endpoint PBS vs Matrigel binding. **g,** Representative example of Matrigel retention of three free L chains and rapid elution of an antibody (Rituximab). **h,** Dissociation from Matrigel of AL, GL and Fabs (λ, control) expressed as the amount of protein retained in Matrigel droplets after 2 hours elution.

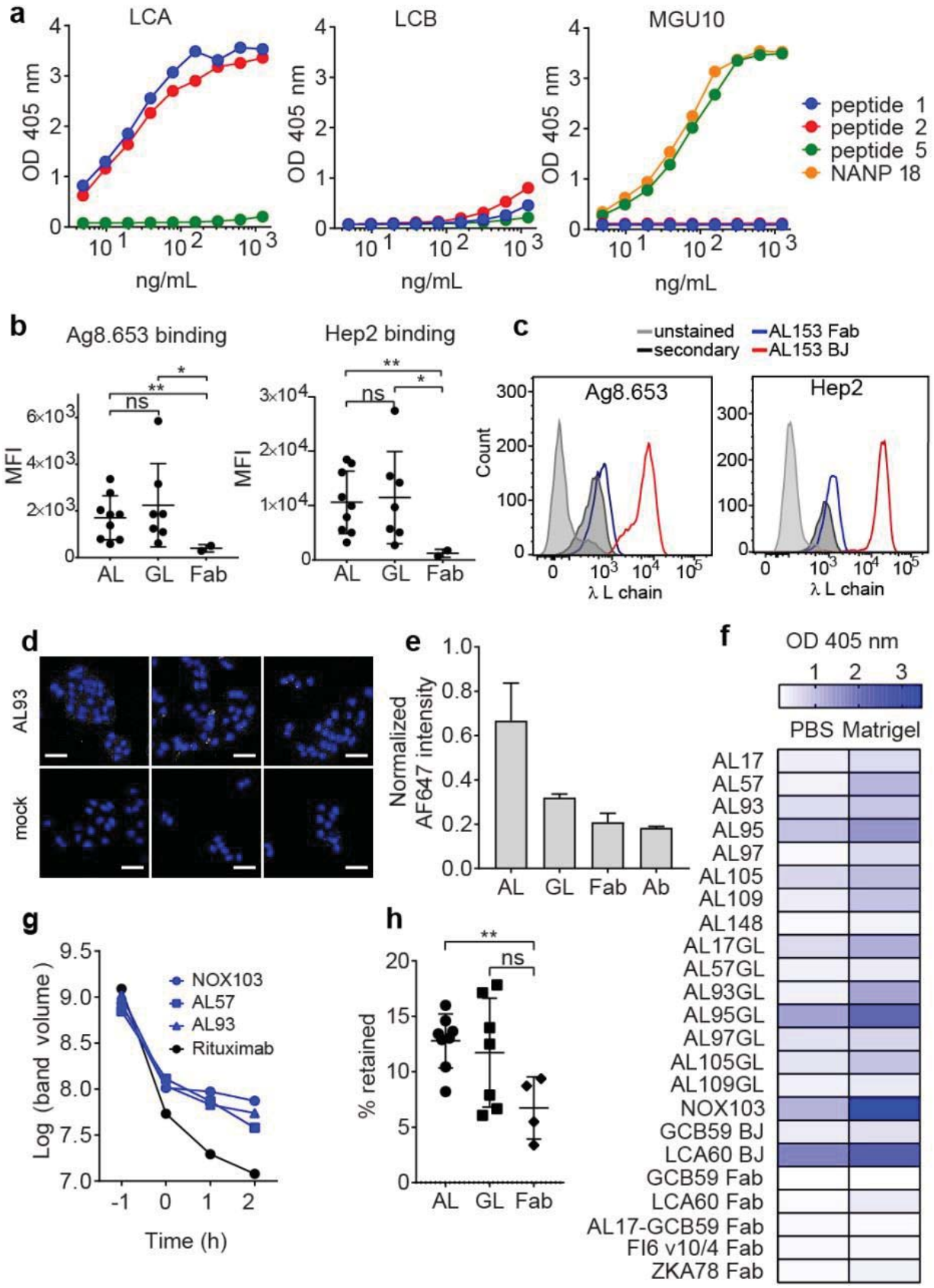
a
LCA
LCB
MGU10
OD 405 nm
ng/mL
peptide 1
peptide 2
peptide 5
NANP 18
b
Ag8.653 binding
Hep2 binding
MFI
ns
AL
GL
Fab
c
unstained
secondary
AL153 Fab
AL153 BJ
Ag8.653
Hep2
Count
λ L chain
d
AL93
mock
e
Normalized AF647 intensity
AL
GL
Fab
Ab
f
OD 405 nm
PBS Matrigel
AL17
AL57
AL93
AL95
AL97
AL105
AL109
AL148
AL17GL
AL57GL
AL93GL
AL95GL
AL97GL
AL105GL
AL109GL
NOX103
GCB59 BJ
LCA60 BJ
GCB59 Fab
LCA60 Fab
AL17-GCB59 Fab
FI6 v10/4 Fab
ZKA78 Fab
g
Log (band volume)
NOX103
AL57
AL93
Rituximab
Time (h)
h
% retained

7. Experimental Procedures

Selection of samples. L chain sequences were selected from the Amyloid Light Chain Database (ALBase) (Bodi *et al.*, 2009) or from a dataset of sequences from the group of our collaborator Prof. Merlini, Amyloidosis Research and Treatment Center, Fondazione IRCCS Policlinico San Matteo and Department of Molecular Medicine, University of Pavia. All other, non AL amyloidosis related sequences were selected from a dataset of sequences either from the laboratory of Prof. Lanzavecchia or from Dr. Davide Corti from Humabs Biomed, a subsidiary of Vir. All sequences were synthesized by Genscript, and their accuracies were confirmed by sequencing.

Sequence analysis of antibodies and reversion to germline The usage of VL genes and the amount of somatic mutations were determined by analysing the homology of sequences to known human V, D and J genes by the IMGT (international ImMunoGeneTics information system) database (Lefranc *et al.*, 2009). Sequences of "germline L chains" (GL) were determined by reverting mutations to the germline sequence while retaining the original CDR3 junctions and terminal deoxy-nucleotidyl transferase (TdT) N nucleotides.

Molecular biology. Paired H and L chains sequences were obtained from BM cells Tryzol lysate provided by the group of our collaborator Prof. Merlini. RNA was extracted using Direct-zol RNA MiniPrep Zymo-Spin IIC Columns (Zymo Research) and used for cDNA synthesis employing the template switching technique approach (Picelli *et al.*, 2014). Ig genes were amplified with specific primers and a library of unique sequences was obtained by Zero Blunt® TOPO® PCR Cloning Kit (Life Technologies) and subsequent analysis of single colonies.

B cell immortalization. Peripheral blood samples were obtained from healthy donors. Memory B cells were isolated using anti-PE microbeads (Miltenyi Biotec) following staining of PBMCs with CD19-PE-Cy7 (BD Phamingen), and were immortalized with Epstein-Barr virus (EBV) and CpG in multiple wells as described previously (Traggiai *et al.*, 2004).

Production of proteins. All proteins were produced by trasfection of Expi293 cells (Thermo Fisher scientific) and purified by affinity chromatography using Column Hitrap LambdaFabSelect (GE Healthcare) for L chains, CaptureSelect™ Pre-packed Column IgG-CH1 (GE Healthcare) for Fabs and HiTrap® rprotein A Fast Flow (GE Healthcare) for antibodies with glycine 0.1 M pH 2.7 elution. Positive fractions were neutralized with Tris HCl 1 M pH 9 and desalted with HiPrep™ 26/10 Desalting, column L × I.D. 10 cm × 26 mm, 17-132 µm particle size columns (GE Healthcare). Purified proteins were concentrated using VIVASPIN 20 PES 50.000 MWCO

or VIVASPIN 20 PES 10.000 MWCO (Sartorius) to more than 1 mg/ml, quantified with Nanodrop and filter sterilized through Millex-GP, 0,22 µm, PES filters (Merck Millipore).

Circular Dicroism. Far-UV spectra of 0.1 mg/ml proteins were recorded and analyzed using CAPITO, a CD Analysing and Plotting tool (Wiedemann, Bellstedt and Görlach, 2013). The secondary structure prediction of an IgG antibody was used as a control.

Size exclusion chromatography. 150 µg protein were diluted to a volume of 600 µl with PBS, spun at 16,000 g, 20 minutes, 4 °C. The supernatant was loaded on a Superdex 200 Increase 10/300 GL column (GE Healthcare) or a Superdex 75 Increase 10/300 GL (GE Healthcare). Fractions were eluted by isocratic elution with PBS, 0.2 ml/minute and collected in multiwell plates. The stability of the fractions was assessed by incubation at 37 °C for increasing time intervals and non-reducing SDS-PAGE analysis of aliquots.

Protein Electrophoresis and Western Blotting. Samples were diluted in either in bolt LDS 4X sample loading buffer or Nupage LDS 4X sample loading buffer, with or without 10X sample reducing agent and loaded on Bolt™ 4-12% Bis-Tris Plus Gels (Life Technologies), 15-well. Gels were run at 200 Volts for 20 minutes. For Commassie Staining Imperial™ Protein Stain (Life Technologies) was used following manufacturer protocol. For Western Blotting gels were briefly washed with milliQ water and transferred using iBlot 2 PVDF Mini Transfer Stacks (Life Technologies) with the iBlot™ 2 Gel Transfer Device (Life Technologies). Membranes were blocked by 30 minutes incubation with 10% Blotting-grade non-fat dry milk (Bio-Rad Laboratories) in TBST. Membranes were probed with different combinations of primary and secondary antibodies, including Goat anti Human Lambda (Southern Biotechnology Associates), Rabbit Anti-Goat IgG (H+L), HRP conjugate (Southern Biotechnology Associates). Briefly, primary antibody was incubated for 90 minutes at room temperature or over-night at 4 °C, washed 3 times for 5 minutes with TBST. Secondary antibody was incubated 45 minutes at room temperature and washed 3 times for 5 minutes with TBST and once with TBS for 5 minutes. Membranes were developed with SuperSignal™ West Pico PLUS Chemiluminescent Substrate (Life Technologies) and imaged either with ImageQuant LAS 4000 (GE Healthcare) or Amersham Imager 600 imager (GE Healthcare). Bands were quantified with Multi Gauge image analysis software (FUJIFILM) .

Aggregation tests. Aggregation tests were performed in Corning® 96 well NBS™ Microplates. 100 µl 0.5-1 mg/ml L chains dilutions were incubated with 0-100 µM DTT, 0-20% (v/v) seeds, 0.05% NaN_3. Plates were sealed with MicroAmp™ Optical Adhesive Film (Life Technologies)

and incubated in Biotek plate reader with linear shaking at 37°C. Aggregation was monitored by turbidity measurement, as OD560 nm. Aggregation curves were plotted with Graph-pad prism and their kinetic parameters were extrapolated after non-linear fitting. End-point CR binding was measured adapting the protocol described by Klunk and collaborators (Klunk, Pettegrew and Abraham, 1989). 12 µl of protein solutions were mixed to 5 µl of 360 µM CR in a final volume of 100 µl. CR binding was calculated as follows:

$$CR_{binding}(a.u.) = \left[\frac{A_{540}}{25.295} - \frac{A_{480}}{46.306}\right] \cdot 1000$$

Alternatively, aggregation tests were performed in Corning® 96 well NBS™ Microplates. 100 µl 0.5-1 mg/ml L chains dilutions were incubated with 0-100 µM DTT, 40 µM ThT, 0.05% NaN_3. Plates were sealed with MicroAmp™ Optical Adhesive Film (Life Technologies) and incubated in Cytation 3 reader (Biotek) with double orbital shaking at 37°C, with excitation 440 nm and emission at 484 nm.

Thermal Shift assay. 18 µl 0.1 mg/ml protein were added to 2 µl 100X Sypro Orange (from a 5000X stock) in MicroAmp™ Fast Optical 96-Well Reaction Plates, 0.1mL Plates (Life Technologies); plates were sealed with MicroAmp™ Optical Adhesive Film (Life Technologies) and analyzed in a 7900HT Fast Real-Time PCR System (Life Technologies) with the ROX reporter. Dissociation curves were normalized and the melting temperatures were extrapolated from the minima of first derivative of the dissociation curves. Hydrophobicity was computed as the Fluorescence measurement at 37°C.

Free thiol assay. 20 µl of serial dilutions of proteins were prepared in PBS and added to 10 µl of CPM (7-Diethylamino-3-(4'-Maleimidylphenyl)-4-Methylcoumarin) 150 µM in 384 plates. Plates were incubated in the dark for 15 minutes and read in a Cytation 3 reader (Biotek) with excitation and emission at 384/470 nm. Cysteine was used as a standard and Bovine Serum Albumin (BSA) as a positive control. After subtraction of blank, the free thiol level was estimated as a ratio of free thiol divided for the molar concentration of protein.

Flow cytometry. Cells were fixed/permeabilized with Acetone:Methanol 1:1 and probed with 1 µM L chains or Fabs as "primary antibody" and 1/100 dilution of Goat Anti-Human Lambda-Alexa Fluor® 647 (Southern Biotechnology Associates) as secondary antibody. Samples were acquired with BD FACSCanto or BD Fortessa and analyzed with FlowJo software.

Immunofluorescence staining. For Hep2 staining, 300,000 cells were cells were seeded on glass coverslips in 6 well plates; after 2 days cells were washed twice with PBS++ and fixed by

Acetone:Methanol 1:1, probed with 50 μg/ml L chains as "primary antibody" and 1/100 dilution of Goat Anti-Human Lambda-Alexa Fluor 647 (Southern Biotechnology Associates) as secondary antibody. Coverslips were mounted with Vectashield Mounting Medium with DAPI (Rectolab). For mouse heart staining, a C57BL/6 mouse was sacrificed; organs were perfused with PBS, fixed with 4% Paraformaldehyde for 1 hour on ice and dehydrated by overnight incubation in 30% sucrose at 4°C. 20 μm sections were cut using a cryostat, permeabilized with 0.5% Triton X-100 for 5 minutes, washed twice with TBST and stained overnight at 4 °C with 200 nM sample dilutions in TBST with 5% goat serum. After two washes with TBST, slides were incubated for 30 minutes with 1/100 dilution Goat Anti-Human Lambda-Alexa Fluor 647 (Southern Biotechnology Associates), then washed twice with TBST and mounted with Vectashield Mounting Medium with DAPI (Rectolab). All images were acquired using a TCS SP5 Leica confocal microscope and analyzed with ImaJ software. We are thankful to Dr. Marcus Thelen and Dr. Egle Radice for support and access to reagents for mouse heart staining.

ELISA. For Matrigel binding, Microplates 96 well polystyrene Half Area clear flat bottom High Bind (Corning) were coated overnight at 4°C with 1/8 dilution of ECM Gel from Engelbreth-Holm-Swarm murine sarcoma (Matrigel) (Sigma Aldrich Chemie GmbH) in PBS. Wells were washed once with ice cold PBS and blocked for 60 minutes with blocking buffer (PBS 1% BSA). Wells were washed twice with PBST (PBS 0.05% Tween20) and incubated with serial dilutions of the samples of interest for 90 minutes. Wells were washed 4 times with PBST and incubated for 60 minutes with 1/500 secondary antibody dilution Goat Anti-Human Lambda-AP (Southern Biotechnology Associates) or Goat Anti-Human IgG AP (Southern Biotechnology Associates). Wells were washed 4 times with PBST and incubated with 4-Nitrophenyl phosphate disodium salt hexahydrate (Sigma Aldrich Chemie GmbH). OD405 nm was measured at several time points. For peptide display ELISA, Microplates 96 well polystyrene Half Area clear flat bottom High Bind (Corning) were coated overnight at 4°C with 10 μg/ml Avidin. Wells were washed twice with PBST (PBS 0.05% Tween20) and blocked for 60 minutes with blocking buffer (PBS 1% BSA). Wells were washed twice with PBST and incubated with 10 μg/ml biotinylated-peptides. Wells were washed twice with PBST and incubated with serial dilutions of the samples of interest for 90 minutes. Wells were washed 4 times with PBST and incubated for 60 minutes with 1/500 secondary antibody dilution Goat Anti-Mouse IgG, Human ads-AP (Southern Biotechnology Associates). Wells were washed times with PBST and incubated with 4-Nitrophenyl phosphate disodium salt hexahydrate (Sigma Aldrich Chemie GmbH). OD405 nm was measured at several time points.

ECM binding assay. 96 well flat bottom plates were coated with 5 µl-drops of ECM Gel from Engelbreth-Holm-Swarm murine sarcoma (Matrigel) (Sigma Aldrich Chemie GmbH). Matrigel was polymerized for 5 minutes at 37 °C. Wells were blocked with 150 µl warm blocking buffer (PBS 1% BSA) for 30 minutes at 37°C. Matrigel drops were briefly washed with 150 µl PBS and incubated for 1 hour at room temperature with 50 µl 5-50 µg/ml sample. Drops were briefly washed with 150 µl PBS and either lysed for 30 minutes at 4 °C with 20 µl 2X NuPAGE™ LDS Sample Buffer (Life Technologies) or incubated for one hour at room temperature with 150 µl PBS (1st wash). After the 1st wash drops were briefly washed and either lysed for 30 minutes at 4 °C with 20 µl 2X NuPAGE™ LDS Sample Buffer (Life Technologies) or incubated for one hour at room temperature with 150 µl PBS (2nd wash). After the 2nd wash drops were briefly washed and lysed for 30 minutes at 4 °C with 20 µl 2X NuPAGE™ LDS Sample Buffer (Life Technologies). 2 µl sample input and 16 µl lysed samples were diluted to reach 1X NuPAGE™ LDS Sample Buffer, in reducing conditions using 10X Bolt™ Sample Reducing Agent (Life Technologies) and run on SDS-PAGE as previously described. Bands were quantified and normalized to the total amount of input protein and the percentage of retained material was calculated.

Phage display. Peptide display experiments were performed adapting the protocol of Ph.D.-12 Phage Display Peptide Library Kit (New England Biolabs) as follows. For the first round of panning for each sample a well of a 96 well MicroWell™ MaxiSorp™ flat bottom plate (Nunc) was coated with 4 µg of Target (IgG-like molecules displaying two identical VL domains on the Light and Heavy chains) in 75 µl TBS overnight at 4 °C, then washed once with TBS, blocked for 1 hour with TBS 1% BSA, then washed once with TBS and incubated for 2 hours with $2 \cdot 10^9$ phages in 75 µl ($2{,}6 \cdot 10^{10}$ pfu/ml). Subsequently wells were washed 6 times with TBST, 3 times with TBS and binding phages were eluted with 100 µl 0.2 M Glycine pH 2.2 for 5 minutes and neutralized with 15 µl Tris HCl 1M pH 9. From the eluted phages 1 µl was used for titration with IPTG/Xgal plates and the remaining was used for amplification following the manufacturer instructions. Phages were purified following the manufacturer instructions and for the second to third round of panning an additional step of negative selection with an irrelevant target (irrelevant IgG) was employed in order to deplete phages binding to the constant region of the antibody or to BSA. For each sample 3 wells of a Maxisorp plate were coated with 4 µg of irrelevant target in 75 µl TBS overnight at 4°C and one well of a Maxisorp plate was coated with 4 µg of Target in 75 µl TBS overnight at 4 °C. The first irrelevant target-coated well was washed once with TBS, blocked for 1 hour with TBS 3% BSA, then washed once with TBS and incubated for 1 hour with $2 \cdot 10^9$ amplified phages in 75 µl ($2{,}6 \cdot 10^{10}$ pfu/ml). In parallel, the second irrelevant target-coated well

was washed, blocked for 1 hour with TBS 3% BSA and washed once with TBS. The phage solution was then transferred from the first irrelevant target-coated well to the second irrelevant target-coated well and incubated for 1 hour. In parallel, the third irrelevant target-coated well and the target-coated well were washed, blocked for 1 hour with TBS 3% BSA and washed once with TBS. The phage solution was diluted 2X with TBS then half of it was transferred to the third irrelevant target-coated well and half to target-coated well and incubated for 1 hour for the second round of panning, 45 minutes for the third and 30 minutes for the fourth. Subsequently wells were washed 6 times with TBST, 3 times with TBS and binding phages were eluted with 100 µl 0.2 M Glycine pH 2.2 for 5 minutes and neutralized with 15 µl Tris HCl 1M pH 9. From the eluted phages 1 µl was used for titration with IPTG/Xgal plates and the remaining was used for amplification following the manufacturer instructions. From the second round onward, an enrichment score was calculated by dividing the target-coated well for the yield of eluted phages from irrelevant-coated well (Mock). Enrichments of ten-fold or more were considered sufficient for sequencing. Phages were sequenced with 96 III REV primer following the manufacturer instructions after amplifying single colonies and extracting DNA by standard Miniprep.

TEM imaging of aggregates. TEM grids (Quantifoil, Carbon film, 400 mesh) were glow discharged for 45 seconds with negative polarity immediately before use (in EMITECH glow discharger). The sample was adsorbed to the grid by placing the grid onto a 5 µl droplet for 1 min. Then the grid was blotted dry to remove excess solution and washed briefly by touching on a droplet of staining solution. After blotting, the sample was negatively stained for 30 seconds (grid on droplet) and blotted again before air drying. All steps are performed at room temperature. Two staining solutions were tested: 2% aqueous uranyl acetate and 2% aqueous phosphotungstic acid (PTA), pH 7.2. PTA was found better suitable for these samples. Samples were imaged in a TEM (FEI Morgagni, Thermo Fischer Scientific) at 100 kV. We are grateful to Dr. M. Lucas, ScopeM, ETH Zurich, for generous support and access to the instrument.

Secretion of free thiols by moDCs. moDCs where differentiated as previously described (Sallusto, 1994). Increasing numbers of day 5 moDCs where plated in complete medium and their maturation was induced by the addition of 1 µg/ml LPS or 2.5 µg/ml R848 for 6 or 18 hours. Cells where washed twice and fresh, serum-free RPMI medium was added. Free thiol content in the supernatants was quantified with the CPM assay.

BJ and Fab modeling using Rosetta Antibody. We modelled Bence Jones (BJ) and AL153Fab structure using RosettaAntibody protocol, as previously described (Weitzner *et al.*, 2017). To obtain the model of the full-length structure, the conformation of constant domain and the initial

mutual orientation of variable and constant domains is modeled based on pdb entry 4FQH. In order to create our BJ models, we first grafted the variable domain of a Fab, using the light chain sequence of interest, to following build the corresponding BJ, and choosing a putative heavy chain to model an initial Fab which will be then used to create our homodimeric BJ structure. Therefore, as result of this first modelling step we obtained the variable domain's model of a Fab containing the light chain of interest. Then, starting from the modelled Fab, we generated the homodimeric BJ structure based on pdb entry 2OLD to obtain the initial mutual orientation of LC-LC variable domain. The generated models are finally subject to relaxing simulation in explicit water using AMBER ff14SB force field (Maier *et al.*, 2015) the TIP3P model for water (Jorgensen *et al.*, 1983), and the parameters proposed for the counter-ions (Joung and Cheatham, 2008). To minimize the obtained models we performed a two-step computational protocol consisting of an energy minimization for 10,000 steps, restraining the backbone atomic coordinates with a harmonic restraint (k = 20 kcal/mol/Å2), followed by an unrestrained energy minimization for 100,000 steps. Modeling was performed by Maura Garofalo and Dr. Andrea Cavalli, Institute for Research in Biomedicine (IRB), Università della Svizzera Italiana (USI).

In-silico prediction of protein thermodynamic stability changes upon mutations. The FoldX energy function version 4.0 was used to estimate the free-energy change upon mutations of the light chains of the Bence Jones germline structures in order to predict the effect of somatic mutations on the thermodynamic proteins' stability. The RepairPDB function of FoldX was first applied to the BJ germline structures to identify and repair amino acids which have bad torsion angles, or VanderWaals' clashes, or total energy. Then the BuildModel function was used to perform FoldX calculations to estimate the free-energy change upon mutations of the different BJ germline structures. Five independent runs were performed and then averaged. The typical predicted error for FoldX is around 0.8 kcal/mol (Guerois, Nielsen and Serrano, 2002). On the variable domain of the light chains of the AL153 BJ, AL153 Fab saturation mutagenesis was performed. Structures for this study were built using an in-house Python script which allows to perform all the possible point mutation at each position of the light chains using multithreading calculations. Then the BuildModel function was used as described above to calculate the free-energy change upon mutation. In-silico prediction of protein thermodynamic stability changes upon mutations was performed by Maura Garofalo and Dr. Andrea Cavalli, Institute for Research in Biomedicine (IRB), Università della Svizzera Italiana (USI).

Molecular dynamics (MD) and binding free energy calculations with MM-GBSA. To estimate the affinity of the AL153BJ, and AL153Fab structures, we performed 100ns MD

simulations in explicit water using AMBER16 and we used the corresponding trajectories to compute the binding energy ΔG with MM-GBSA, a computational method already used to compute the binding affinity of protein complexes. The BJ and the Fab structures were solvated in a water box with a minimum distance from the protein surface of 10 Å. The total charge of the system was neutralized adding a proper number of Cl-/Na+ ions. All molecular dynamics simulations were carried out using the ff14SB force field for the protein, the TIP3P model for water, and the parameters proposed by Joung et al. for the counter-ions. The BJ and the Fab structures were first relaxed with a two-step computational protocol consisting of an energy minimization for 10,000 steps, restraining the backbone atomic coordinates with a harmonic restraint (k = 20 kcal/mol/Å2), followed by an unrestrained energy minimization for 100,000. The systems were then heated to their final temperature of 310K in 40 ps. The simulations were run at constant volume, during the first 20 ps, subsequently, the velocities were reassigned and the systems equilibrated for 20 ps at constant pressure (1 Atm). Finally, all complexes were simulated for 100 ns and the obtained trajectories were used for the MM-GBSA calculations. Water molecules and counter-ions were stripped, while the BJ and the Fab complexes were parametrized using the same force field as in MD simulations. The polar contribution to solvation energy was computed with the Onufriev, Bashford and Case model (Onufriev, Bashford and Case, 2004) setting the dielectric constant to 1 for the solute and 80 for the solvent. MD and MM-GBSA calculations were performed by Maura Garofalo and Dr. Andrea Cavalli, Institute for Research in Biomedicine (IRB), Università della Svizzera Italiana (USI).

8. Discussion and Outlook

Our analysis reveals several novel aspects of free L chains biology: their heterogeneity and instability, their distinctive specificity and the remarkable structural and biophysical variation due to their homo-dimerization over their hetero-dimerization with H chains.

A first crucial aspect of our research was the use of recombinant L chains produced in mammalian cells. The production of reasonable amounts of amyloidogenic proteins represents a general challenge in the field of amyloidosis. Hence, several different biochemical approaches have been reported for the production of amyloidogenic L chains. Initially, based on the assumption that amyloid deposits were composed only of VL domains, most studies have been performed on L chain N-terminal domains, which are easily recombinantly produced and purified from bacteria, but do not genuinely represent the precursor species secreted by PCs (Lavatelli *et al.*, 2008; Vrana *et al.*, 2009). Only recently, expression and purification of full-length L chains from bacteria, based on the refolding of denatured protein, were described (Rognoni *et al.*, 2013). Compared to the limitations of those methods, a valuable alternative is represented by the purification of urine-derived BJ proteins, which however presents several constraints, namely the limited availability of samples and the potentially different biochemical properties of urine-derived L chains, which might not reflect those of their circulating counterparts (Lavatelli *et al.*, 2011).

Considering that the identity of the partially folded precursor of L chains amyloid aggregates is still controversial and that L chains are secretory proteins, which rely on ER folding and on possible Golgi apparatus-mediated post-translational modifications, the use of eukaryotic cells to study amyloidogenic L chains could be extremely advantageous, in order to obtain sufficient amounts of L chains in a conformation as close as the one displayed by the species circulating in the sera of patients. Besides limited pioneering studies (Arosio *et al.*, 2012; Klimtchuk *et al.*, 2017), our experimental approach empowered us to appreciate crucial features of L chain biology, which are lost by current protein production and purification strategies, such as their intrinsic heterogeneity and instability, which are in accordance with the recently described model of L chain transient unfolding after secretion, resulting in a mixed ensemble of L chains, with distinct susceptibility to amyloidogenesis (Morgan, Usher and Kelly, 2017).

In detail, by SEC and non-reducing SDS-PAGE analysis we could appreciate the high degree of heterogeneity in terms of L chain MW distribution, suggesting the co-existence of several entities. Our findings extend the observation of a population of L chains isoforms, characterized by multiple charge isoforms and N-terminal amino acid losses (Lavatelli *et al.*, 2011). Interestingly,

the distribution of L chains seemed to reflect GL-dependent characteristics, besides a general tendency to populate covalently linked and non-covalently linked dimeric species, together with monomers, at least for some L chains; most importantly, the MW assemblies observed are in agreement with the non-reducing SDS-PAGE profiles of immunoprecipitated free L chains from AL amyloidosis patients sera (Lavatelli *et al.*, 2011), emphasizing that the mammalian expression system is suitable to produce samples resembling patient-derived L chains.

The observation of non-covalently linked species was corroborated by the presence of free thiols, especially located at the terminal Cysteine residue. Moreover, the residual proportion of free thiols observed in C105S mutants indicates that, at the population level, a small proportion of L chains presents reduced inter-molecular disulphide bridges either in the VL or in the CL domain; based on this finding, we postulate that partially reduced L chains, despite present in low proportions, may become relevant amyloidogenic species when L chains are secreted in large amounts by clonally expanded malignant PCs (Morgan, Usher and Kelly, 2017).

Additionally, our finding is supported by previously described post-translational modifications occurring at the Cysteine residue usually involved in the formation of the intra-molecular disulphide bridge of the CL domain, which imply the presence, at least in a transient stage, of a free thiol at that location and a consequent rearrangement in the pattern of disulphide bridges (Lavatelli *et al.*, 2011). A potential pro-amyloidogenic role of free thiols is supported by the description in an extended family affected by an hereditary form of systemic amyloidosis of a Serine to Cysteine mutation in the CK domain (Benson, Liepnieks and Kluve-Beckerman, 2015).

Somatically mutated AL L chains did not globally present either a higher heterogeneity or a higher proportion of monomeric species, despite in some cases, such as for AL57, the impact of somatic mutations on L chain heterogeneity was remarkable. The presence of L chains monomers and dimers has been described by several studies (Aucouturier *et al.*, 1993; Andrich *et al.*, 2017), however the presence of non-canonic dimeric L chains represents a novel observation, which could prove significant by demonstrating that non-canonic L chains dimers represent a crucial entity in the pathway of amyloid formation. The structural determinants for the GL-specific MW ensembles and their potential association with AL amyloidosis need to be further investigated by the combination of computational and structural studies, namely Small-angle X-ray scattering (SAXS), and by the analysis of other L chains belonging to the same GLs.

Additionally, both AL and GL L chains presented a similar level of hydrophobicity at 37 °C as measured through the binding of the fluorescent dye Sypro Orange. It is particularly meaningful

to analyze the hydrophobicity of amyloidogenic proteins, considering that hydrophobic patches are chemical groups that should remain buried in the protein core under native conditions; accordingly, the exposure of hydrophobic moieties is widely considered a peculiar characteristic of misfolded precursor species of oligomers in the context of several amyloid-associated disorders (Bolognesi *et al.*, 2010; Campioni *et al.*, 2010; Knowles, Vendruscolo and Dobson, 2014). In the same line, we speculate that also the exposure of free thiols observed in all L chains, which is seldom reported in antibodies, where rare free thiols remain buried in the protein core (Hongcheng Liu* and Kimberly May, 2012; Zhang *et al.*, 2012), could be considered as another example of unusual display of chemical, even reactive, groups on the surface of an amyloidogenic protein.

Interestingly, somatic mutations favored a more rapid exposure of additional hydrophobic moieties at higher temperatures, suggesting that AL L chains were characterized by a lower thermodynamic stability, in line with previous studies, which reported that the thermodynamic instability of a single AL amyloidosis BJ protein could be dependent on somatic mutations (Baden *et al.*, 2008). Globally, our data indicate L chains present aberrant structural properties that are aggravated by somatic mutations. Remarkably, the results obtained in vitro correlated with in silico data, predicting through FoldX energy function a lower thermodynamic folding stability for AL L chains as compared to GL L chains both in the monomeric and dimeric form; importantly, the difference of the calculated thermodynamic stability of AL and GL L chains, expressed as $\Delta\Delta G$, was characterized by values of up to 25 times the prediction error of FoldX, which is estimated to be approximatively 0.8 kcal/mol, supporting the soundness of such computational approach.

In line with previous reports (Morgan and Kelly, 2016), we observed that full-length L chains, even if thermodynamically unstable, do not readily aggregate in native conditions, supporting the notion that the CL domain can exert an anti-amyloidogenic role. The study of the kinetics of aggregation in a reasonable experimental setting to describe phenomena that take place over several years in patients (Knowles, Vendruscolo and Dobson, 2014) requires the use of conditions that increase the concentration of the misfolded precursor responsible for the initiation of amyloid aggregation. Previous studies employed a wide array of stimuli to trigger VL or full-length L chains aggregation, spanning from high salt concentration to extreme pH conditions (Ramirez-Alvarado, 2013).

Considering that one of the most intriguing biophysical properties of L chains described in this study is the presence of a varying proportion of free thiols, we reasoned that a further

enhancement of L chain reduction could potentially either trigger or accelerate L chains aggregation into amyloid material by putatively increasing the concentration of the misfolded aggregation-prone amyloid precursor species. Indeed, the use of a reducing agent, as previously suggested (Andrich *et al.*, 2017), not only led to L chains aggregation, but also allowed us to discriminate between L chains from AL amyloidosis patients and their GL counterparts, providing a valuable tool to address the role of somatic mutations in the context of AL amyloidosis. The different rate and extent of aggregation of the L chain tested, corroborated by the seeding experiments, suggest that only a fraction of total L chains is the primary substrate for aggregation. Interestingly, the prominent aggregation of AL L chains, which are characterized by lower melting temperatures, compared to their GL counterparts is in line with the current models for amyloid state thermodynamic and kinetic accessibility (Baldwin *et al.*, 2011; Knowles, Vendruscolo and Dobson, 2014).

While reducing agents appear to be essential in the time frame and constraints of an in vitro experiment, it remains to be established whether the slow process of in vivo deposition might be dependent from the local production of reducing agents, such as thioredoxin secreted by dendritic cells and other cell types, especially upon activation (Angelini *et al.*, 2002), or will be fueled by a minor species that is already produced in a reduced form. Remarkably, we could provide evidence that immature moDCs are able to secrete discrete amounts of free thiols in vitro, which become substantial after maturation; considering that in our in vitro system each moDC could secrete approximatively 80 fmol of free thiols, it is noteworthy that in the small-scale volumes associated to the ECM such minute amounts could correspond to considerable local concentrations, as high as 160 mM estimating, by large excess, the volume of a monocyte to be approximatively 500 fL. Our speculation supports the notions that reducing conditions, even more stringent than what appears essential to foster L chains aggregation in vitro, are compatible with the extracellular milieu and suggests that immune cells, namely DCs, could potentially support the reducing environment required to trigger L chains fibrillogenesis.

To support this hypothesis, it could be decisive to systematically assess whether serum circulating L chains in AL amyloidosis patients present higher proportions of free thiols compared to what is observed in healthy donors, extending the preliminary observation of post-translational modifications occurring on L chains Cysteines, which implies the reduction of at least one of the two intra-chain disulphide bonds (Lavatelli *et al.*, 2011). An additional outlook will be the systematic assessment of the post-translational modifications, potentially promoting L chains aggregation, due to L chains co-incubation with moDCs. It is also crucial to consider that

increased oxidative stress is often associated with amyloidosis (Brenner *et al.*, 2004), despite the causal link between L chain aggregation and toxicity and oxidative stress is still controversial. However, considering that several studies described that L chain-related toxicity drives ROS production, it is likely that oxidizing conditions could be a consequence of amyloidosis rather than a cause thereof.

An intriguing perspective investigated in this thesis regards the divergent features of Fabs and L chains and the resulting impact on AL amyloidosis. In this regard, it is critical to note that most AL amyloidosis patients are characterized by the presence of a monoclonal component consisting of both free L chains and a full antibody counterpart, however it is still enigmatic why only free L chains are the causative agent of the disease, an observation that is corroborated by the fact that also patients characterized by deletions in the IgH locus, who present only free L chains as monoclonal component, can suffer from amyloidosis. If the sequence of each amyloidogenic L chains dictated its intrinsic instability, L chains and constructs thereof would be characterized by aberrant properties. This interpretation would imply that also amyloidogenic L chains-containing antibodies, due to L chains instability per se, could become pathogenic if they reached a critical concentration in target tissues. However, due to the MW-dependent differential distribution of antibodies and free L chains in tissues, only free L chains could be able to trigger amyloidogenesis. Conversely, we were able to observe that, compared to free L chains, the corresponding Fabs displayed no hydrophobic surfaces and no exposed free thiols, consistent with a higher thermodynamic stability, also supported by molecular dynamic simulations and free energy calculation associated to VL/VL and VL/VH dimerization. Our findings are consistent with the notion that L chains are selected, both in the primary and secondary repertoire, only for the formation of stable and functional BCRs.

As a consequence, somatic mutations on L chains are dependent on antigen-driven selection and affinity maturation (Perfetti *et al.*, 1998) operating on the heterodimer comprising the H and the L chain. We can assimilate the process of affinity maturation to any in vitro or in silico method aimed at screening and selecting high-affinity or high stability binding partners from a library, where selection operates thanks to the ability of the BCR to trigger an intracellular signaling cascade; considering that free L chains represent a by-product of antibody production rather than the species undergoing selection, it is straightforward that mutations leading to gain of affinity in the paired VH-VL domains could potentially generate deleterious effects on the L chain homodimer. Examples of this phenomenon are represented by conditional secretory L chains, where the presence of specific mutations generates L chains that cannot be secreted alone but that

can be rescued in the presence of an H chain partner (Dul, Burrone and Argon, 1992), and the evolutionary pressure on the VL/VH interface aimed at stabilizing highly affine antigen-antibody complexes (Sarel Fleishman, personal communication).

In this regard, it should be remarked that free LCs, as soluble species, devoid of any effector function and intrinsic signaling capacity, are able to escape the appropriate selection and stability checkpoint mechanisms; this phenomenon represents a failure of the basic principle of quality control of multi-protein complexes and exposes the individual to the risk of secreting unstable, aberrant proteins, potentially leading to a protein aggregation disorder once L chains are produced in large excess.

The inability of positive and negative selection to operate on free L chains led us to speculate that L chains could develop into rogue proteins that are not only prone to denaturation and aggregation but could also be endowed with the ability to bind self-antigens. Our data show a previously unappreciated property of L chain dimers, consisting of their distinctive specificity that can be described in terms of differential peptides binding but also extends to a general tendency to bind to cell surfaces and to the ECM. The latter properties are found in polyreactive or "sticky" antibodies which however are under control by negative selection (Wardemann *et al.*, 2003), while L chain dimer specificity is not. Intriguingly, none of the Fab analyzed, even at high concentration, displayed significant binding to the antigens tested. A putative rationale for L chains interaction with cell surfaces and the ECM could reside in the nature of their solvent exposed surface, where hydrophobic moieties and free thiols groups are present; likewise, the display of chemical groups that under normal physiological conditions should reside in the protein core is a distinctive feature of misfolded amyloid precursor species that has been hypothesized to lead to aberrant interactions with cellular components (Olzscha *et al.*, 2011; Knowles, Vendruscolo and Dobson, 2014).

The observation of L chain distinctive specificity suggests two major mechanisms that could be crucial for the sake of amyloidogenesis: an increase in L chain tissue concentration due to interaction with the ECM and a putative tissue-specific tropism. The former property, revealed by our ECM binding assay, is extremely significant, because it could clarify why free L chains are the causative agent of AL amyloidosis; not only free L chains will distribute in target organs better than their antibody counterparts due to their lower MW, but they will also be retained in the extracellular milieu, thus leading to a significant increase in the local concentration of thermodynamically unstable species, which could readily increase the critical concentration required to trigger amyloid aggregation, in agreement with the current model of amyloidogenesis

(Knowles, Vendruscolo and Dobson, 2014). In parallel, an intriguing perspective that could link binding to tissues and aggregation could be represented by a putative conformational change of the L chains triggered by binding to an antigen, resembling the conformational change of prion protein promoted by the engagement of its flexible tail by an antibody, resulting in aggregation and neurotoxicity (Sonati *et al.*, 2013). Further studies are needed to assess the binding of L chains to specific cellular and ECM-associated components, in order to evaluate whether interaction with specific antigens, rather than a general tendency to spuriously bind cells and tissues, could modulate L chain misfolding, trigger nucleation or enhance aggregation kinetics.

In parallel, through selection from a library of peptides, we could show a L chain-specific binding to linear peptides; our data provide a proof of principle that VL/VL dimers could be able to bind with high affinity and specificity given antigens. It is tempting to speculate that L chains binding to tissue-specific antigens could be responsible for AL L chains organ tropism, a concept that is supported by the association of specific organs involvement and IgL gene usage (Kourelis *et al.*, 2017). As previously mentioned, low affinity L chains interaction with self-antigens can be tolerated and is a direct consequence of their escape from positive and negative selection mechanisms. Future studies should take advantage of libraries of conformational epitopes to confirm L chain-specific binding and to guide the identification of potential tissue-specific antigens.

Altogether, our data support the importance of analyzing paired H and L chains expressed by amyloidogenic clones, as recently suggested by pioneering studies (Klimtchuk *et al.*, 2017). We were able to include in our analysis one representative example (AL153), for which we could retrieved paired sequences; however, a major limitation is represented by the unavailability of the H chain sequences corresponding to L chain sequences from databases like ALBase. Future experiments should extend our preliminary observations on additional VL/VL and VH/VL counterparts, by short-term culture of BM PCs from AL amyloidosis patients that could allow to analyze and compare the species produced by PCs to recombinantly produced ones.

In parallel, it will be critical to validate our hypothesis by analyzing through in vitro and in silico stability approaches whether somatic mutations that are associated to Fab affinity maturation could result into destabilization of the free L chains counterpart, corroborating our theory on L chains evasion from quality checkpoints, due to their impracticable selection. Finally, the same set of analysis should be performed on κ L chains that, as stated in the introduction, are seldom associated to AL amyloidosis, in order to ascertain whether their lower amyloidogenic propensity is due to a higher stability or to the lack of interaction with self. Collectively, our analysis, by

emphasizing the complexity of AL amyloidosis pathophysiology, is in close agreement with the notion that protein misfolding diseases can arise from small perturbations of protein homeostasis, spanning from mutations and post-translational modification to failure of quality checkpoints and increased concentration (Knowles, Vendruscolo and Dobson, 2014).

Specifically, we speculate that the break of homeostasis occurs at several levels through a combination of factors that involve L chains concentration, their escape from positive and negative selection and the micro-environment. In order to observe aggregation L chains concentration should reach an maintain a critical level for extensive periods of time due to the expansion of a malignant B cell clone and to reduced metabolic clearance, as supported not only by the presence of high levels of circulating free L chains years before the onset of the disease but also by the description of an hereditary form of AL amyloidosis, where age-related metabolic factors increase in the concentration of a species that has been present from birth, thus dictating the late-onset of the disease (Weiss *et al.*, 2014; Benson, Liepnieks and Kluve-Beckerman, 2015). High levels of free L chains are also associated to MM, where no amyloid aggregation is observed; however we could speculate that, due to the more severe pathogenic mechanisms of MM, the low patients survival could limit the possibility to observe amyloid formation. A second failure of protein homeostasis is represented by the failure of quality and tolerance checkpoints, which can be considered a general characteristic of L chains rather than a property of amyloidogenic L chains. In parallel, the tissue micro-environment might act as an enhancer of L chains intrinsic aberrant properties, by supporting a dramatic increase in the local concentration via binging to tissue cells and to the ECM and putatively providing the source for post-translational modifications.

9. Appendix

9.1 List of Figures

9.2 References

Aguzzi, A., Kranich, J. and Krautler, N. J. (2014) 'Follicular dendritic cells: Origin, phenotype, and function in health and disease', *Trends in Immunology*. doi: 10.1016/j.it.2013.11.001.

Allen, C. D. C. *et al.* (2007) 'Imaging of germinal center selection events during affinity maturation', *Science*. doi: 10.1126/science.1136736.

Ami, D. *et al.* (2016) 'In situ characterization of protein aggregates in human tissues affected by light chain amyloidosis: a FTIR microspectroscopy study', *Scientific Reports*. doi: 10.1038/srep29096.

Andrich, K. *et al.* (2017) 'Aggregation of full-length immunoglobulin light chains from systemic light chain amyloidosis (AL) patients is remodeled by epigallocatechin-3-gallate', *Journal of Biological Chemistry*. doi: 10.1074/jbc.M116.750323.

Angelini, G. *et al.* (2002) 'Antigen-presenting dendritic cells provide the reducing extracellular microenvironment required for T lymphocyte activation', *Proceedings of the National Academy of Sciences*. doi: 10.1073/pnas.022630299.

Arendt, B. K. *et al.* (2008) 'Biologic and genetic characterization of the novel amyloidogenic lambda light chain-secreting human cell lines, ALMC-1 and ALMC-2', *Blood*. doi: 10.1182/blood-2008-03-143040.

Arosio, P. *et al.* (2012) 'In vitro aggregation behavior of a non-amyloidogenic λ light chain dimer deriving from U266 multiple myeloma cells', *PLoS ONE*. doi: 10.1371/journal.pone.0033372.

Attaelmannan, M. and Levinson, S. S. (2000) 'Understanding and identifying monoclonal gammopathies', in *Clinical Chemistry*.

Aucouturier, P. *et al.* (1993) 'Monoclonal Ig L chain and L chain V domain fragment crystallization in myeloma-associated Fanconi's syndrome.', *Journal of immunology (Baltimore, Md. : 1950)*.

Azimzadeh, A. and Van Regenmortel, M. H. V. (1990) 'Antibody affinity measurements', *Journal of Molecular Recognition*. doi: 10.1002/jmr.300030304.

Baden, E. M. *et al.* (2008) 'Altered dimer interface decreases stability in an amyloidogenic protein', *Journal of Biological Chemistry*. doi: 10.1074/jbc.M705347200.

Baldwin, A. J. *et al.* (2011) 'Metastability of native proteins and the phenomenon of amyloid formation', *Journal of the American Chemical Society*. doi: 10.1021/ja2017703.

Bannard, O. and Cyster, J. G. (2017) 'Germinal centers: programmed for affinity maturation and antibody diversification', *Current Opinion in Immunology*. Elsevier Ltd, 45, pp. 21–30. doi: 10.1016/j.coi.2016.12.004.

Barclay, A. N. (2003) 'Membrane proteins with immunoglobulin-like domains - A master superfamily of interaction molecules', *Seminars in Immunology*. doi: 10.1016/S1044-5323(03)00047-2.

Basnayake, K. *et al.* (2011) 'The biology of immunoglobulin free light chains and kidney injury', *Kidney International*. Elsevier Masson SAS, 79(12), pp. 1289–1301. doi: 10.1038/ki.2011.94.

Bassing, C. H., Swat, W. and Alt, F. W. (2002) 'The mechanism and regulation of chromosomal

V(D)J recombination', *Cell*. doi: 10.1016/S0092-8674(02)00675-X.

Basso, K. and Dalla-Favera, R. (2015) 'Germinal centres and B cell lymphomagenesis', *Nature Reviews Immunology*. Nature Publishing Group, 15(3), pp. 172–184. doi: 10.1038/nri3814.

Basten, A. and Silveira, P. A. (2010) 'B-cell tolerance: Mechanisms and implications', *Current Opinion in Immunology*. doi: 10.1016/j.coi.2010.08.001.

Batuman, V. *et al.* (1998) 'Myeloma light chains are ligands for cubilin (gp280).', *The American journal of physiology*.

Batuman, V., Dreisbach, A. W. and Cyran, J. (1990) 'Light-chain binding sites on renal brush-border membranes', *Am J Physiol*.

Batuman, V. and Guan, S. (1997) 'Receptor-mediated endocytosis of immunoglobulin light chains by renal proximal tubule cells.', *The American journal of physiology*. doi: 10.1111/j.1365-294X.2011.05389.x.

Benson, M. D., Liepnieks, J. J. and Kluve-Beckerman, B. (2015) 'Hereditary systemic immunoglobulin light-chain amyloidosis', *Blood*. doi: 10.1182/blood-2014-12-618108.

Berek, C. and Milstein, C. (1987) 'Mutation Drift and Repertoire Shift in the Maturation of the Immune Response', *Immunological Reviews*. doi: 10.1111/j.1600-065X.1987.tb00507.x.

Bernard, O., Hozumi, N. and Tonegawa, S. (1978) 'Sequences of mouse immunoglobulin light chain genes before and after somatic changes', *Cell*. doi: 10.1016/0092-8674(78)90041-7.

Bernasconi, N. L., Traggiai, E. and Lanzavecchia, A. (2002) 'Maintenance of serological memory by polyclonal activation of human memory B cells', *Science*. doi: 10.1126/science.1076071.

Blancas-Mejia, L. M. *et al.* (2018) 'Immunoglobulin light chain amyloid aggregation', *Chemical Communications*. Royal Society of Chemistry, 54(76), pp. 10664–10674. doi: 10.1039/C8CC04396E.

Blancas-Mejía, L. M. and Ramirez-Alvarado, M. (2016) 'Recruitment of Light Chains by Homologous and Heterologous Fibrils Shows Distinctive Kinetic and Conformational Specificity', *Biochemistry*. doi: 10.1021/acs.biochem.6b00090.

Bochtler, T. *et al.* (2011) 'Hyperdiploidy is less frequent inAL amyloidosis compared with monoclonal gammopathy of undetermined significance and inversely associated with translocation t(11;14)', *Blood*. doi: 10.1182/blood-2010-02-268987.

Bodi, K. *et al.* (2009) 'AL-Base: A visual platform analysis tool for the study of amyloidogenic immunoglobulin light chain sequences', *Amyloid*. doi: 10.1080/13506120802676781.

Bodin, K. *et al.* (2010) 'Antibodies to human serum amyloid P component eliminate visceral amyloid deposits', *Nature*. doi: 10.1038/nature09494.

Bolognesi, B. *et al.* (2010) 'ANS binding reveals common features of cytotoxic amyloid species', *ACS Chemical Biology*. doi: 10.1021/cb1001203.

Bork, P., Holm, L. and Sander, C. (1994) 'The immunoglobulin fold: Structural classification, sequence patterns and common core', *Journal of Molecular Biology*. doi: 10.1006/jmbi.1994.1582.

Brack, C. *et al.* (1978) 'A complete immunoglobulin gene is created by somatic recombination',

Cell. doi: 10.1016/0092-8674(78)90078-8.

Brenner, D. A. *et al.* (2004) 'Human Amyloidogenic Light Chains Directly Impair Cardiomyocyte Function Through an Increase in Cellular Oxidant Stress', *Circulation Research*. doi: 10.1161/01.RES.0000126569.75419.74.

Brink, R. (2014) 'The imperfect control of self-reactive germinal center B cells', *Current Opinion in Immunology*. Elsevier Ltd, 28(1), pp. 97–101. doi: 10.1016/j.coi.2014.03.001.

Burnet, F. M. (1976) 'A Modification of Jerne's Theory of Antibody Production using the Concept of Clonal Selection', *CA: A Cancer Journal for Clinicians*. doi: 10.3322/canjclin.26.2.119.

Burnett, D. L. *et al.* (2018) 'Germinal center antibody mutation trajectories are determined by rapid self/foreign discrimination', *Science*, 360(6385), pp. 223–226. doi: 10.1126/science.aao3859.

Buxbaum, J. N. (2009) 'Animal models of human amyloidoses: Are transgenic mice worth the time and trouble?', *FEBS Letters*. doi: 10.1016/j.febslet.2009.07.031.

Cambier, J. C. *et al.* (2007) 'B-cell anergy: From transgenic models to naturally occurring anergic B cells?', *Nature Reviews Immunology*, 7(8), pp. 633–643. doi: 10.1038/nri2133.

Campioni, S. *et al.* (2010) 'A causative link between the structure of aberrant protein oligomers and their toxicity', *Nature Chemical Biology*. doi: 10.1038/nchembio.283.

Castillo, J. J. (2016) 'Plasma Cell Disorders', *Primary Care - Clinics in Office Practice*. Elsevier Inc, 43(4), pp. 677–691. doi: 10.1016/j.pop.2016.07.002.

Chiti, F. *et al.* (1999) 'Designing conditions for in vitro formation of amyloid protofilaments and fibrils', *Proceedings of the National Academy of Sciences*. doi: 10.1073/pnas.96.7.3590.

Chiti, F. and Dobson, C. M. (2009) 'Amyloid formation by globular proteins under native conditions', *Nature Chemical Biology*. doi: 10.1038/nchembio.131.

Chung, J. B., Silverman, M. and Monroe, J. G. (2003) 'Transitional B cells: Step by step towards immune competence', *Trends in Immunology*. doi: 10.1016/S1471-4906(03)00119-4.

Comenzo, R. L. *et al.* (2001) 'The tropism of organ involvement in primary systemic amyloidosis: Contributions of Ig VLgerm line gene use and clonal plasma cell burden', *Blood*. doi: 10.1182/blood.V98.3.714.

Davis, M. M. and Bjorkman, P. J. (1988) 'T-cell antigen receptor genes and T-cell recognition [published erratum appears in Nature 1988 Oct 20;335(6192):744]', *Nature*.

Defrance, T., Taillardet, M. and Genestier, L. (2011) 'T cell-independent B cell memory', *Current Opinion in Immunology*. doi: 10.1016/j.coi.2011.03.004.

Detanico, T. *et al.* (2013) 'Somatic mutagenesis in autoimmunity', *Autoimmunity*. doi: 10.3109/08916934.2012.757597.

Diomede, L. *et al.* (2014) 'A Caenorhabditis elegans-based assay recognizes immunoglobulin light chains causing heart amyloidosis', *Blood*. doi: 10.1182/blood-2013-10-525634.

Duhamel, S. *et al.* (2017) 'Incidence and Prevalence of Light Chain Amyloidosis: A Population-Based Study', *Blood*.

Dul, J. L. *et al.* (1996) 'lg Light Chains Are Secreted Predominantly as Monomers', *The journal of immunology*. doi: 10.1152/ajpgi.00394.2001.

Dul, J. L., Burrone, O. R. and Argon, Y. (1992) 'A conditional secretory mutant in an Ig L chain is caused by replacement of tyrosine/phenylalanine 87 with histidine.', *Journal of immunology (Baltimore, Md. : 1950)*.

Duong, B. H. *et al.* (2010) 'Decoration of T-independent antigen with ligands for CD22 and Siglec-G can suppress immunity and induce B cell tolerance in vivo', *The Journal of Experimental Medicine*. doi: 10.1084/jem.20091873.

Duty, J. A. *et al.* (2009) 'Functional anergy in a subpopulation of naive B cells from healthy humans that express autoreactive immunoglobulin receptors', *The Journal of Experimental Medicine*. doi: 10.1084/jem.20080611.

Eanes, E. D. and Glenner, G. G. (1968) 'X-ray diffraction studies on amyloid filaments.', *The journal of histochemistry and cytochemistry : official journal of the Histochemistry Society*. doi: 10.1177/16.11.673.

Eisen, H. N. and Siskind, G. W. (1964) 'Variations in Affinities of Antibodies during the Immune Response', *Biochemistry*. doi: 10.1021/bi00895a027.

Enqvist, S., Sletten, K. and Westermark, P. (2009) 'Fibril protein fragmentation pattern in systemic AL-amyloidosis', *Journal of Pathology*. doi: 10.1002/path.2607.

Fändrich, M. and Dobson, C. M. (2002) 'The behaviour of polyamino acids reveals an inverse side chain effect in amyloid structure formation', *EMBO Journal*. doi: 10.1093/emboj/cdf573.

Feige, M. J. *et al.* (2009) 'An Unfolded CH1 Domain Controls the Assembly and Secretion of IgG Antibodies', *Molecular Cell*. doi: 10.1016/j.molcel.2009.04.028.

Feige, M. J., Hendershot, L. M. and Buchner, J. (2010) 'How antibodies fold', *Trends in Biochemical Sciences*. doi: 10.1016/j.tibs.2009.11.005.

Fitzpatrick, A. W. P. *et al.* (2013) 'Atomic structure and hierarchical assembly of a cross-amyloid fibril', *Proceedings of the National Academy of Sciences*. doi: 10.1073/pnas.1219476110.

Fugmann, S. D. *et al.* (2000) 'The RAG Proteins and V(D)J Recombination: Complexes, Ends, and Transposition', *Annual Review of Immunology*. doi: 10.1146/annurev.immunol.18.1.495.

Garay Sánchez, S. A. *et al.* (2017) 'Stability and aggregation propensity do not fully account for the association of various germline variable domain gene segments with light chain amyloidosis', *Biological Chemistry*. doi: 10.1515/hsz-2016-0178.

Gertz, M. A. *et al.* (2016) 'First-in-human phase I/II study of NEOD001 in patients with light chain amyloidosis and persistent organ dysfunction', *Journal of Clinical Oncology*. doi: 10.1200/JCO.2015.63.6530.

Glenner, G. G. *et al.* (1969) 'Physical and chemical properties of amyloid fibers. II. Isolation of a unique protein constituting the major component from human splenic amyloid fibril concentrates.', *The journal of histochemistry and cytochemistry : official journal of the Histochemistry Society*. doi: 10.1177/17.12.769.

Goodnow, C. C. *et al.* (1988) 'Altered immunoglobulin expression and functional silencing of

self-reactive B lymphocytes in transgenic mice', *Nature*. doi: 10.1038/334676a0.

Goodnow, C. C. *et al.* (2005) 'Cellular and genetic mechanisms of self tolerance and autoimmunity', *Nature*. doi: 10.1038/nature03724.

Goto, Y., Azuma, T. and Hamaguchi, K. (1979) 'Refolding of the immunoglobulin light chain', *Journal of Biochemistry*. doi: 10.1093/oxfordjournals.jbchem.a132470.

Guan, J. *et al.* (2013) 'Stanniocalcin1 is a key mediator of amyloidogenic light chain induced cardiotoxicity', *Basic Research in Cardiology*. doi: 10.1007/s00395-013-0378-5.

Guan, J. *et al.* (2014) 'Lysosomal dysfunction and impaired autophagy underlie the pathogenesis of amyloidogenic light chain-mediated cardiotoxicity', *EMBO Molecular Medicine*. doi: 10.15252/emmm.201404190.

Guerois, R., Nielsen, J. E. and Serrano, L. (2002) 'Predicting changes in the stability of proteins and protein complexes: A study of more than 1000 mutations', *Journal of Molecular Biology*. doi: 10.1016/S0022-2836(02)00442-4.

Haas, I. G. and Wabl, M. (1983) 'Immunoglobulin heavy chain binding protein', *Nature*. doi: 10.1038/306387a0.

Halaby, D. M. and Mornon, J. P. E. (1998) 'The immunoglobulin superfamily: An insight on its tissular, species, and functional diversity', *Journal of Molecular Evolution*. doi: 10.1007/PL00006318.

Halverson, R., Torres, R. M. and Pelanda, R. (2004) 'Receptor editing is the main mechanism of B cell tolerance toward membrane antigens', *Nature Immunology*. doi: 10.1038/ni1076.

Hartley, S. B. *et al.* (1993) 'Elimination of self-reactive B lymphocytes proceeds in two stages: Arrested development and cell death', *Cell*. doi: 10.1016/0092-8674(93)90111-3.

Hendershot, L. M. and Sitia, R. (2003) 'Immunoglobulin Assembly and Secretion', in *Molecular Biology of B Cells*. doi: 10.1016/B978-012053641-2/50018-6.

Hippen, K. L. L., Tze, L. E. E. and Behrens, T. W. W. (2000) 'CD5 maintains tolerance in anergic B cells.', *Journal of Experimental Medicine*. doi: 10.1084/jem.191.5.883.

Hombach, J. *et al.* (1990) 'Molecular components of the B-cell antigen receptor complex of the IgM class', *Nature*. doi: 10.1038/343760a0.

Hongcheng Liu* and Kimberly May (2012) 'Disulfide bond structures of IgG molecules', *mAbs*. doi: 10.4161/mabs.4.1.18347.

Hozumi, N. and Tonegawa, S. (1976) 'Evidence for somatic rearrangement of immunoglobulin genes coding for variable and constant regions.', *Proceedings of the National Academy of Sciences*. doi: 10.1073/pnas.73.10.3628.

Hrncic, R. *et al.* (2000) 'Antibody-mediated resolution of light chain-associated amyloid deposits', *American Journal of Pathology*. doi: 10.1016/S0002-9440(10)64639-1.

Huang, Z. Q. *et al.* (1993) 'Bence Jones proteins bind to a common peptide segment of Tamm-Horsfall glycoprotein to promote heterotypic aggregation', *Journal of Clinical Investigation*, 92(6), pp. 2975–2983. doi: 10.1172/JCI116920.

Huang, Z. Q. and Sanders, P. W. (1997) 'Localization of a single binding site for immunoglobulin

light chains on human Tamm-Horsfall glycoprotein', *Journal of Clinical Investigation*, 99(4), pp. 732–736. doi: 10.1172/JCI119218.

Huber, R. *et al.* (1976) 'Crystallographic structure studies of an IgG molecule and an Fc fragment', *Nature*. doi: 10.1038/264415a0.

Hurle, M. R. *et al.* (1994) 'A role for destabilizing amino acid replacements in light-chain amyloidosis.', *Proceedings of the National Academy of Sciences*. doi: 10.1073/pnas.91.12.5446.

Imperlini, E. *et al.* (2017) 'Proteotoxicity in cardiac amyloidosis: Amyloidogenic light chains affect the levels of intracellular proteins in human heart cells', *Scientific Reports*. doi: 10.1038/s41598-017-15424-3.

Jacob, J. *et al.* (1991) 'Intraclonal generation of antibody mutants in germinal centres', *Nature*. doi: 10.1038/354389a0.

Jorgensen, W. L. *et al.* (1983) 'Comparison of simple potential functions for simulating liquid water', *The Journal of Chemical Physics*. doi: 10.1063/1.445869.

Joung, I. S. and Cheatham, T. E. (2008) 'Determination of alkali and halide monovalent ion parameters for use in explicitly solvated biomolecular simulations', *Journal of Physical Chemistry B*. doi: 10.1021/jp8001614.

Jucker, M. and Walker, L. C. (2011) 'Pathogenic protein seeding in Alzheimer disease and other neurodegenerative disorders', *Annals of Neurology*. doi: 10.1002/ana.22615.

Jung, D. *et al.* (2006) 'Mechanism and Control of V(D)J Recombination At the Immunoglobulin Heavy Chain Locus', *Annual Review of Immunology*, 24(1), pp. 541–570. doi: 10.1146/annurev.immunol.23.021704.115830.

Jung, D. and Alt, F. W. (2004) 'Unraveling V(D)J Recombination: Insights into Gene Regulation', *Cell*. doi: 10.1016/S0092-8674(04)00039-X.

Kalmanson, G. M. and Bronfenbrenner, J. (1942) 'The reversal of Pneumococcus quellung by digestion of the antibody with papain', *Science*. doi: 10.1126/science.96.2479.21.

Kara, E. E. and Nussenzweig, M. C. (2018) 'Redemption for self-reactive antibodies', *Science*, 360(6385), pp. 152–153. doi: 10.1126/science.aat5758.

Keeling, J., Teng, J. and Herrera, G. A. (2004) 'AL-amyloidosis and light-chain deposition disease light chains induce divergent phenotypic transformations of human mesangial cells', *Laboratory Investigation*. doi: 10.1038/labinvest.3700161.

Kim, Y. S. *et al.* (2000) 'Thermodynamic modulation of light chain amyloid fibril formation', *Journal of Biological Chemistry*. doi: 10.1074/jbc.275.3.1570.

Klassen, R. B. S. *et al.* (2005) 'Light chains are a ligand for megalin.', *Journal of applied physiology (Bethesda, Md. : 1985)*. doi: 10.1152/japplphysiol.01090.2003.

Klimtchuk, E. S. *et al.* (2017) 'In vitro co-expression of human amyloidogenic immunoglobulin light and heavy chain proteins: a relevant cell-based model of AL amyloidosis', *Amyloid*. doi: 10.1080/13506129.2017.1336996.

Klinman, N. R. (1996) 'The "clonal selection hypothesis" and current concepts of B cell tolerance', *Immunity*. doi: 10.1016/S1074-7613(00)80314-3.

Klunk, W. E., Pettegrew, J. W. and Abraham, D. J. (1989) 'Quantitative evaluation of Congo red binding to amyloid-like proteins with a beta-pleated sheet conformation', *Journal of Histochemistry and Cytochemistry*. doi: 10.1177/37.8.2666510.

Knarr, G. *et al.* (1995) 'BiP binding sequences in antibodies', *Journal of Biological Chemistry*. doi: 10.1074/jbc.270.46.27589.

Knowles, T. P. J. *et al.* (2009) 'An analytical solution to the kinetics of breakable filament assembly', *Science*. doi: 10.1126/science.1178250.

Knowles, T. P. J., Vendruscolo, M. and Dobson, C. M. (2014) 'The amyloid state and its association with protein misfolding diseases', *Nature Reviews Molecular Cell Biology*. doi: 10.1038/nrm3810.

Kourelis, T. V. *et al.* (2017) 'Clarifying immunoglobulin gene usage in systemic and localized immunoglobulin light-chain amyloidosis by mass spectrometry', *Blood*. doi: 10.1182/blood-2016-10-743997.

Kuehl, W. M. and Bergsagel, P. L. (2012) 'Molecular pathogenesis of multiple myeloma and its premalignant precursor', *Journal of Clinical Investigation*. doi: 10.1172/JCI61188.

Kumar, S. K. *et al.* (2011) 'Recent improvements in survival in primary systemic amyloidosis and the importance of an early mortality risk score', *Mayo Clinic Proceedings*. doi: 10.4065/mcp.2010.0480.

Kuraoka, M. *et al.* (2016) 'Complex Antigens Drive Permissive Clonal Selection in Germinal Centers', *Immunity*. doi: 10.1016/j.immuni.2016.02.010.

Kurosaki, T., Kometani, K. and Ise, W. (2015) 'Memory B cells', *Nature Reviews Immunology*. Nature Publishing Group, 15(3), pp. 149–159. doi: 10.1038/nri3802.

Kyle, R. A. *et al.* (1992) 'Incidence and natural history of primary systemic amyloidosis in Olmsted County, Minnesota, 1950 through 1989.', *Blood*.

Kyle, R. and Gertz, M. (1995) 'Primary Amyloidosis - Clinical and Laboratory Features in 474 cases.pdf', *Seminars in Hematology*.

Labbadia, J. and Morimoto, R. I. (2015) 'The Biology of Proteostasis in Aging and Disease', *Annual Review of Biochemistry*. doi: 10.1146/annurev-biochem-060614-033955.

Laffleur, B. *et al.* (2013) 'AID-induced remodeling of immunoglobulin genes and B cell fate IgM memory', *Oncotarget*, 5(5), pp. 1118–1131. doi: 10.18632/oncotarget.1546.

Landgren, O. *et al.* (2009) 'Monoclonal gammopathy of undetermined significance (MGUS) consistently precedes multiple myeloma: A prospective study', *Blood*. doi: 10.1182/blood-2008-12-194241.

Lanzavecchia, A. (1985) 'Antigen-specific interaction between T and B cells', *Nature*. doi: 10.1038/314537a0.

Lau, C. M. *et al.* (2005) 'RNA-associated autoantigens activate B cells by combined B cell antigen receptor/Toll-like receptor 7 engagement', *The Journal of Experimental Medicine*. doi: 10.1084/jem.20050630.

Lavatelli, F. *et al.* (2008) 'Amyloidogenic and Associated Proteins in Systemic Amyloidosis Proteome of Adipose Tissue', *Molecular & Cellular Proteomics*. doi: 10.1074/mcp.M700545-

MCP200.

Lavatelli, F. *et al.* (2011) 'A novel approach for the purification and proteomic analysis of pathogenic immunoglobulin free light chains from serum', *Biochimica et Biophysica Acta - Proteins and Proteomics*. doi: 10.1016/j.bbapap.2010.12.012.

Lavatelli, F. *et al.* (2015) 'Novel mitochondrial protein interactors of immunoglobulin light chains causing heart amyloidosis', *FASEB Journal*. doi: 10.1096/fj.15-272179.

Leadbetter, E. A. *et al.* (2002) 'Chromatin-IgG complexes activate B cells by dual engagement of IgM and Toll-like receptors', *Nature*. doi: 10.1038/416603a.

Lebien, T. W. and Tedder, T. F. (2008) 'B lymphocytes : how they develop and function - ASH 50th anniversary review', *The american society of hematology*, 112(5), pp. 1570–1580. doi: 10.1182/blood-2008-02-078071.

Lefranc, M. P. *et al.* (2009) 'IMGT (R), the international ImMunoGeneTics information system (R)', *Nucleic Acids Research*. doi: Doi 10.1093/Nar/Gkn838.

Leitzgen, K., Knittler, M. R. and Haas, I. G. (1997) 'Assembly of immunoglobulin light chains as a prerequisite for secretion: A model for oligomerization-dependent subunit folding', *Journal of Biological Chemistry*. doi: 10.1074/jbc.272.5.3117.

Leung-Hagesteijn, C. *et al.* (2013) 'Xbp1s-Negative Tumor B Cells and Pre-Plasmablasts Mediate Therapeutic Proteasome Inhibitor Resistance in Multiple Myeloma', *Cancer Cell*. doi: 10.1016/j.ccr.2013.08.009.

Levinson, R. T. *et al.* (2013) 'Role of mutations in the cellular internalization of amyloidogenic light chains into cardiomyocytes', *Scientific Reports*. doi: 10.1038/srep01278.

Lin, Y. C. *et al.* (2010) 'A global network of transcription factors, involving E2A, EBF1 and Foxo1, that orchestrates B cell fate', *Nature Immunology*. doi: 10.1038/ni.1891.

Linke, R. P. (2012) 'On Typing Amyloidosis Using Immunohistochemistry. Detailled Illustrations, Review and a Note on Mass Spectrometry', *Progress in Histochemistry and Cytochemistry*, 47(2), pp. 61–132. doi: 10.1016/j.proghi.2012.03.001.

Lohr, J. G. *et al.* (2014) 'Widespread genetic heterogeneity in multiple myeloma: Implications for targeted therapy', *Cancer Cell*. doi: 10.1016/j.ccr.2013.12.015.

Lu, L. L. *et al.* (2018) 'Beyond binding: Antibody effector functions in infectious diseases', *Nature Reviews Immunology*. Nature Publishing Group, 18(1), pp. 46–61. doi: 10.1038/nri.2017.106.

Lührs, T. *et al.* (2005) '3D structure of Alzheimer's amyloid-beta(1-42) fibrils.', *Proceedings of the National Academy of Sciences of the United States of America*. doi: 10.1073/pnas.0506723102.

Ma, K. K., Ogawa, T. and De Bold, A. J. (2004) 'Selective upregulation of cardiac brain natriuretic peptide at the transcriptional and translational levels by pro-inflammatory cytokines and by conditioned medium derived from mixed lymphocyte reactions via p38 MAP kinase', *Journal of Molecular and Cellular Cardiology*. doi: 10.1016/j.yjmcc.2004.01.001.

Madan, S. *et al.* (2010) 'Clinical features and treatment response of light chain (AL) amyloidosis diagnosed in patients with previous diagnosis of multiple myeloma', *Mayo Clinic Proceedings*.

doi: 10.4065/mcp.2009.0547.

Maier, J. A. *et al.* (2015) 'ff14SB: Improving the Accuracy of Protein Side Chain and Backbone Parameters from ff99SB', *Journal of Chemical Theory and Computation*. doi: 10.1021/acs.jctc.5b00255.

Manz, R. A. *et al.* (1998) 'Survival of long-lived plasma cells is independent of antigen', *International Immunology*. doi: 10.1093/intimm/10.11.1703.

Marin-Argany, M. *et al.* (2016) 'Cell damage in light chain amyloidosis fibril internalization, toxicity and cell-mediated seeding', *Journal of Biological Chemistry*. doi: 10.1074/jbc.M116.736736.

Martin, D. J. and Ramirez-Alvarado, M. (2011) 'Glycosaminoglycans promote fibril formation by amyloidogenic immunoglobulin light chains through a transient interaction', *Biophysical Chemistry*. doi: 10.1016/j.bpc.2011.05.011.

De Matteis, M. A. *et al.* (2017) 'The 5-phosphatase OCRL in Lowe syndrome and Dent disease 2', *Nature Reviews Nephrology*, 13(8), pp. 455–470. doi: 10.1038/nrneph.2017.83.

Mayer, C. T. *et al.* (2017) 'The microanatomic segregation of selection by apoptosis in the germinal center', *Science*. doi: 10.1016/0301-6226(82)90033-1.

McHeyzer-Williams, M. *et al.* (2012) 'Molecular programming of B cell memory', *Nature Reviews Immunology*. Nature Publishing Group, 12(1), pp. 24–34. doi: 10.1038/nri3128.

Mclaughlin, R. W. *et al.* (2006) 'The effects of sodium sulfate, glycosaminoglycans, and Congo red on the structure, stability, and amyloid formation of an immunoglobulin light-chain protein', *Protein Science*. doi: 10.1110/ps.051997606.

McWilliams-Koeppen, H. P. *et al.* (2015) 'Light chain amyloid fibrils cause metabolic dysfunction in human cardiomyocytes', *PLoS ONE*. doi: 10.1371/journal.pone.0137716.

Melchers, F. (2005) 'The pre-B-cell receptor: Selector of fitting immunoglobulin heavy chains for the B-cell repertoire', *Nature Reviews Immunology*. doi: 10.1038/nri1649.

Merlini, G. *et al.* (2018) 'Systemic immunoglobulin light chain amyloidosis', *Nature Reviews Disease Primers*, 4(1), p. 38. doi: 10.1038/s41572-018-0034-3.

Merlini, G. and Bellotti, V. (2003) 'Molecular Mechanisms of Amyloidosis', *New England Journal of Medicine*. doi: 10.1056/NEJMra023144.

Merlini, G. and Stone, M. J. (2006) 'Dangerous small B-cell clones', *Blood*. doi: 10.1182/blood-2006-03-001164.

Mesin, L., Ersching, J. and Victora, G. D. (2016) 'Germinal Center B Cell Dynamics', *Immunity*. Elsevier Inc., 45(3), pp. 471–482. doi: 10.1016/j.immuni.2016.09.001.

Mian, I. S., Bradwell, A. R. and Olson, A. J. (1991) 'Structure, function and properties of antibody binding sites', *Journal of Molecular Biology*. doi: 10.1016/0022-2836(91)90617-F.

Miettinen, T. A. and Kekki, M. (1967) 'Effect of impaired hepatic and renal function on [131]bence jones protein catabolism in human subjects', *Clinica Chimica Acta*. doi: 10.1016/0009-8981(67)90036-8.

Migrino, R. Q. *et al.* (2011) 'Human microvascular dysfunction and apoptotic injury induced by

AL amyloidosis light chain proteins', *AJP: Heart and Circulatory Physiology*. doi: 10.1152/ajpheart.00503.2011.

Miralles, G. D., O'Fallon, J. R. and Talley, N. J. (1992) 'Plasma-Cell Dyscrasia with Polyneuropathy', *New England Journal of Medicine*. doi: 10.1056/NEJM199212313272705.

Mishra, S. *et al.* (2013) 'Human amyloidogenic light chain proteins result in cardiac dysfunction, cell death, and early mortality in zebrafish', *AJP: Heart and Circulatory Physiology*. doi: 10.1152/ajpheart.00186.2013.

Mond, J. J. *et al.* (1995) 'T cell independent antigens', *Current Opinion in Immunology*. doi: 10.1016/0952-7915(95)80109-X.

Monis, G. F. *et al.* (2006) 'Role of endocytic inhibitory drugs on internalization of amyloidogenic light chains by cardiac fibroblasts', *American Journal of Pathology*. doi: 10.2353/ajpath.2006.060183.

Monroe, J. G. (2006) 'ITAM-mediated tonic signalling through pre-BCR and BCR complexes', *Nature Reviews Immunology*. doi: 10.1038/nri1808.

Morgan, G. J. and Kelly, J. W. (2016) 'The Kinetic Stability of a Full-Length Antibody Light Chain Dimer Determines whether Endoproteolysis Can Release Amyloidogenic Variable Domains', *Journal of Molecular Biology*. doi: 10.1016/j.jmb.2016.08.021.

Morgan, G. J., Usher, G. A. and Kelly, J. W. (2017) 'Incomplete Refolding of Antibody Light Chains to Non-Native, Protease-Sensitive Conformations Leads to Aggregation: A Mechanism of Amyloidogenesis in Patients?', *Biochemistry*. doi: 10.1021/acs.biochem.7b00579.

Mostoslavsky, R., Alt, F. W. and Rajewsky, K. (2004) 'The lingering enigma of the allelic exclusion mechanism', *Cell*. doi: 10.1016/j.cell.2004.08.023.

Nemazee, D. (2017) 'Mechanisms of central tolerance for B cells', *Nature Reviews Immunology*, 17(5), pp. 281–294. doi: 10.1038/nri.2017.19.

Nielsen, R. and Christensen, E. I. (2010) 'Proteinuria and events beyond the slit', *Pediatric Nephrology*. doi: 10.1007/s00467-009-1381-9.

Nimmerjahn, F. and Ravetch, J. V. (2008) 'Fc receptors', in *How the Immune System Recognizes Self and Nonself: Immunoreceptors and Their Signaling*. doi: 10.1007/978-4-431-73884-8_6.

Nokwe, C. N. *et al.* (2015) 'The Antibody Light-Chain Linker Is Important for Domain Stability and Amyloid Formation', *Journal of Molecular Biology*. doi: 10.1016/j.jmb.2015.09.012.

Nutt, S. L. *et al.* (2015) 'The generation of antibody-secreting plasma cells', *Nature Reviews Immunology*. Nature Publishing Group, 15(3), pp. 160–171. doi: 10.1038/nri3795.

Nutt, S. L. and Kee, B. L. (2007) 'The Transcriptional Regulation of B Cell Lineage Commitment', *Immunity*. doi: 10.1016/j.immuni.2007.05.010.

Nuvolone, M. *et al.* (2017) 'Regulated expression of amyloidogenic immunoglobulin light chains in mice', *Amyloid*. doi: 10.1080/13506129.2017.1289914.

Nyström, S. N. and Westermark, G. T. (2012) 'AA-Amyloid is cleared by endogenous immunological mechanisms', *Amyloid*. doi: 10.3109/13506129.2012.711391.

Oberti, L. *et al.* (2017) 'Concurrent structural and biophysical traits link with immunoglobulin

light chains amyloid propensity', *Scientific Reports*. doi: 10.1038/s41598-017-16953-7.

Obici, L. *et al.* (2005) 'Clinical aspects of systemic amyloid diseases', in *Biochimica et Biophysica Acta - Proteins and Proteomics*. doi: 10.1016/j.bbapap.2005.08.014.

Oliva, L. *et al.* (2017) 'The amyloidogenic light chain is a stressor that sensitizes plasma cells to proteasome inhibitor toxicity', *Blood*. doi: 10.1182/blood-2016-08-730978.

Olzscha, H. *et al.* (2011) 'Amyloid-like aggregates sequester numerous metastable proteins with essential cellular functions', *Cell*. doi: 10.1016/j.cell.2010.11.050.

Onufriev, A., Bashford, D. and Case, D. A. (2004) 'Exploring Protein Native States and Large-Scale Conformational Changes with a Modified Generalized Born Model', *Proteins: Structure, Function and Genetics*. doi: 10.1002/prot.20033.

Packard, T. A. and Cambier, J. C. (2013) 'B lymphocyte antigen receptor signaling: initiation, amplification, and regulation', *F1000Prime Reports*. doi: 10.12703/P5-40.

Palladini, G. *et al.* (2006) 'Circulating amyloidogenic free light chains and serum N-terminal natriuretic peptide type B decrease simultaneously in association with improvement of survival in AL', *Blood*. doi: 10.1182/blood-2005-11-4385.

Pepys, M. B. *et al.* (1994) 'Human serum amyloid P component is an invariant constituent of amyloid deposits and has a uniquely homogeneous glycostructure', *Proc Natl Acad Sci U S A*. doi: 10.1073/pnas.91.12.5602.

Pérez-Persona, E. *et al.* (2007) 'New criteria to identify risk of progression in monoclonal gammopathy of uncertain significance and smoldering multiple myeloma based on multiparameter flow cytometry analysis of bone marrow plasma cells', *Blood*. doi: 10.1182/blood-2007-05-088443.

Perfetti, V. *et al.* (1998) 'Evidence that amyloidogenic light chains undergo antigen-driven selection.', *Blood*. doi: http://dx.doi.org/10.1016/j.stemcr.2016.12.007.

Perfetti, V. (2002) 'Analysis of Vlambda -Jlambda expression in plasma cells from primary ({AL}) amyloidosis and normal bone marrow identifies 3r (lambda {III}) as a new amyloid-associated germline gene segment', *Blood*, 100(3), pp. 948–953. doi: 10.1182/blood-2002-01-0114.

Perfetti, V. *et al.* (2012) 'The repertoire of λ light chains causing predominant amyloid heart involvement and identification of a preferentially involved germline gene, IGLV1-44', *Blood*, 119(1), pp. 144–150. doi: 10.1182/blood-2011-05-355784.

Phipps, J. E. *et al.* (2010) 'Inhibition of pathologic immunoglobulin-free light chain production by small interfering RNA molecules', *Experimental Hematology*. doi: 10.1016/j.exphem.2010.07.001.

Picelli, S. *et al.* (2014) 'Full-length RNA-seq from single cells using Smart-seq2', *Nature Protocols*. doi: 10.1038/nprot.2014.006.

Poshusta, T. L. *et al.* (2009) 'Mutations in specific structural regions of immunoglobulin light chains are associated with free light chain levels in patients with AL amyloidosis', *PLoS ONE*. doi: 10.1371/journal.pone.0005169.

Qin, Z. *et al.* (2007) 'Structural characterization of the partially folded intermediates of an

immunoglobulin light chain leading to amyloid fibrillation and amorphous aggregation', *Biochemistry*. doi: 10.1021/bi061716v.

Radbruch, A. *et al.* (2006) 'Competence and competition: The challenge of becoming a long-lived plasma cell', *Nature Reviews Immunology*. doi: 10.1038/nri1886.

Ramirez-Alvarado, M. *et al.* (2012) 'Differences in immunoglobulin light chain species found in urinary exosomes in light chain amyloidosis (AL)', *PLoS ONE*. doi: 10.1371/journal.pone.0038061.

Ramirez-Alvarado, M. (2013) 'Amyloid Formation in Light Chain Amyloidosis', *Current Topics in Medicinal Chemistry*. doi: 10.2174/1568026611212220007.

Ravetch, J. V. and Lanier, L. L. (2000) 'Immune inhibitory receptors', *Science*. doi: 10.1126/science.290.5489.84.

Ravetch, J. V and Kinet, J. P. (1991) 'Fc receptors.', *Annual review of immunology*. doi: 10.1146/annurev.iy.09.040191.002325.

Reth, M. (1992) 'Antigen Receptors on B Lymphocytes', *Annual Review of Immunology*. doi: 10.1146/annurev.iy.10.040192.000525.

Richards, D. B. *et al.* (2015) 'Therapeutic Clearance of Amyloid by Antibodies to Serum Amyloid P Component', *New England Journal of Medicine*. doi: 10.1056/NEJMoa1504942.

Richardson, J. S. and Richardson, D. C. (2002) 'Natural -sheet proteins use negative design to avoid edge-to-edge aggregation', *Proceedings of the National Academy of Sciences*. doi: 10.1073/pnas.052706099.

Rognoni, P. *et al.* (2013) 'A Strategy for Synthesis of Pathogenic Human Immunoglobulin Free Light Chains in E. coli', *PLoS ONE*. doi: 10.1371/journal.pone.0076022.

Rooney, S., Chaudhuri, J. and Alt, F. W. (2004) 'The role of the non-homologous end-joining pathway in lymphocyte development', *Immunological Reviews*. doi: 10.1111/j.0105-2896.2004.00165.x.

Ru, H. *et al.* (2015) 'Molecular Mechanism of V(D)J Recombination from Synaptic RAG1-RAG2 Complex Structures', *Cell*. doi: 10.1016/j.cell.2015.10.055.

Sallusto, F. (1994) 'Efficient presentation of soluble antigen by cultured human dendritic cells is maintained by granulocyte/macrophage colony-stimulating factor plus interleukin 4 and downregulated by tumor necrosis factor alpha', *Journal of Experimental Medicine*. doi: 10.1084/jem.179.4.1109.

Sanders, P. W. and Booker, B. B. (1992) 'Pathobiology of cast nephropathy from human Bence Jones proteins', *Journal of Clinical Investigation*. doi: 10.1172/JCI115629.

Sawaya, M. R. *et al.* (2007) 'Atomic structures of amyloid cross-β spines reveal varied steric zippers', *Nature*. doi: 10.1038/nature05695.

Schiffer, M. *et al.* (1970) 'A preliminary crystallographic investigation of human L-type Bence-Jones protein.', *Journal of Biological Chemistry*.

Schmechel, D. E. *et al.* (1993) 'Increased amyloid beta-peptide deposition in cerebral cortex as a consequence of apolipoprotein E genotype in late-onset Alzheimer disease.', *Proceedings of the National Academy of Sciences*. doi: 10.1073/pnas.90.20.9649.

Schroeder, H. W. *et al.* (2010) 'Structure and function of immunoglobulins.', *The Journal of allergy and clinical immunology*. doi: 10.1016/j.jaci.2009.09.046.

Seligmann, M. *et al.* (1979) 'Heavy Chain Diseases: Current Findings and Concepts', *Immunological Reviews*. doi: 10.1111/j.1600-065X.1979.tb00302.x.

Serio, T. R. *et al.* (2000) 'Nucleated conformational conversion and the replication of conformational information by a prion determinant', *Science*. doi: 10.1126/science.289.5483.1317.

Shaffer, A. L. *et al.* (2008) 'IRF4 addiction in multiple myeloma', *Nature*. doi: 10.1038/nature07064.

Shapiro-Shelef, M. and Calame, K. C. (2005) 'Regulation of plasma-cell development', *Nature Reviews Immunology*. doi: 10.1038/nri1572.

Shi, J. *et al.* (2010) 'Amyloidogenic light chains induce cardiomyocyte contractile dysfunction and apoptosis via a non-canonical p38 MAPK pathway', *Proceedings of the National Academy of Sciences*. doi: 10.1073/pnas.0912263107.

Shirahama, T. and Cohen, A. S. (1967) 'High-resolution electron microscopic analysis of the amyloid fibril.', *The Journal of cell biology*. doi: 10.1083/jcb.33.3.679.

Shlomchik, M. J. *et al.* (1987) 'The role of clonal selection and somatic mutation in autoimmunity', *Nature*. doi: 10.1038/328805a0.

Da Silva Filho, M. I. *et al.* (2017) 'Genome-wide association study of immunoglobulin light chain amyloidosis in three patient cohorts: Comparison with myeloma', *Leukemia*. doi: 10.1038/leu.2016.387.

Slifka, M. K., Matloubian, M. and Ahmed, R. (1995) 'Bone Marrow Is a Major Site of Long-Term Antibody Production after Acute Viral Infection', *JOURNAL OF VIROLOGY*.

Smith, K. G. C. *et al.* (1997) 'The extent of affinity maturation differs between the memory and antibody-forming cell compartments in the primary immune response', *EMBO Journal*. doi: 10.1002/jez.10030.

Solomon, A. (1985) '[6] Light chains of human immunoglobulins', *Methods in Enzymology*. doi: 10.1016/S0076-6879(85)16008-8.

SOLOMON, A. *et al.* (1964) 'Metabolism of Bence Jones Proteins.', *The Journal of clinical investigation*, 43(1), pp. 103–117. doi: 10.1172/JCI104884.

Solomon, A., Weiss, D. T. and Pepys, M. B. (1992) 'Induction in mice of human light-chain-associated amyloidosis.', *The American journal of pathology*.

Solomon, A., Weiss, D. T. and Wall, J. S. (2003) 'Immunotherapy in Systemic Primary (AL) Amyloidosis Using Amyloid-Reactive Monoclonal Antibodies', *Cancer Biotherapy and Radiopharmaceuticals*. doi: 10.1089/108497803322702824.

Sonati, T. *et al.* (2013) 'The toxicity of antiprion antibodies is mediated by the flexible tail of the prion protein', *Nature*. doi: 10.1038/nature12402.

Stevens, F. J. (2000) 'Four structural risk factors identify most fibril-forming kappa light chains', *Amyloid*. doi: 10.3109/13506120009146835.

Tangye, S. G. *et al.* (2003) 'Intrinsic Differences in the Proliferation of Naive and Memory Human B Cells as a Mechanism for Enhanced Secondary Immune Responses', *The Journal of Immunology*. doi: 10.4049/jimmunol.170.2.686.

Tas, J. M. J. *et al.* (2016) 'Visualizing antibody affinity maturation in germinal centers', *Science*. doi: 10.1126/science.aad3439.

Tennent, G. A., Lovat, L. B. and Pepys, M. B. (1995) 'Serum amyloid P component prevents proteolysis of the amyloid fibrils of Alzheimer disease and systemic amyloidosis', *Medical Sciences*. doi: 10.1073/pnas.92.10.4299.

Tiller, T. *et al.* (2007) 'Autoreactivity in Human IgG+ Memory B Cells', *Immunity*. doi: 10.1016/j.immuni.2007.01.009.

Townsend, C. L. *et al.* (2016) 'Significant differences in physicochemical properties of human immunoglobulin kappa and lambda CDR3 regions', *Frontiers in Immunology*. doi: 10.3389/fimmu.2016.00388.

Traggiai, E. *et al.* (2004) 'An efficient method to make human monoclonal antibodies from memory B cells: Potent neutralization of SARS coronavirus', *Nature Medicine*. doi: 10.1038/nm1080.

Traggiai, E., Puzone, R. and Lanzavecchia, A. (2003) 'Antigen dependent and independent mechanisms that sustain serum antibody levels', *Vaccine*. doi: 10.1016/S0264-410X(03)00198-1.

Trinkaus-Randall, V. *et al.* (2005) 'Cellular response of cardiac fibroblasts to amyloidogenic light chains', *American Journal of Pathology*. doi: 10.1016/S0002-9440(10)62244-4.

Vinuesa, C. G. *et al.* (2016) 'Follicular Helper T Cells.', *Annual review of immunology*. doi: 10.1146/annurev-immunol-041015-055605.

Vrana, J. A. *et al.* (2009) 'Classification of amyloidosis by laser microdissection and mass spectrometry-based proteomic analysis in clinical biopsy specimens', *Blood*. doi: 10.1182/blood-2009-07-230722.

Waldmann, T. A., Strober, W. and Mogielnicki, R. P. (1972) 'The renal handling of low molecular weight proteins. II. Disorders of serum protein catabolism in patients with tubular proteinuria, the nephrotic syndrome, or uremia.', *The Journal of clinical investigation*. doi: 10.1172/JCI107023.

Ward, J. E. *et al.* (2011) 'Doxycycline reduces fibril formation in a transgenic mouse model of AL amyloidosis', *Blood*. doi: 10.1182/blood-2011-04-351643.

Wardemann, H. *et al.* (2003) 'Predominant autoantibody production by early human B cell precursors', *Science*. doi: 10.1126/science.1086907.

Wardemann, H., Hammersen, J. and Nussenzweig, M. C. (2004) 'Human Autoantibody Silencing by Immunoglobulin Light Chains', *The Journal of Experimental Medicine*. doi: 10.1084/jem.20040818.

Wardemann, H. and Nussenzweig, M. C. (2007) 'B-Cell Self-Tolerance in Humans', *Advances in Immunology*. doi: 10.1016/S0065-2776(07)95003-8.

Weiss, B. M. *et al.* (2014) 'Increased serum free light chains precede the presentation of immunoglobulin light chain amyloidosis', *Journal of Clinical Oncology*, 32(25), pp. 2699–2704.

doi: 10.1200/JCO.2013.50.0892.

Weitzner, B. D. *et al.* (2017) 'Modeling and docking of antibody structures with Rosetta', *Nature Protocols*. doi: 10.1038/nprot.2016.180.

Wiedemann, C., Bellstedt, P. and Görlach, M. (2013) 'CAPITO - A web server-based analysis and plotting tool for circular dichroism data', *Bioinformatics*. doi: 10.1093/bioinformatics/btt278.

Williams, A. F. and Barclay, A. N. (1988) 'The Immunoglobulin Superfamily—Domains for Cell Surface Recognition', *Annual Review of Immunology*. doi: 10.1146/annurev.iy.06.040188.002121.

Wochner, R. D. (1967) 'THE ROLE OF THE KIDNEY IN THE CATABOLISM OF BENCE JONES PROTEINS AND IMMUNOGLOBULIN FRAGMENTS', *Journal of Experimental Medicine*. doi: 10.1084/jem.126.2.207.

Wyatt, A. R. *et al.* (2012) 'Roles of extracellular chaperones in amyloidosis', *Journal of Molecular Biology*. doi: 10.1016/j.jmb.2012.01.004.

Xu, Z. *et al.* (2012) 'Immunoglobulin class-switch DNA recombination: Induction, targeting and beyond', *Nature Reviews Immunology*. Nature Publishing Group, 12(7), pp. 517–531. doi: 10.1038/nri3216.

Yang, J. and Reth, M. (2010) 'Oligomeric organization of the B-cell antigen receptor on resting cells', *Nature*. doi: 10.1038/nature09357.

Zhang, C., Huang, X. and Li, J. (2017) 'Light chain amyloidosis: Where are the light chains from and how they play their pathogenic role?', *Blood Reviews*. doi: 10.1016/j.blre.2017.03.002.

Zhang, T. *et al.* (2012) 'Identification and characterization of buried unpaired cysteines in a recombinant monoclonal igg1 antibody', *Analytical Chemistry*. doi: 10.1021/ac301426h.

Zhu, L. *et al.* (1995) 'Pathogenesis of glomerulosclerosis in light chain deposition disease. Role for transforming growth factor-beta', *Am J Pathol*.